Delay effects on synchronization in networks of dynamical systems

D I S S E R T A T I O N

zur Erlangung des akademischen Grades

Dr. Rer. Nat.
im Fach Physics

eingereicht an der
Mathematisch-Naturwissenschaftlichen Fakultät I
Humboldt-Universität zu Berlin

von
Dipl.-Phys. Manju Shrii Murugesan

Präsident der Humboldt-Universität zu Berlin:
Prof. Dr. Jan-Hendrik Olbertz

Dekan der Mathematisch-Naturwissenschaftlichen Fakultät I:
Prof. Stefan Hecht, Ph. D.

Gutachter:
1. Prof. Dr. Dr. h.c. mult. Jürgen Kurths
2. Prof. Dr. M. Lakshmanan
3. PD Dr. Sten Rüdiger

Tag der mündlichen Prüfung: 06.11.2013

To Senthil and Nidhika

Abstract

Synchronization is a fundamental nonlinear phenomenon observed in diverse natural systems. The underlying phenomenon is universal and can be understood within a common framework based on modern nonlinear dynamics. Investigations on synchronization of chaos has become an active area of research not only from theoretical perspectives but also in view of its potential applications in diverse areas of science and technology. Soon after understanding the concept of synchronization in two coupled chaotic systems, a flurry of research activities was provoked in understanding this phenomenon as an emergent behavior of an ensemble of dynamical systems with different topologies.

Deducing the conditions for stable synchronization is an important issue in the synchronization studies for its applications. In this regard, the framework of the master stability formalism has been largely employed in analyzing the stability of networks, which allows one to separate the local dynamics of the individual oscillators from the coupling matrix characterizing the topology of the underlying network. Similarly, time-delay is ubiquitous in many physical systems and investigations on the influence of connection delays in networks of nonlinear dynamical systems have been an active area of research in the domain of synchronization studies in recent times. Now, it has been understood the connection delays can actually be conductive to synchronization, so that it is possible for the delayed system to synchronize where the undelayed system does not.

In this thesis, we will explore the effect of delay coupling on networks of chaotic dynamical systems using the framework of master stability formalism. We will investigate the phenomenon of delay-enhanced and delay-induced stable synchronization in an arbitrary delay coupled network of time-continuous dynamical systems. We will demonstrate that there always exist an extended regime of stable synchronous state as a function of coupling strength for appropriate coupling delays, which cannot be observed without any delay in the coupling. We will also propose a partial delay coupling as a combination of both the instantaneous and the completely delay coupling with certain weights determining their contributions. We will show that the partial delay coupling outperforms both limiting cases of the instantaneous and the completely delay coupling on the synchronizability of networks. The framework of master stability formalism is extended to a network of intrinsic time-delay systems, whose node dynamics are described by delay differential equations, for the first time in the literature and illustrated the generic behavior of the master stability function in networks of scalar time-delay systems based on the synchronization properties of the network. We also investigate the interplay of noise and delay in the phenomenon of noise-enhanced phase synchronization in both unidirectionally and bidirectionally coupled time-delay systems.

Abstract

Synchronisation ist ein grundlegendes nichtlineare Phänomen in vielfältigen natürlichen beobachteten systeme. Die zugrunde liegende Phänomen ist universell und kann in einem gemeinsamen Rahmen auf der Grundlage verstanden werden modernen nichtlinearen Dynamik. Untersuchungen zur Synchronisation des Chaos geworden ein aktives Gebiet der Forschung nicht nur aus theoretischen Perspektiven, aber auch im Hinblick auf von ihrer möglichen Anwendungen in den verschiedensten Bereichen von Wissenschaft und Technik. Bald nach Verständnis des Konzepts der Synchronisation in zwei gekoppelten chaotischen Systemen, eine Flut von Forschungsarbeiten wurde im Verständnis dieses Phänomens provoziert als entstehender Verhalten eines Ensembles von dynamischen Systemen mit unterschiedlichen Topologien.

Ableitung die Voraussetzungen für eine stabile Synchronisation ist ein wichtiges Thema in der Synchronisations-Studien für ihre Anwendungen. In dieser Hinsicht ist die Rahmen der Master Stabilität Formalismus wurde weitgehend in der Analyse der Stabilität des Netzwerks, einer um die lokalen Dynamiken der einzelnen Oszillatoren von der Koppelmatrix Charakterisierung der Topologie der zugrundeliegenden Netzwerk trennen können eingesetzt werden. Ebenso ist Zeitverzögerung allgegenwärtig in vielen physikalischen Systemen und Untersuchungen über den Einfluss der Verbindung Verzögerungen in Netzwerken nichtlinearer dynamischer Systeme haben ein aktives Gebiet der Forschung im Bereich der Synchronisation Studien in der letzten Zeit. Nun hat es verstanden die Verbindung Verzögerungen tatsächlich leitend, um die Synchronisation, so dass es möglich für das verzögerte System synchronisiert wo das unverzögerte System nicht.

In dieser Dissertation werden wir die Wirkung der Verzögerung Kupplung auf Netzwerke von chaotischen erkunden dynamischer Systeme mit dem Rahmen der Master Stabilität Formalismus. Wir werden untersuchen das Phänomen der Verzögerung verstärkter und Verzögerungen induzierte stabile Synchronisation in einer willkürlichen Verzögerung gekoppelt Netzwerk von zeitkontinuierlichen dynamischen Systemen. Wir demonstrieren, dass es immer existieren eine erweiterte Regime des stabilen synchronen Zustand als eine Funktion der Kopplungsstärke geeignete Verbindung Verzögerungen, die nicht ohne Verzögerung in die Kupplung beobachtet werden kann. Wir schlagen eine partielle verzögerung Verbindung als eine Kombination von sowohl den momentanen und der komplett Verzögerung Verbindung mit gewissen Gewichten Bestimmung ihrer Beiträgen. Wir werden zeigen, dass die partielle Verzögerung Verbindung beide Grenzfälle des momentanen und der komplett Verzögerung Kupplung am synchronizabilit von Netzwerken übertrifft. Der Rahmen fuer Master Stabilität Formalismus ist mit einem Netzwerk von intrinsischen Zeitverzögerung Systeme, deren Knoten Dynamik durch Verzögerung Differentialgleichungen beschrieben erweitert, zum ersten Mal in der Literatur und veranschaulicht das allgemeine Verhalten des Master-Stabilisierungsfunktion in Netzwerken skalare Zeit Einschaltverzögerung Systeme auf den Synchronisations-Eigenschaften des Netzes. Ausserdem untersuchen wir das Zusammenspiel von Lärm und verzögert in das Phänomen der Lärmverstärkter Phasensynchronisierung in beiden unidirektional und bidirektional gekoppelt zeitverzögerung systeme.

List of Publications

In International Journals :

1. **M. Manju Shrii**, D. V. Senthilkumar and J. Kurths, Delay coupling enhances synchronization in complex networks, *Europhys. Lett.* **98** (2012) 10003(1-6).

2. **M. Manju Shrii**, D. V. Senthilkumar and J. Kurths, Delay-induced synchrony in complex networks with conjugate coupling, *Phys. Rev. E* **85** (2012) 057203(1-5).

3. D. V. Senthilkumar, **M. Manju Shrii** and J. Kurths, Noise-enhanced phase synchronization in time-delayed systems, *Phys. Rev. E* **85** (2012) 026218(1-6).

4. **M. Manju Shrii**, D. V. Senthilkumar, Wei Zou and J. Kurths, Effects of partial time-delay on synchronization of neuronal networks, *submitted (2013)*

5. **M. Manju Shrii**, D. V. Senthilkumar and J. Kurths, synchronization in a network of intrinsic time-delay systems, *submitted (2013)*

Invited Book Chapter :

6. D. V. Senthilkumar, **M. Manju Shrii** and J. Kurths, Chapter 31 on "**Phase and complete synchronizations in time-delay systems**" in the book on the 75th birthday of Prof. Leon Chua entitled "**Chaos, CNN, Memristors and Beyond**" *World Scientific* (2013).

In Proceedings (peer reviewed):

7. **M. Manju Shrii**, D. V. Senthilkumar and J. Kurths, *Noise enhanced phase synchronization in coupled time-delay systems*, Proc. Fifth National Conference on "Nonlinear Systems & Dynamics", (2011).

Acknowledgement

I would like to express my deep gratitude to Prof. Jürgen kurths, my research supervisor, for his patient guidance, enthusiastic encouragement and useful critiques of this research work. I would like to express my very great appreciation to Dr. D. V. Senthilkumar for his valuable and constructive suggestions during the planning and development of this research work. His willingness to give his time so generously has been very much appreciated especially at the final stage of my research work. Special thanks should be given to Dr. Eulalie Joell Ngamga Ketchamen, for her professional and personal guidance. I would like to extend my thanks to Dr. Norbert Marwan for his constant support. I would like to thank Dr. Sabrina Hempel and Andreas Muller for their help, suggestion and straight forward comments. I wish to acknowledge the informations provided by Dr. Jonathan Donges and Dr. Kira Rehfeld for preparing this thesis. I would like to express my very great appreciation to all the members of Prof. Kurths group for their valuable critics and comments that helps me to proceed in right direction in my research work. I would also like to acknowledge the support of Ms. Heike Prietzel, Mr. Till Hollmann and Ms. Gabriele Pilz.

Contents

List of Figures

1 Introduction to synchronization and its stability in dynamical systems

1.1 Introduction

Synchronization, a fundamental nonlinear phenomenon, is ubiquitous in nature and can be observed in diverse areas of science, engineering, technology, and even in social life. Systems as diverse as clocks, adjacent organ pipes, singing crickets, firing neurons, cardiac pacemakers, and applauding audiences exhibit a tendency to operate in synchrony. The underlying phenomenon is universal and can be understood within a common framework based on modern nonlinear dynamics [Pikovsky et al., 2001, Winfree, 1980, Kuramoto, 1984, Boccaletti et al., 2002, Blekhman, 1988, Arenas et al., 2008]. Historically, the phenomenon of synchronization dates back to the period of the Dutch physicist Christiaan Huygens (1629-1695), who observed that two very weakly coupled pendulum clocks hanging from a same support swing exactly in opposite phase to each other, exhibiting anti-phase synchronization [Huygens, Christiaan, 1673]. Another important earliest observation was synchrony of organ pipes described by the English physicist Lord Rayleigh in his "Theory of Sound" [Rayleigh, 1877].

Despite being one of the first scientifically studied nonlinear phenomenon, synchronization was understood only in the late 1920s when Edward Appleton [Appleton, 1922] and Balthasar van der Pol [van der Pol and van der Mark, 1927] reported synchronization of triode oscillators both theoretically and experimentally. They demonstrated that the frequency of a generator can be entrained (synchronized) by a weak external signal of a slightly different frequency. These investigations have received a great physical significance and practical importance because triode generators were the basic elements of radio communication systems in those days. The phenomenon of synchronization was used to stabilize the frequency of a powerful generator with the help of one which was weak but very precise.

For a very long time, it was believed that synchronization is possible only among periodic systems and investigations on synchronization are restricted to such systems. For classical examples on synchronization in periodic systems, one may refer to [Blekhman, 1988]. Similarly, nonlinear systems were essentially studied under linear approximations, barring a few exceptions. However, in early sixties numerical works on the fluid convection model describing the atmospherical weather condition by E. N. Lorenz and on the initial value problem of the Korteweg-de-Veries (KdV) equation by Zabusky and Kruskal paved the way for identifying two important basic concepts, namely *Chaos* and *Soliton*, thereby triggering the golden era of modern nonlinear dynamics. Subsequently, different analytical methods and numerical tools have been developed to unravel the

hidden dynamical properties of nonlinear dynamical systems. In recent times increasing attention has been paid on exploring real technological applications of nonlinear dynamics. In particular, the notion of synchronization of coupled chaotic systems has emerged as an active area of research during the past twenty years or so in view of its potential applications.

Despite a substantial understanding on the phenomenon of synchronization well before the notion of chaos was realized and appreciated, it was considered that synchronization of chaos in chaotic dynamical systems was not possible because of their hallmark property of sensitivity dependence on initial conditions. This implies that two identical chaotic dynamical systems starting from an infinitesimal difference in their starting points will evolve such that their trajectories diverge exponentially in the course of time. Consequently, dynamical systems in a chaotic regime intrinsically defy synchronization as two identical systems starting from very slightly different initial conditions would evolve in an unsynchronized manner. This is a relevant practical problem even now a days in experiments, insofar as experimental initial conditions are never known perfectly.

However, it was realized later in 1980s that synchronization in chaotic dynamical systems can be achieved by introducing appropriate coupling between identical chaotic dynamical systems due to the works of Pecora and Carroll and the earlier works of Fujisaka and Yamada. [Fujisaka and Yamada, 1983, 1984, Pecora and Carroll, 1990, Afraimovich et al., 1986, Pikovsky, 1984, Pecora and Carroll, 1991]. After these seminal works on synchronization of chaos, this phenomenon has attracted considerable research activity in different areas of science and technology. Furthermore, several generalizations of this phenomenon and interesting applications have been developed. Investigations on synchronization of chaos have become an active area of research not only from theoretical perspectives but also in identifying potential applications in diverse subjects such as laser, chemical, electrical, biological, neurological, fluid mechanical systems as well as in secure communication, cryptography and so on.

In the following, a brief account on the different kinds of chaos synchronization and some directions of investigations in this area will be provided. It is to be noted that the literature on this subject is exhaustive and it is not possible, and appropriate, to give a complete review here. As a consequence of investigations on the phenomenon of synchronization with suitable couplings pertaining to real world connections, different types of synchronizations, characterized by the difference in the degree of correlation between the interacting dynamical systems, have been identified. Some of the basic types of synchronization includes

1. Phase synchronization (PS): PS means entrainment of phases of the interacting systems, $n\Phi_X - m\Phi_Y = const.$ (n and m are integers), while their amplitudes remain chaotic and are often uncorrelated [Rosenblum et al., 1996, Yalcinkaya and Lai, 1997],

2. Complete synchronization (CS): It refers to the identical evolution of the interacting systems, $Y(t) = X(t)$ [Fujisaka and Yamada, 1983, Pecora and Carroll, 1990],

3. Generalized synchronization (GS): GS is observed in coupled nonidentical systems,

where there exists some functional relation between the states of the coupled systems, that is, $Y(t) = F(X(t))$ [Rulkov et al., 1995, Kocarev and Parlitz, 1996, Brown, 1998],

4. Lag synchronization (LS): LS refers to the phenomenon, where the state of the response system lags the state of the drive system with a lag time $\tau > 0$, $Y(t) = X(t - \tau)$ [Rosenblum et al., 1997, Rim et al., 2002, Zhan et al., 2002] and

5. Anticipatory synchronization (AS): AS corresponds to the fact that the state of the response system anticipates the state of the drive system with an anticipating time $\tau > 0$, $Y(t) = X(t + \tau)$ [Voss, 2000, 2001, Masoller, 2001], etc.

Further, several variants of the above types of synchronizations such as their intermittent synchronizations, imperfect synchronizations have also been investigated.

Synchronization of chaotic systems with coexisting attractors indicates that the route to complete synchronization is characterized by a sequence of type-I and on-off intermittencies, intermittent phase synchronization, anticipatory synchronization and period-doubling phase synchronization [Pisarchik et al., 2006]. A transition from one kind of synchronizations to a other, coexistence of different kinds of synchronization in time series and also the nature of transitions has been studied extensively [Rosenblum et al., 1997, Rim et al., 2002, Zhan et al., 2002, 2003, Locquet et al., 2001] in coupled chaotic systems. The role of parameter mismatch in synchronization phenomenon is quite versatile and it has also been widely reported in the literature [Boccaletti and Valladares, 2000, Masoller, 2001, Zhu and Lai, 2001, Taherion and Lai, 1999, Locquet et al., 2002, Shahverdiev et al., 2002a,b]. Attempts has also been made to define a unifying framework for the overall class of synchronizations [Boccaletti et al., 2001, Brown and Kocarev, 2000, Hramov and Koronovskii, 2004]. For a critical discussion on the interrelationship between various kinds of synchronizations, one may refer to [Brown and Kocarev, 2000, Boccaletti et al., 2001]. Reviews on the phenomenon of chaos synchronization can also be found in [Pikovsky et al., 2001, Boccaletti et al., 2002, Kurths, 2000, Pecora, 1997]. From now onward we will restrict our discussions only on complete synchronization and its characterizations as we intended to investigate complete synchronization in networks of chaotic dynamical systems with delay coupling in this thesis, except in the last Chapter in which phase synchronization in intrinsic time-delay systems will be discussed. In particular, we explore the effect of two different types of delay coupling, namely, (i) completely delay coupling and (ii) partial delay coupling with certain proportion of both instantaneous coupling and delay coupling, in a network of continuous time dynamical systems. Further, we will also investigate the existence of stable synchronization in networks of intrinsic time-delay systems described by delay differential equation. We would like to point out that time-delay systems are essentially infinite-dimensional in nature and analyzing them is a challenging task both theoretically and numerically.

1.1.1 Synchronization in two coupled chaotic oscillators

Synchronization of chaotic systems can be defined as a process wherein two or more chaotic systems adjust to a given property of motion due to coupling or forcing. As

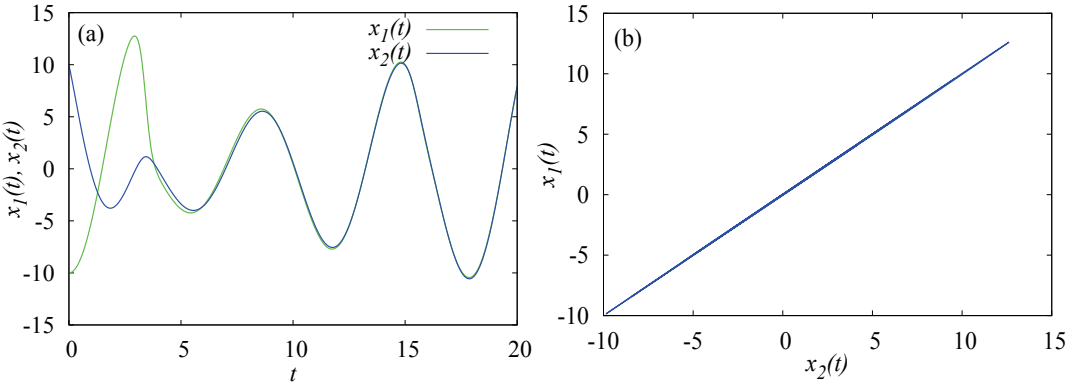

Figure 1.1: Identical synchronization between two Rössler systems with drive-response configuration (1.3). (a) Time trajectories of the drive $x_1(t)$ and the response $x_2(t)$ systems, and (b) Phase space plot of the drive and the response.

discussed above, there are different kinds of synchronization depending upon the nature of the interacting systems and the coupling schemes [Winfree, 1980, Kuramoto, 1984, Pikovsky et al., 2001, Boccaletti et al., 2002]. Among them, identical or complete synchronization (CS) was widely investigated in great detail [Fujisaka and Yamada, 1983, Pecora and Carroll, 1990]. This type of synchronization is also some times referred to as conventional synchronization. It is now known that the two chaotic dynamical systems $X \in \mathbb{R}^n$ and $Y \in \mathbb{R}^n$ exhibiting chaotic oscillations are said to be completely synchronized only when the systems evolve identically ($X = Y$) over a course of time, despite its chaotic behavior. This is achieved for a suitable coupling strength ε by coupling the two systems appropriately. The nature of coupling configuration is broadly classified into two main types as (i) unidirectional and (ii) bidirectional coupling.

When the evolution of one of the coupled systems is unaltered by the coupling, the resulting configuration is called *unidirectional coupling* or *drive-response coupling*, as one of the dynamical systems, X, drive the other (response, Y) in a one way communication channel.

$$\dot{X} = F(X), \tag{1.1a}$$
$$\dot{Y} = F(Y, S(t)), \tag{1.1b}$$

where F is a vector field $F : \mathbb{R}^n \to \mathbb{R}^n$ and $S(t)$ is some function of $X(t)$ and $Y(t)$ corresponding to the driving signal. In this case, the evolution of one of the coupled system, Y, is forced to follow the evolution of the other system, X.

As an illustrative example of the above general coupling scheme for drive-response configuration, we will consider a drive system given by the paradigmatic Rössler sys-

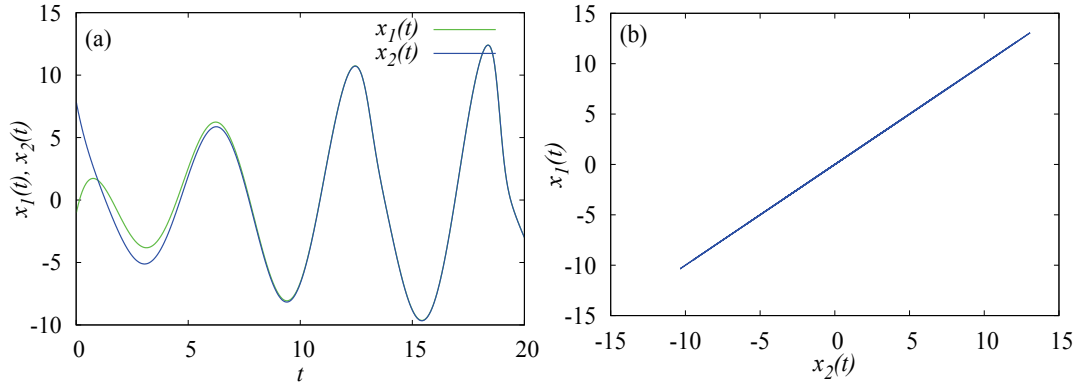

Figure 1.2: Identical synchronization between two mutually coupled Rössler systems (1.5). (a) Time trajectories of the drive $x_1(t)$ and the response $x_2(t)$ systems, and (b) Phase space plot of the drive and the response.

tem [Pecora, 1997],

$$\dot{x}_1 = -(y_1 + z_1), \tag{1.2a}$$
$$\dot{y}_1 = x_1 + 0.2y_1, \tag{1.2b}$$
$$\dot{z}_1 = 1.0 + z_1(x_1 - 7.0), \tag{1.2c}$$

and the response system (x_2, y_2, z_2) by

$$\dot{x}_2 = (y_2 + z_2) + \varepsilon(x_1 - x_2), \tag{1.3a}$$
$$\dot{y}_2 = x_2 + 0.2y_2, \tag{1.3b}$$
$$\dot{z}_2 = 1.0 + z_2(x_2 - 7.0), \tag{1.3c}$$

where ε defines the coupling strength. The response system is driven unidirectionally by the driving signal x_1, while the drive system remains unaffected by the response system. Beyound a certain critical value of the coupling strength, the response system synchronizes to the state of the drive system. The time trace of the variables $x_1(t)$ and $x_2(t)$ evolving identical to each other after some transient time is depicted in Fig. 1.1(a) and the diagonal line in the phase space of $(x_1(t), x_2(t))$ confirming the existence of complete synchronization between the two unidirectionally coupled systems is shown in Fig. 1.1(b) for the value of the coupling strength $\varepsilon = 0.5$.

On the other hand, when the coupling configuration is bidirectional (or mutual), the systems are coupled in such a way that they mutually influence each others evolution as represented by the following equations.

$$\dot{X} = F(X, S(t)), \tag{1.4a}$$
$$\dot{Y} = F(Y, S(t)), \tag{1.4b}$$

In this case of bidirectionally coupled systems, both systems X and Y drive each other and adjust their rhythms to reach a common dynamical behavior above a critical coupling strength. Let us consider an example of mutually coupled Rössler systems, whose equation of motion is represented by

$$\dot{x}_{1,2} = -(y_{1,2} + z_{1,2}) + \varepsilon(x_{2,1} - x_{1,2}), \tag{1.5a}$$
$$\dot{y}_{1,2} = -x_{1,2} + 0.2y_{1,2}, \tag{1.5b}$$
$$\dot{z}_{1,2} = 1.0 + z_{1,2}(x_{1,2} - 7.0). \tag{1.5c}$$

Figure 1.2(a) shows the time trajectory plot of $x_1(t)$ and $x_2(t)$ illustrating identical evolution of both systems after initial transients and the diagonal line in Fig. 1.2(b) for the coupling strength $\varepsilon = 1.0$ corroborates the existence of complete synchronization between the mutually coupled Rössler systems. For detail descriptions about the Rössler system, one may refer to Ref. [Rössler, 1976].

1.1.2 Stability of synchronization

The most challenging and important aspect of the synchronization studies is to ascertain the stability of CS solution as stable synchronization is essential to many practical applications [Pikovsky et al., 2001, Boccaletti et al., 2002]. One of the most important and widely used criteria to determine the nature of the stability is the use of the Lyapunov exponents, which quantifies the degree of convergence or divergence of small displacements (perturbation) along the synchronized trajectory [Wolf et al., 1985, Wylie and Barrett, 1995, Lakshmanan and Rajasekar, 2003].

In order to provide a much deeper insight into this concept, let us consider a system of two coupled identical chaotic systems, whose temporal evolution is ruled by the Eq. (1.4). The problem of the stability of synchronization in the identically coupled systems (1.4) can be determined by addressing the stability of the CS manifold $X \equiv Y$, or equivalently by studying the temporal evolution of the synchronization error $\mathbf{e} \equiv Y - X$. The evolution of $\mathbf{e}$ is given by

$$\dot{\mathbf{e}} = F(X, S(t)) - F(Y, S(t)). \tag{1.6}$$

A necessary condition for the existence of stable CS between the coupled systems is that the synchronization manifold is asymptotically stable for all possible $S(t)$ within the phase space spanned by the trajectories of the chaotic attractor. This property can be proved by using the stability analysis of the linearized system for small $\mathbf{e}$,

$$\dot{\mathbf{e}} = D(S(t))\mathbf{e}, \tag{1.7}$$

where D is the Jacobian of the vector field F evaluated onto the driving signal $S(t)$. It is to be noted that when the driving signal is either periodic or a fixed point, then the stability is determined directly by evaluating the eigenvalues of D or the Floquet multipliers. For chaotic driving signal $S(t)$, one has to estimate the Lyapunov exponents of the Eq. (1.7) to ascertain about the stability of synchronization.

Lyapunov Exponents may be defined as

$$\lambda(S_0, \mathbf{d}_0) \equiv \lim_{t\to\infty} \frac{1}{t} ln \left(\frac{|\mathbf{e}(t)|}{|\mathbf{e}(0)|} \right) = \lim_{t\to\infty} \frac{1}{t} ln |Z(S_0, t).\mathbf{d}_0|, \tag{1.8}$$

where S_0 is the initial condition of the driving signal, $\mathbf{d}_0 = \mathbf{e}(0)/|\mathbf{e}(0)|$ defines the initial orientation of the infinitesimal displacement and $Z(S_0, t)$ is the matrix solution of the linearized equation,

$$dZ/dt = D_X(S(t))Z, \tag{1.9}$$

subject to the initial condition $Z(0) = I$. The synchronization error $\mathbf{e}$ evolves according to $\mathbf{e}(t) = Z(S_0, t)\mathbf{e}_0$ and the matrix Z determines whether the error diverge or converge in a particular direction. When the error diverges, then the ratio $\frac{|\mathbf{e}(t)|}{|\mathbf{e}(0)|}$ in the Eq. (1.8) has at least one-component with value greater than unity and hence the largest Lyapunov exponent

$$\lambda(S_0, \mathbf{d}_0)_{max} > 0, \tag{1.10}$$

and will always be positive. In contrast, when the error converges, then the ratio $\frac{|\mathbf{e}(t)|}{|\mathbf{e}(0)|}$ is less than unity resulting in

$$\lambda(S_0, \mathbf{d}_0)_{max} < 0, \tag{1.11}$$

the negative values for the largest Lyapunov exponent. For chaotic dynamical systems, the Lyapunov exponents cannot be estimated analytically and hence one should rely on numerical techniques [Wylie and Barrett, 1995, Lakshmanan and Rajasekar, 2003, Wolf et al., 1985].

Thus, it is clear that the negative value of the largest Lyapunov exponent (1.11) correspond to the convergence of the nearby trajectories and it assures the stability of the CS exhibited by the coupled system (1.4). These Lyapunov exponents are called as *transverse Lyapunov exponents* because they characterize the nature of the perturbations transverse to the CS manifold. In the context of drive-response coupling schemes, these exponents are usually called as *conditional Lyapunov exponents* because they correspond to the Lyapunov exponents of the response system under the explicit condition (or constraint) that they are estimated on the drive system. The negative value of the transverse (or conditional) Lyapunov exponent is a necessary condition for the global stability of the synchronized state over the whole chaotic attractor. Nevertheless, it does not assures the local stability within the CS manifold as it is an average quantity over a long time evolution by definition. Local desynchronization events could occur within the CS manifold due to the presence of small parameter mismatch between the coupled systems and low levels of noise, which are unavoidable effects in experimental devices and in numerical integrations.

However, the local stability condition is assured by the use of appropriate positive definite Lyapunov functional $L(t)$ [Krasvoskii, 1963, Wolf et al., 1985, Wylie and Barrett, 1995]. The stability condition is deduced from the requirement that the derivative of the Lyapunov functional on the evolution equation corresponding to the synchronization manifold $\dot{\mathbf{e}}$ should be less than zero. Hence the Lyapunov functional assures stable syn-

chronization all the way along the evolution of the synchronization manifold $\dot{\mathbf{e}}$, ensuring the local stability. The stability condition deduced from the Lyapunov function is a sufficiency condition. More details on the Lyapunov functional theory can be found in Ref. [Krasvoskii, 1963, Lakshmanan and Rajasekar, 2003].

1.2 Synchronization in ensemble of oscillators with regular topologies

In many natural systems, synchronization is observed as an emergent collective phenomenon of a large population of systems. For example, synchronized flashing of fireflies, creeping of insects, croaking of frogs, synchronized spiking-bursting of neurons in the cortex, etc. With the existing knowledge on chaos synchronization in two coupled chaotic systems along with ample of real world applications, a flurry of research activities is provoked in understanding the synchronization phenomenon as an emergent behavior of ensemble of dynamical systems. The stability aspects that will be discussed in Sec. 1.3.2 for an arbitrary network will also valid for regular network topologies. As our main objective is to investigate synchronization in an arbitrary network that includes complex network topolgies, we provide more attention to details on complex networks and its synchronization properties. Detailed reviews on the literature on synchronization in coupled oscillators with regular topologies can be found in [Pikovsky et al., 2001, Winfree, 1980, Kuramoto, 1984, Boccaletti et al., 2002, Pecora, 1997].

1.3 Complex networks

Networks of coupled dynamical systems have been used to model chemical and biological oscillators [Winfree, 1980, Kuramoto, 1984, Strogatz, 1993], Josephson junction arrays [Braiman et al., 1995, Wiesenfeld, 1996], excitable media [Gerhardt and Schuster, 1990], neural networks [Collins et al., 1995, Abbott and Vreeswijk, 1993], genetic networks [Kauffman, 1969], etc. Networks can be conveniently modeled as an ensemble of nodes (vertex) representing the individual dynamical units that interact by means of complex wiring of edges (links) representing connection between them. Historically, the study of networks has been the domain of a branch of discrete mathematics known as graph theory (where the networks are usually completely regular or completely random), which has witnessed many exciting developments after the publication of the solution to the Königsberg bridge problem by Leonhard Euler in 1736.

The concept of networks has received a central importance in the context of social sciences in early 1920s, where the focus is on the relationship among the social entities such as communication or acquaintanceship among the group of members, trades among the nations, etc. The pioneering work of Milgram in this context in 1960s highlighted that social networks have the property of being *small world*. The last decade has witnessed the birth of a new movement of interest and research activity in the study of *complex networks* (networks whose structure is irregular, complex and dynamically evolving in time) with special attention to the properties of networks of dynamical units

and this was triggered by two seminal papers, that by Watts and Strogatz on small-world networks [Watts and Strogatz, 1998] and that by Barabási and Albert on scale free networks [Albert and Barbasi, 2002].

The comparative analysis of real world networks such as World Wide Web, mobile network, internet, transportation network, actor's collaborations network in movie database, scientific co-authorship and citation network from the Science Citation Index, neural networks, genetic, metabolic and protein networks, etc. has uncovered a series of unexpected results, which stimulated a renewed effort of defining new concepts and measures to characterize the observed topologies. The main results have been the identification of a series of unifying principles and statistical properties common to most of the real world networks.

In particular, it was observed in many cases of real networks that the degree distribution (the probability that a node chosen uniformly at random has a given number of direct connections to other nodes) exhibits power law (scale-free) tail with an exponent taking value between 2 and 3 which deviates from the Poisson distribution expected for random graph models. Moreover real networks are also characterized by correlations in the node degree by having relatively short paths between any two nodes (small-world) and large clustering coefficients.

These findings has initiated a revival of network modeling with scientists developing new models to mimic the growth of network and to reproduce the structural properties observed in real topologies. This was also motivated by the expectation that understanding and modeling the structure of a network would lead to a better knowledge of its evolutionary mechanisms, its dynamical and functional behavior. Indeed, it was shown that the coupling architecture has important consequences on the network functional robustness and response to external perturbations such as random failures or targeted attacks.

While researchers are dealing with the structural issues for a decade, recent interest in the subject has switched to investigate the dynamical behavior of networks with a special emphasis on how the network structure affects the properties of a networked dynamical system. For instance, considerable attention have been shown to study the emergence of collective synchronized dynamics in complex networks from the view point of synchronizability (including the desynchronization dynamics) of networks due to the interplay between the topology and the local properties of the coupled dynamical systems. The emergence of collective and synchronized dynamics in a network of coupled dynamical systems has been investigated in different contexts and in a variety of fields [Boccaletti et al., 2006, chaos, 2006]. Detail reviews on this subject can be found in Ref. [Boccaletti et al., 2006, Arenas et al., 2008].

1.3.1 Synchronization in complex networks

Historically, the study of synchronization in complex networks was started by dealing with oscillators whose topology of interactions showed either the scale free or the small-world properties [Nishikawa et al., 2003, Gade and Hu, 2000, Jost and Joy, 2002] and later it was mainly concentrated on complete synchronization of identical nonlinear sys-

tems as they allowed for analytical approaches. As enormous amount of research activity has been provoked in this direction soon after the first network models were proposed, only the most significant results on the synchronization of complex networks will be briefly discussed in the following.

The pioneering works on conditions and effects of synchronization in complex networks were reported by Watts [Watts, 1999] and Barahona and Pecora [Barahona and Pecora, 2002]. The Kuramoto model with small-world topology was studied numerically by Watts, while the analytical condition for complete synchronization of chaotic systems on different kinds of graphs was addressed by Barahona and Pecora. With the growing interest in understanding the dynamics of complex networks, several groups have investigated the onset and the mechanism leading to synchronization in Kuramoto model with various forms of complex wirings, as this model allows for both analytical and fast numerical simulations [Acebron et al., 2005, Moreno and Pacheco, 2004, Lee, 2005]. Other than the master stability formalism discussed in the previous sections, efforts have also been made to introduce different analytical approaches such as mean field theory [Lee, 2005], generalized mean-field approach and their variants.

Recent studies [Nishikawa et al., 2003, Lee, 2005] on the degree of synchronization produced by complex topologies revealed that the ability of a given network to synchronize is strongly ruled by the structure of connections. Some of the studies suggest that small-world wirings always lead to an enhancement of synchronization compared to regular networks due to decrease in average path length. However, it was latter shown that it is not always true and that under certain circumstances the addition of random short cuts lead to destabilization of synchronized state [Jiang et al., 2003]. Nevertheless the relationship between the emergence of small-world regime and the arising of collective synchronized behaviors remain under debate. Furthermore, synchronization of dynamical systems on scale-free networks was also demonstrated [Jalan and Amritkar, 2003]. In addition to this, desynchronization mechanisms in the complex network has also been reported by many researchers.

It has also shown that the maximum synchronizability in complex networks is achieved when the network of couplings is weighted and directed with the overall cost involved in the couplings is minimum [Motter et al., 2005]. It was shown that synchronizability of random networks is determined by two leading parameters: the mean degree and the heterogeneity of the distribution of node's intensity [Zhou et al., 2006a]. It was also demonstrated that the dynamical organization of connection weights, adaptive process, enhances significantly the synchronizability of the networks [Zhou and Kurths, 2006] and the results on synchronization dynamics in the cortical brain network of the cat provide insights into the relationship between network topology and functional organization of complex brain networks [Zhou et al., 2006b].

1.3.2 Stability of synchronization in an arbitrary network

To deal with the stability of synchronization in an ensemble of coupled dynamical systems, the master stability formalism was first put forward analytically by Fujisaka and Yamada [Fujisaka and Yamada, 1983, 1984], later extended theoretically and experi-

mentally by Pecora and Carroll for an ensemble of coupled chaotic oscillators with regular topologies [Pecora and Carroll, 1990, Pecora et al., 1997], and later on extended to more complex topologies by Barhona and Pecora [Pecora and Barahona, 2002]. This framework allows one to separate the local dynamics of the individual oscillators from the coupling matrix characterizing the topology of the underlying network [Pecora and Carroll, 1998]. Now, we will describe this approach in some detail as we will employ the master stability formalism to determine the stability nature of networks of delay coupled chaotic low-dimensional dynamical systems described by ordinary differential equations (ODEs) and in intrinsic time-delay systems described by delay differential equations (DDEs).

Consider an arbitrary network composed of N identical chaotic units represented by the equation of motion

$$\dot{X}_i(t) = F(X_i(t)) + \sigma \sum_{j=1}^{N} g_{ij} h(X_j(t)), \qquad i = 1, \ldots, N \tag{1.12}$$

where $X \in \mathbb{R}^m$, F is a nonlinear function describing the dynamics of the individual systems, σ is the overall coupling strength, $G = g_{ij}$ is a $N \times N$ connectivity matrix, which determines the topology of the arbitrary network and h is a $m \times m$ coupling function. The $N-1$ constraints $X_1 = ... = X_N = X_s$ defines the invariant synchronization manifold, which is assured by the requirement of the zero row sum for each row, i.e., $\sum_{j=1}^{N} g_{ij} = 0 \ \forall i$. Hence the equation of motion of all the oscillators is the same in the synchronized state and the solution of the synchronization manifold X_s is the same as that of the uncoupled individual dynamical system $\dot{X} = F(X)$.

The above dynamical equation, (1.12), representing the evolution of the network can be recasted for convenience as

$$\dot{X}_i = I_N \otimes F + \sigma (G \otimes I_N)(h \otimes I_N), \tag{1.13}$$

where $\otimes$ stands for the direct product between the matrices and I_N is a $N \times N$ identity matrix.

A necessary condition for the stability of the synchronization manifold is that all the $(N-1) * m$ Lyapunov exponents that characterize the perturbations in the transverse directions to the synchronization manifold should be negative. This corroborates that the transverse perturbations converge to the synchronization manifold so that it is a stable manifold. To determine the stability nature, let us consider a small perturbation δX_i applied to the ith state vector from its synchronized state, such that $X_i = X_s + \delta X_i$.

The perturbed equation of motions (referred to as the variational equations) of the ith oscillator can be written as

$$\delta \dot{X}_i = \left(I_N \otimes DF + \sigma (G \otimes I_N)(Dh \otimes I_N)\right) \delta X_i, \tag{1.14}$$

where DF and Dh are the Jacobian matrices of the nonlinear function F and the coupling function h, respectively, evaluated on the synchronization manifold X_s. Using the

property $(A \otimes B)(C \otimes D) = (AC) \otimes (BD)$, the above equation of motion becomes

$$\delta \dot{X}_i = (I_N \otimes DF + \sigma G \otimes Dh)\delta X_i. \tag{1.15}$$

Now, let us project δX_i into the eigenspace spanned by the eigenvectors V_i of the coupling matrix G. Then the corresponding variational equation can be written as

$$\delta X_i = \sum_{i=1}^{N} V_i \otimes \eta_i(t) \tag{1.16}$$

where $\eta_i(t) = (\eta_{1,i}(t), \eta_{2,i}(t), ..., \eta_{m,i}(t))$ is the eigenmode associated with eigenvalue γ_i of G. Let $\gamma_i, i = 0, 1, 2, \ldots, N-1$ be the set of real eigenvalues and V_i be the associated orthonormal eigenvectors such that $GV_i = \gamma_i V_i$ and $V_j^T \times V_i = \delta_{ij}$. Then the corresponding block diagonalized variational equations, with each block having the same form, is represented as

$$\dot{\eta} = (DF + \varepsilon Dh)\eta, \tag{1.17}$$

where the normalized coupling parameter $\varepsilon = \sigma\gamma_i$. The zero row sum condition ensures that the spectrum is entirely semi-positive i.e. $\gamma_i \geq 0 \ \forall i$, $\gamma_0 = 0$ is associated with the eigenvector $V_0 = \pm 1/\sqrt{N}(1, 1, ..., 1)^T$ that entirely defines the synchronization manifold and all the other eigenvalues $\gamma_i (i = 1, 2, ..., N-1)$ have the associated eigenvectors spanning in all the other directions of the hyper-dimensional phase space transverse to the synchronization manifold. It is to be noted that the eigenvalue γ_i is more generic because of the arbitrary G and it could be the eigenvalue corresponding to any specific topology determined by G. Now, the stability of the synchronization manifold is governed by the eigenvalues of G and the block diagonalized variational equations (1.17) for the transverse modes. The stability of the synchronized state of a given network topology is assured by the negative value of the largest transverse Lyapunov exponent, $\lambda_{max}(\varepsilon) < 0$, of the variational equations (1.17). The generic variational equation is referred to as the master stability equation and $\lambda_{max}(\varepsilon)$ as the master stability function (MSF).

First, it was considered that G is symmetric with real eigenvalues and later it is extended to the case of asymmetric coupling matrix G, which can be characterized by complex eigenvalues $\varepsilon = \sigma\gamma_i = (\alpha + i\beta)$. The generic variational equation (master stability equation) in the complex (α, β) plane can be written as

$$\dot{\eta} = (DF + (\alpha + i\beta)Dh)\eta, \tag{1.18}$$

where α and β are the real and imaginary parts of the eigenvalue. The largest transverse Lyapunov exponent $(\lambda_{max}(\alpha, \beta))$ estimated from the generic variational equation yields a complex surface in the (α, β) plane, namely, the master stability surface (MSF) of the network of oscillators. For a given value of the coupling strength σ, one can locate a point in the complex surface and the sign of λ_{max} at that point determines the stability of the synchronization manifold. It is to be noted that only the real terms in the above equation contribute to the stability of the synchronized state, whereas the imaginary terms have a rotational effect among different eigenmodes [Pecora and Carroll, 1998].

1.3.3 Coupling matrix G with non-zero row sum

Most of the investigations using the master stability formalism for determining the stability of a network of coupled oscillators assume the coupling matrix G to be zero row sum, so that the spectrum of eigenvalues of G is entirely semi-positive, i. e., the eigenvalues $\gamma_i \geq 0 \; \forall i$. Further, this ensures that the solution of the synchronization manifold X_s is the same as that of the individual uncoupled system $\dot{X} = F(X)$ and the identical evolution of the network of coupled systems in the synchronization manifold (invariant synchronization manifold).

Similar analysis can also be performed with a constant row sum of the coupling matrix G, i.e. $\gamma_i \geq c \; \forall i$. It is to be noted that, in the latter case, X_s is no more a solution of the uncoupled original dynamical system $\dot{X} = F(X)$ instead it is a solution of the equation $\dot{X} = F(X) + ch\left(X(t)\right)$, as $G = g_{ij}$ is replaced by $G = g_{ij} - c\delta_{ij}$ to make it zero row sum [Pecora et al., 2000]. Now the corresponding variational equation can be written as

$$\dot{\eta_i} = \left(DF + cDh + \sigma \sum_{j=1}^{N} (g_{ij} - c\delta_{ij}) Dh \right) \eta_i. \tag{1.19}$$

This is similar to Eq. (1.17), except that cDh is added to the first term of the variational equation and now G has zero row sum. Hence the equation of motions of the synchronization manifold becomes

$$\dot{X}_s = F(X_s) + ch(X_s). \tag{1.20}$$

For mathematical simplification, it is usually assumed that the coupling matrix G has zero row sum and block diagonalizable even for the asymmetric coupling.

1.3.4 Asymmetric, nondiagonalizable coupling matrix G

The framework of master stability formalism is also extended to networks of identical oscillators with asymmetric, nondiagonalizable coupling matrix and the stability of synchronization in such networks was determined using Jordan canonical form G [Nishikawa and Motter, 2006a,b, 2010]. Directed and weighted networks are characterized with asymmetric, nondiagonalizable coupling matrix, and hence the stability of synchronization in such networks can now be analyzed using the extended master stability formalism.

Now, the coupling matrix G is characterized by $g_{ij} \neq g_{ji}$ and it is defined by $g_{ij} = -a_{ij}w_{ij}$, where $A = a_{ij}$ is the adjacency matrix with entry $a_{ij} = 1$ when the nodes i and j are linked otherwise $a_{ij} = 0$. The weighted matrix $W = w_{ij}$ characterizes the weights and the directions of the links.

The $N \times N$ coupling matrix G is transformed into Jordan canonical form $J = P^{-1}GP$, where P is the invertible matrix of the generalized eigenvectors of G. Now, J can be

written as

$$J = \begin{pmatrix} 0 & & & \ldots & \\ & B_1 & & \ldots & \\ & & B_2 & \ldots & \\ . & . & . & \ldots & . \\ . & . & . & \ldots & . \\ & & \ldots & & B_l \end{pmatrix},$$

where

$$B_j = \begin{pmatrix} \gamma & & \ldots & \\ 1 & \gamma & \ldots & \\ & 1 & \gamma & \ldots \\ . & . & \ldots & . \\ . & . & \ldots & . \\ & \ldots & 1 & \gamma \end{pmatrix}.$$

γ is one of the (may be complex) eigenvalues of the connection matrix G. By applying these condition, the corresponding variational equation becomes

$$\dot{\xi} = DF(X_s)\xi - \varepsilon Dh(X_s)\xi G^T. \tag{1.21}$$

Applying the change of variable $\eta = \xi P^T$, the variational equation becomes,

$$\dot{\eta} = DF\eta - \varepsilon Dh\eta J^T. \tag{1.22}$$

Each block B_i in the Jordan canonical form corresponds to a subset of equations in (1.22). For example, if the block B_i is $k \times J$, then it takes the form

$$\dot{\eta}_1 = (DF - \varepsilon Dh)\eta_1, \tag{1.23a}$$
$$\dot{\eta}_2 = (DF - \varepsilon Dh)\eta_2 - \varepsilon Dh\eta_1, \tag{1.23b}$$
$$\vdots \tag{1.23c}$$
$$\dot{\eta}_k = (DF - \varepsilon Dh)\eta_k - \varepsilon Dh\eta_{k-1}, \tag{1.23d}$$

where $\eta = (\eta_1, \eta_2, \ldots, \eta_k)$ are perturbation modes in the generalized eigenspace of eigenvalue γ. If $\varepsilon = \sigma\gamma$ is complex then the Eq. (1.23a) is the master stability equation and the corresponding largest transverse Lyapunov exponent λ_{max} determines the stability of Eq. (1.23a). The stability of the other subsequent equations depend on the stability of the previous one, which can be realized from the second part of the equations. Assuming that Dh is bounded, when $\lambda_{max} < 0$, $\eta_1 \to 0$ exponentially as $t \to 0$ then the second term in Eq. (1.23b) is small. Hence, the same stability condition $\lambda_{max} < 0$ assures the convergence of the both terms in Eq. (1.23b) resulting in $\eta_2 \to 0$ exponentially as $t \to 0$. Extending the similar argument repeatedly to all the other equations in Eq. (1.23), one may realize that $\lambda_{max} < 0$ is a necessary and sufficient condition for the linear stability equations in each block B_i. Thus, the MSF of the master stability equation determines the stability of nondiagonalizable networks.

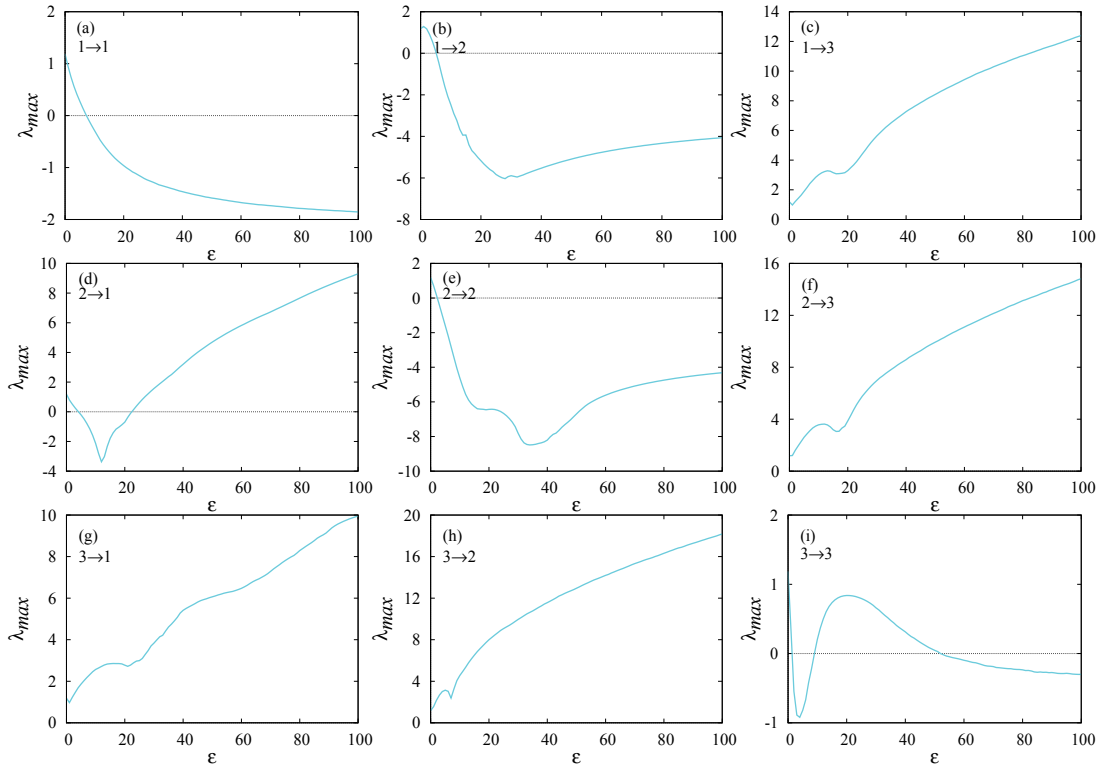

Figure 1.3: The master stability function λ_{max}, the largest transverse Lyapunov exponent of the generic variational equation (1.17), in the real plane as a function of normalized coupling parameter ε for an arbitrary network of Lorenz system with all possible one-component couplings. The notation $i \to j$ indicates the coupling as being from ith component of one oscillator to the jth component of another one.

If G is diagonalizable, then all the Jordan blocks are of the form 1×1 with only Eq. (1.23a) and hence all the eigenmodes are independent of each other. As the topology of any complex network can be broadly classified under either symmetric diagonalizable or asymmetric nondiagonalizable coupling matrix G, the stability of synchronization of any network can be determined using the master stability function λ_{max}, the largest transverse Lyapunov exponent corresponding to the largest transverse eigenmode of the variational equations.

1.3.5 Classification of the master stability function (MSF)

Recently, Huang et al classified the typical behaviors of the MSF into different categories by examining all possible one-component linear coupling configurations in several prototype three-dimensional systems [Huang et al., 2009]. The classification is carried out based on the behavior of the largest transverse Lyapunov exponent λ_{max} as a function of

the normalized coupling parameter ε (see Fig. 1.3). The classification depends upon the zero crossing of the λ_{max} and the classes are represented as Γ_n, where n represents the number of cross points with the zero-axis. According to their classification, the classes

1. Γ_0 has no finite cross points across the zero-axis and hence λ_{max} is positive for all the values of the normalized coupling parameter elucidating that the oscillators will never synchronize.

2. Γ_1 possess only one zero crossing at ε_1, i.e., the system is in unsynchronized state for $\varepsilon < \varepsilon_1$ with positive values for the λ_{max}. When the normalized coupling parameter is increased, the λ_{max} reaches zero at ε_1 and acquires negative values corroborating the existence of synchronization. Further, the corresponding system remain synchronized forever for further larger values of $\varepsilon > \varepsilon_1$ with $\lambda_{max} < 0$.

3. The λ_{max} of class Γ_2 possesses two successive crossings with the zero-axis at ε_1 and ε_2, resulting in a finite interval of stable synchronization in a finite range of the normalized coupling parameter $\varepsilon \in (\varepsilon_1, \varepsilon_2)$.

4. Γ_3 and Γ_4 represents multiple stable synchronized state with 3 and > 3 crossing points with the zero-axis, respectively.

In order to illustrate the above classification based on the behavior of the MSF, let us consider the Lorenz system as nodes in an arbitrary network. The generic variational equation (1.17) with real eigenvalues is used to estimate the master stability function, λ_{max}, and to determine the nature of the stability of synchronization in the network of Lorenz systems. The dynamical equations representing the Lorenz systems [Lorenz, 1963] is represented as

$$\dot{x} = \sigma(x - y), \tag{1.24a}$$
$$\dot{y} = x(r - z) - y, \tag{1.24b}$$
$$\dot{z} = xy - bz, \tag{1.24c}$$

where the variable x represents the amplitude of the convection motion, y and z measure the horizontal and vertical temperature variations, respectively. Here, $\sigma = 10.0$ represents the Prandtl number, $r = 28.0$ is the Rayleigh number and $b = 2.0$ is a geometric factor.

The behavior of the MSF for all possible one-component linear coupling configurations is shown in Fig. 1.3 [Huang et al., 2009]. Figures 1.3(c), (f) and (h) belongs to the class Γ_0 with positive values for λ_{max} for all the values of the normalized coupling parameter ε indicating that $x \to z$, $y \to z$ and $z \to y$ component couplings does not induce any synchronization in the corresponding network. Figures 1.3(a), (b) and (e) comes under the class Γ_1 with a single crossing of the λ_{max} across the zero-axis from positive to negative values and remain synchronized for ever for further larger values of the normalized coupling parameter ε. The class Γ_2 with a finite range of stable synchronized state as a function of ε with two zero crossings at $\varepsilon_1 = 4.2$ and $\varepsilon_2 = 22.5$ is depicted in

Figure 1.3(d). Multiple stable synchronized state, class Γ_3, with zero crossing of λ_{max} at $\varepsilon_1 = 1.4$, $\varepsilon_2 = 9.3$ and $\varepsilon_3 = 49.5$ is illustrated in Fig. 1.3(i).

1.4 Synchronization in complex networks with delay coupling

In the early stages of chaotic synchronization certain regularity in the connection was maintained whereas latter on more general networks with random, small-world, scale-free and hierarchical architectures have been emphasized as suitable models of real world networks. However, more realistic modeling of many large networks with nonlocal interaction inevitably requires connection delays [Atay et al., 2004] to be taken into account. As time-delay is ubiquitous in many physical systems due to finite switching speed of amplifiers, finite signal propagation time in biological networks, finite chemical reaction times, memory effects and so on [Senthilkumar and Lakshmanan, 2011], it is inevitable to consider the individual dynamical units of networks as delay dynamical systems [Masoller and Marti, 2005] with constant or time varying delays to mimic the most of the real network and to unravel their actual hidden dynamics. For example, in populations of spatially separated neurons, the synaptic communications between them depends on the propagation of action of potentials over appreciable distances involve distributed delays [Masoller and Marti, 2005].

Investigations on the influence of connection (or propagation) delay in coupled networks of nonlinear dynamical systems have been an active area of research in recent times in the synchronization studies [Soriano et al., 2013, Dhamala et al., 2004, Atay et al., 2004, Masoller and Marti, 2005, Flunkert et al., 2010, Kozyreff et al., 2000, Kinzel et al., 2009, Fischer et al., 2006, Shrii et al., 2012b,a, Tang J. et al., 2011, Wang et al., 2008, 2009, 2011, Lu et al., 2009, Stepan, 2009, Perez et al., 2011, Liang et al., 2009]. A flurry of research activities have been provoked in unveiling several fascinating features of connection delays on the synchronizability of networks of coupled dynamical systems. It has also been shown that delay in networks enhances the synchronizability of networks and interestingly it leads to the emergence of a wide range of new collective behavior (see [Atay et al., 2004, Masoller and Marti, 2005] and reference therein). On the other hand, it is also shown that connection delays can actually be conducive to synchronization, so that it is possible for the delayed system to synchronize where the undelayed system does not [Atay et al., 2004]. Unfortunately, only a few studies has been carried out along these line so far in midst of lot of recent activity in this subject and it requires immediate attention in order to understand more realistic dynamics of the many natural networks. Furthermore, the notion of the master stability formalism has not yet been successfully exploited in understanding the stability properties of synchronization in delay coupled networks synthesized even from a simple low-dimensional chaotic dynamical systems. Further, the effect of delay on the synchronizability of such a network has not yet been investigated using the MSF. These facts contributes to the motivation behind this thesis.

Despite enormous research activities on both synchronization of delay coupled networks [Atay et al., 2004, Masoller and Marti, 2005, Fischer et al., 2006, Li et al., 2007, Wang et al., 2008, Ponce et al., 2009, Masoller and Atay, 2011, Kozyreff et al., 2000] and

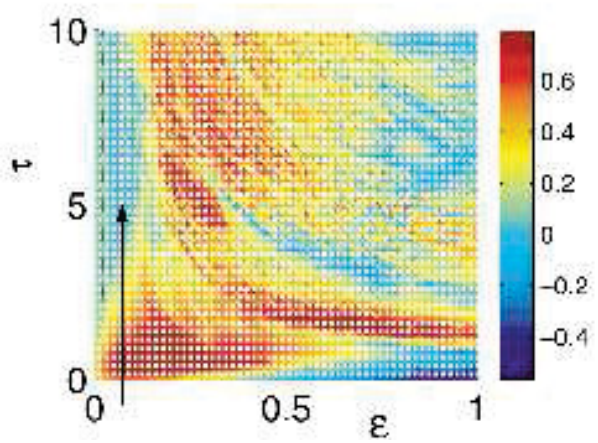

Figure 1.4: Color intensity of the largest transverse Lyapunov exponent, λ_{max}, indicating the degree of synchronization of two mutually delay coupled HR neurons. The arrow points to the region of synchronization at very low coupling strength.

in analysing the stability of synchronization in networks of oscillators by exploiting the MSF [Pecora and Carroll, 1990, Heagy et al., 1995, Pecora, 1997, Pecora and Carroll, 1998, Huang et al., 2009] independently, only a very few recent studies have been dealt with both MSF and delay coupled networks in probing the stability properties of the latter [Dhamala et al., 2004, Kinzel et al., 2009, Englert et al., 2011, Choe et al., 2010, Flunkert et al., 2010]. However, these reports limited their analysis either to phase oscillators [Choe et al., 2010, Flunkert et al., 2010] or to maps [Kinzel et al., 2009, Englert et al., 2011] except in Ref. [Dhamala et al., 2004, Jirsa, 2008], which reported the enhancement of neural synchrony by delay in two diffusively coupled Hindmarsh-Rose (HR) neurons. In the following, we will discuss briefly some of the important contributions along this line of research, which provide some more background knowledge on the problems to be discussed in the main part of this thesis.

1.4.1 Enhancement of neural synchrony by time-delay

The first systematic study of time-delay coupling was carried out by Schuster and Wagner [Schuster and Wagner, 1989], in two coupled phase oscillators and investigated multistability of synchronized solutions. Later, the work of Dhamala et. al. [Dhamala et al., 2004] on the enhancement of neural synchrony by time-delay coupling has attracted the attention of several researchers and re-initiated the investigations on the effects of delay coupling on synchronization of dynamical systems. In particular, Dhamala et. al. has investigated the synchronization of Hindmarsh-Rose (HR) neurons using the master stability formalism with delay coupling. These authors have shown that synchronization of two mutually coupled HR neurons occurs for the value of the coupling strength $\varepsilon > 0.5$

in the absence of delay in the coupling by estimating the largest transverse Lyapunov exponent of the system of two coupled HR neurons. Further, it has been shown that synchronization can be achieved for the value of the coupling strength as low as $\varepsilon > 0.1$ for appropriate delays in the coupling. The degree of synchronization of two coupled HR neurons as a function of the delay τ in the coupling and the coupling strength ε, characterized by the value of the largest transverse Lyapunov exponent, obtained by these authors is depicted in Fig. 1.4 as a color intensity plot. It is clearly seen that the two x-coupled HR neurons reach synchronization for a very low ε for the coupling delay $\tau > 3$ as indicated by the arrow. The dashed line drawn at $\varepsilon \approx 0.036$ delineate the stable and unstable regions. Nevertheless, they could not able to obtain stable synchronized state using the master stability function in a network of delay coupled HR neurons.

1.4.2 Synchronization in networks of delay coupled chaotic maps

consider a finite connected graph Γ with nodes (vertices) i, writing $i \sim j$ when i and j are neighbors, i. e., connected by an edge, and with the number of neighbors of i denoted by n_i. On Γ, one can have a dynamical system with discrete time $t \in \mathbf{Z}$, with the state x_i of i evolving according to

$$x_i(t+1) = f(x_i(t)) + \varepsilon \left(\frac{1}{n_i} \sum_{\substack{j \\ j \sim i}} f(x_j(t-\tau)) - f(x_i(t)) \right). \tag{1.25}$$

Here f is a differentiable function mapping some finite interval, say $[0, 1]$, to itself, $\varepsilon \in [0, 1]$ is the coupling strength, and $\tau \in \mathbf{Z}^+$ is the transmission delay between vertices. For simulation, the function $f(x)$ is chosen as $f(x) = \rho x(1-x)$ with the value of $\rho = 4$, for which the individual uncoupled systems are fully chaotic. Synchronized regions in the parameter space for scale-free, random, small-world and nearest-neighbour coupling are shown in Fig. 1.5(a), 1.5(b), 1.5(c) and 1.5(d), respectively. The authors have considered the same size, $N = 10000$, and the same number of average connections in the networks, even though their architectures are different.

It is evident from Figs. 1.5 that the scale-free and random networks can synchronize for a large range of parameters whereas more regular networks with nearest-neighbor and small-world type coupling do not. In the case of scale-free and random networks, for strong coupling (roughly for $\varepsilon > 0.6$) synchronization is achieved regardless of the actual value of the delay, as long as it is positive as seen in Figs. 1.5(a) and 1.5(b). For intermediate coupling in the range $0.4 < \varepsilon < 0.6$, the value of the delay becomes decisive for synchronization. There are also smaller regions of synchronization that exist for weaker coupling ($0.15 < \varepsilon < 0.20$) and only for odd delays. Note that for zero delay synchronization can occur only for a rather limited range ($\varepsilon > 0.85$). Also, the small regions of synchronization in Figs. 1.5(c) and 1.5(d) occur for nonzero delay only. Hence, the presence of delay can indeed facilitate synchronization.

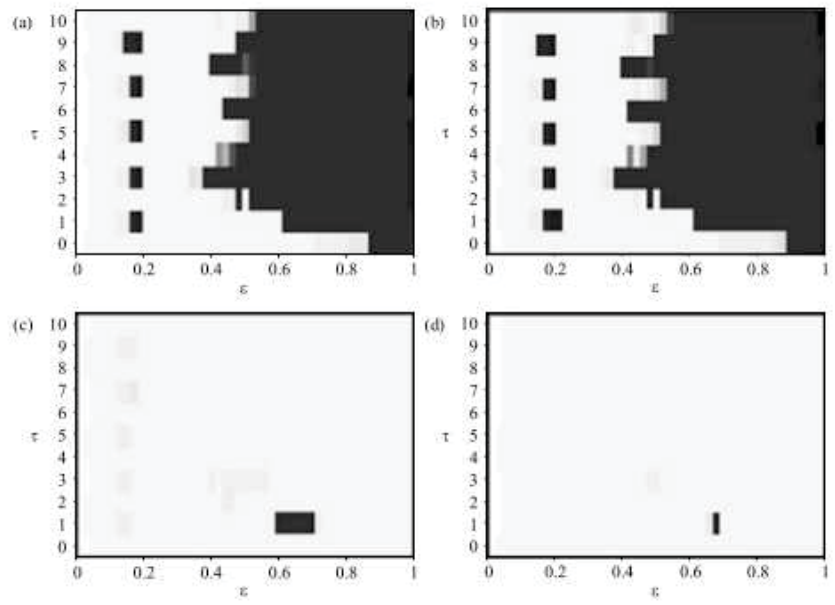

Figure 1.5: Synchronization of coupled logistic maps for different values of coupling strength ε and connection delays τ, for the cases of (a) scale-free, (b) random, (c) small-world, and (d) nearest-neighbor coupling. The grayscale encodes the degree of synchronization, with black regions corresponding to complete synchronization.

1.4.3 Synchronization in networks with random delays

In a similar study, as in the previous section, with random connection delays in networks of coupled chaotic maps, it has been shown that the network is able to synchronize despite the presence of random delays in the coupling. It has also shown that the synchronized state is a homogeneous steady state [Masoller and Marti, 2005], which is in contrast with the investigations on synchronization in network with constant delays [Atay et al., 2004]. The influence of the topology of the connection in the presence of random connection delay is investigated and found that the steady-state synchronization depends mainly on the average number of links per node and not on the architecture of the network unlike instantaneous and fixed-delay couplings [Masoller and Marti, 2005].

1.4.4 Synchronization of delay coupled networks using the MSF

In a recent work [Kinzel et al., 2009], the authors have calculated the master stability function for a network of chaotic units with time-delayed coupling. They have shown that when the delay times of transmission are much larger than any characteristic time scales of the individual units of any arbitrary finite network, the individual units are not synchronized. It is also shown that this holds for any network including the case where the individual units contain self-feedback delays. For several models including chaotic flows and maps, the authors have calculated the master stability function and determined the maximal value of delay time for which synchronization can occur.

In a very recent work [Flunkert et al., 2010], the authors has showed that for large coupling delays synchronizability is related in a simple way to the spectral properties of the network topology. It has been shown that the master stability function has a universal structure in the limit of large delay. The MSF is characterized by rotationally symmetric around the origin and increase monotonically with the radius in the complex plane, which facilitates the universal classification of networks with respect to their synchronization properties.

Among these interesting reports on synchronization in complex networks with connection delays, there are also few studies available in the literature on the effect of connection delays on the synchronization dynamics of several network motifs of different architectures [Gonzalez et al., 2007, Huys et al., 2008, Oguchi et al., 2008].

1.5 Motivations

Now, we will specify clearly how the above discussions contribute to the underlying reasons for the motivation behind this thesis in the following.

1. The framework of the master stability formalism has not yet been successfully employed in probing the stability of synchronization in an network of time continuous dynamical system.

2. Further, delay-enhanced synchronization, i.e, the phenomenon of enlargement of stable synchronization in an extended range of parameter space (usually as a func-

tion of the coupling strength) due to delay in the coupling is widely explored. It is not clear whether the connection delays can induce stable synchronization where there is no synchronization at all without delay in the instantaneous coupling.

3. Whether is it possible to induce or enhance stable synchronization in a much more profound range of parameter space then that induced either by completely instantaneous coupling or completely delayed coupling. For this purpose, we have introduced a partial delay coupling and shown that this type of coupling outperforms both the limiting cases for appropriate weights.

4. The behavior of the MSF has been clearly classified for networks of dynamical systems represented by ordinary differential equations based on their synchronization properties. On the other hand for node dynamics described intrinsic delay differential equations, which forms an important class of dynamical systems and is being widely used in the current literature for synchronization studies due to their potential applications, the framework of the master stability formalism has not yet been employed to our knowledge and we also aim to address this issue.

5. It is also worth to emphasize that the network of delay differential equations impose a challenging task to treat them both analytically and numerically.

In the following, we will explain in these tasks and the obtained results in some detial as outline of the thesis.

1.6 Outline of the Thesis

The Outline of the thesis is as follows:

In Chapter 2, the phenomena of delay-enhanced and delay-induced synchronization due to time-delay is investigated in an arbitrary delay coupled network with chaotic units. Using the master stability formalism for a delay coupled network, we will elaborate that there always exist an extended regime of stable synchronous solutions of the network for appropriate coupling delays. Further, we will show that the stable synchronous state is achieved even at smaller values of coupling strength with delay, which can be attained only at much larger coupling strength without delay. Further, the largest transverse Lyapunov exponents of the master stability equation of the network clearly demarcates the stable synchronous solutions from the unstable ones. The generic nature of our results is also corroborated using four different paradigmatic models, namely, Rössler, Lorenz systems, Hindmarsh-Rose neurons and as well as Chua's circuit systems as nodes in the delay coupled network.

In Chapter 3, we propose a partial delay coupling as a combination of both instantaneous and delay coupling with certain weights and investigate the effect of the partial delay coupling on the synchronization properties of an arbitrary network as a function of the weight. We will estimate the largest transverse Lyapunov exponent corresponding to the largest transverse mode of the network obtained using the master stability formalism to determine the stability of the synchronized state. We will show that the partial delay

coupling outperforms the limiting case of completely delay coupling in inducing an extended regime of stable synchronization for both lower and higher values of the coupling strength for appropriate weights. Further, we will demonstrate that the partial delay coupling is capable of inducing synchronization for appropriate coupling configurations, where both the limiting cases of completely delay coupling and completely instantaneous coupling does not exhibit any synchronization. These results are corroborated using Hindmarsh-Rose neurons and Rössler systems as the nodes of the network.

Chapter 4 deals with the synchronization in network of intrinsic time-delay systems, with the node dynamics are represented by a first-order scalar delay differential equations, using the master stability function (MSF). In this chapter, We will examine the nature of the master stability function (MSF) in an arbitrary network of scalar time-delay system in both chaotic and hyperchaotic regimes. We find that the MSF, that is the largest transverse Lyapunov exponent λ_{max} of the network, exhibits a generic behavior in a network of scalar time-delay systems. The λ_{max} possesses two finite crossings across the zero-axis as a function of the normalized coupling parameter, there by confirming the stable synchronization of the network of scalar time-delay systems in a finite range of coupling strength. We will demonstrate similar behavior of the MSF in networks of four different scalar time-delay systems that have been widely used in synchronization studies, allowing for universal classification of the MSF for networks of scalar time-delay systems with respect to their synchronization properties. This result ensures that one can analyze specific network topologies unambiguously using the eigenratio R, to characterize the synchronizability of a given network of scalar time-delay systems.

In Chapter 5, we will investigate the phenomenon of noise-enhanced phase synchronization (PS) in coupled time-delay systems, which usually exhibit non-phase-coherent attractors with complex topological properties. As a delay system is essentially an infinite dimensional in nature with multiple characteristic time scales, it is interesting and crucial to understand the interplay of noise and the time scales in achieving PS. In an unidirectionally coupled systems, the response system adjust all its time scales to that of the drive, whereas both subsystems adjust their rhythms to a single (main time scale of the uncoupled system) time scale in bidirectionally coupled systems. We have found similar effects for both a common and an independent additive Gaussian noise.

Finally, in Chapter 6, we will summarize briefly the results presented in the thesis. We will point out the possibility of extension of the synchronization studies to specific complex networks of low-dimensional dynamical systems described by ordinary differential equations with delay coupling and intrinsic time-delay systems described by delay differential equations including the interplay of various factors of topology and different types of delays in the coupling.

2 Delay effect on synchronization in networks of chaotic dynamical systems

2.1 Introduction

Understanding the dynamics of collective behaviors of networks or ensembles of oscillators is continued to be an area of active research in view of their potential applications in various fields of science and technology. Examples include self-organization of flock of birds, animal gaits, coherent neural oscillations, laser arrays, etc., [Winfree, 1980, Kuramoto, 1984, Pikovsky et al., 2001, Wu, 2007, Boccaletti et al., 2002, 2006, Arenas et al., 2008, Reddy et al., 1998, Schuster and Wagner, 1989, Koseska et al., 1998, Abrams and Strogatz, 2004, Sethia et al., 2008, Prasad et al., 2006, Atay et al., 2004, Masoller and Marti, 2005]. In addition to facilitating analytical/semi-analytical treatment, a network of oscillators can also exhibit plethora of rich dynamical behaviors, such as multistable states [Schuster and Wagner, 1989, Koseska et al., 1998], amplitude death [Reddy et al., 1998], chimera states [Abrams and Strogatz, 2004, Sethia et al., 2008], phase-flip [Prasad et al., 2006] and Neimark-sacker [Atay et al., 2004] type bifurcations, which the individual units are incapable of producing in isolation. In particular, as pointed out in Chapter 1, synchronization of a network of dynamical systems is a fundamental nonlinear phenomenon observed in diverse natural systems [Pikovsky et al., 2001, Wu, 2007, Boccaletti et al., 2002, 2006, Arenas et al., 2008]. Recent investigations on synchronization is focused on nontrivial effects of delay coupling due to a finite propagation time of information transfer in communication channels [Atay et al., 2004, Masoller and Marti, 2005, Fischer et al., 2006, Li et al., 2007, Wang et al., 2008, Ponce et al., 2009, Masoller and Atay, 2011, Earl and Strogatz, 2003, Kozyreff et al., 2000, Dhamala et al., 2004, Kinzel et al., 2009, Choe et al., 2010, Flunkert et al., 2010, Englert et al., 2011]. It has been shown that delay coupling enhances the synchronizability of networks and interestingly leads to the emergence of a wide range of new collective behavior [Atay et al., 2004, Masoller and Marti, 2005]. Further, it has also been shown that connection delays can actually be conductive to synchronization, so that it is possible for the delayed system to synchronize where the undelayed system does not [Atay et al., 2004].

The master stability formalism have been widely employed in probing the stability of synchronization from regular to complex networks [Arenas et al., 2008, Pikovsky et al., 2001, Boccaletti et al., 2002] as pointed out in the Sec. 1.3.2 of the introduction. Despite the enormous literature on the framework of the master stability formalism on networks of dynamical systems with instantaneous coupling, only a very few recent investigations have employed this framework in investigating the stability of synchroniza-

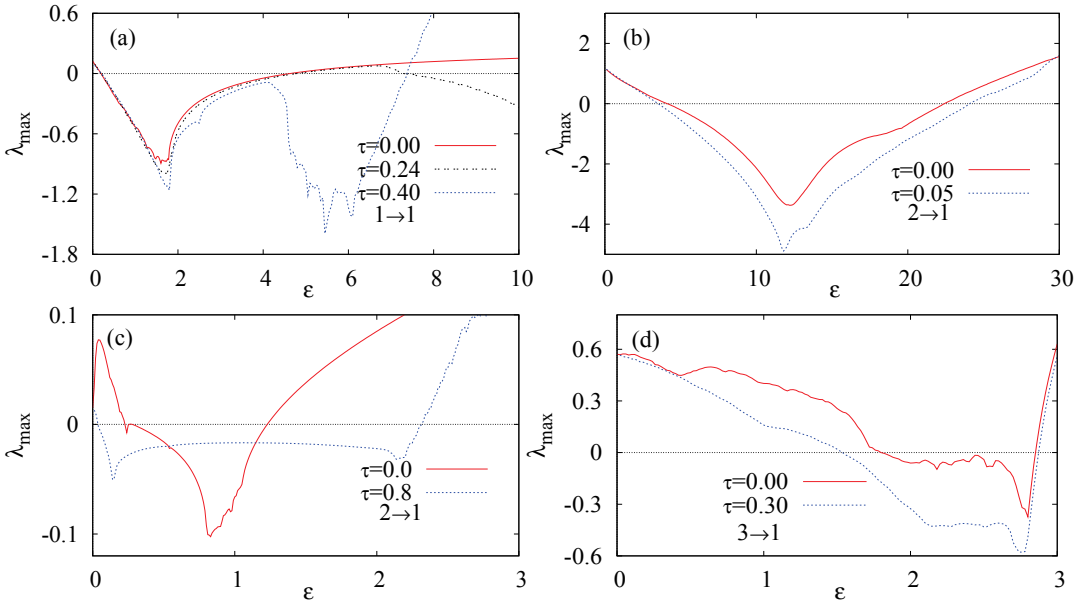

Figure 2.1: The largest transverse Lyapunov exponents λ_{max} of the master stability function (2.2) of a delay coupled network as a function of the normalized coupling parameter ε for different values of the coupling delay τ. The notation $i \rightarrow j$ indicates the coupling as being from ith component of one oscillator to the jth component of another one. (a) Rössler system as nodes with $\tau = 0.0, 0.24$ and 0.4, (b) Lorenz system as nodes with $\tau = 0.0$ and 0.05, (c) HR neurons as nodes with $\tau = 0.0$ and 0.8 and (d) Chua's circuit system as nodes with $\tau = 0.0$ and 0.3.

tion in delay-coupled networks [Dhamala et al., 2004, Flunkert et al., 2010, Kinzel et al., 2009], where the analyses are even restricted to either map or phase oscillators except in Ref. [Dhamala et al., 2004]. Nevertheless, the authors of Ref. [Dhamala et al., 2004] admitted that their analysis could not establish stable synchronized states in the master stability surface of the network of delay coupled HR neurons (please refer to Sec. 1.4.1 for some discussions on the important results of Ref. [Dhamala et al., 2004]). Hence, the master stability formalism has not yet been successfully employed in determining the stability of delay coupled networks of time continuous dynamical systems.

In this chapter, we aim at filling void in the literature by analyzing an arbitrary delay coupled network using the master stability formalism discussed in Sec. 1.3.2 of the introduction. In particular, we find that the maximal transverse Lyapunov exponent, estimated from the master stability equation using the framework of the master stability formalism, displays an extended regime of a stable synchronized state as a function of the coupling strength for appropriate values of the delay coupling resulting in delay-enhanced synchronization. In addition, we also find that the delay in the coupling can induce synchronization in certain coupling configurations, which does not show any syn-

chronized behavior without delay, elucidating delay-induced synchronization. Further, the stable synchronous state is achieved even at smaller values of the coupling strength with delay, which is actually attained at larger coupling strength without delay in the coupling. We will also illustrate the stable synchronized state in the master stability surface (MSF), i.e. the maximal transverse Lyapunov exponent of the master stability equation, of the delay coupled network. We demonstrate our results using several paradigmatic models.

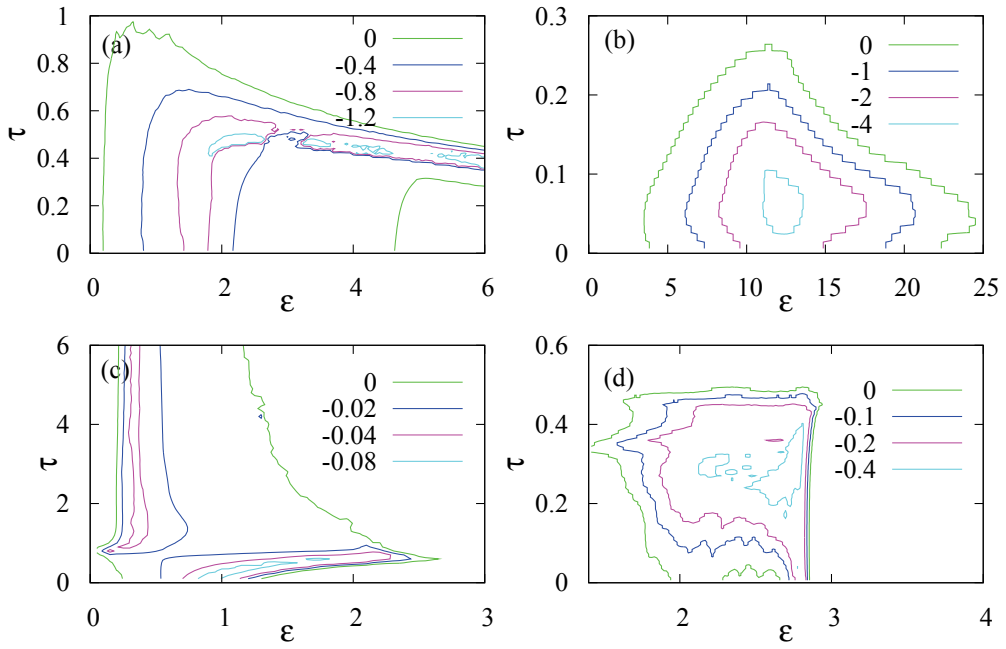

Figure 2.2: Contours of the largest transverse Lyapunov exponent λ_{max} in the real plane of the master stability function (2.2) as a function of ε and the coupling delay τ. (a) $x \to x$ coupled Rössler systems, (b) $y \to x$ coupled Lorenz systems, (c) $y \to x$ coupled Hindmarsh-Rose neurons and (d) $z \to x$ coupled Chua's circuit systems. Contours correspond to different values of λ_{max} encompassing the stable synchronous states.

2.2 Master stability formalism for a delay coupled network

We consider an arbitrary undirected delay coupled network with N identical chaotic units, whose equation of motion is represented as follows:

$$\dot{X}_i(t) = F\left[X_i(t)\right] - \sigma \sum_{j=1}^{N} g_{ij} h\left[X_j(t-\tau)\right], \tag{2.1}$$

where $X_i \in \mathbb{R}^m, i = 1, \ldots, N$, F is a nonlinear function describing the dynamics of the individual units, σ is the overall coupling strength, $G = g_{ij}$ is a $N \times N$ matrix, which determines the topology of an arbitrary network, h is a coupling function and τ is the coupling delay. Note that when we set the connection delay $\tau = 0$ in the above equation, then it is identical to the arbitrary network with instantaneous coupling given by Eq. (1.12). The identical evolution of the network of coupled systems in the synchronization manifold, that is $X_1(t) = X_2(t) = X_N(t) = X_s(t)$ (invariant synchronization manifold), is assured by the requirement of the row sum $\sum_{j=1}^{N} g_{ij}$ to be the same for each row. We consider the constant row sum to be $\sum_{j=1}^{N} g_{ij} = 0 \ \forall \ i$. Now, $X_s(t)$ is a solution of the uncoupled original dynamical system $\dot{X} = F(X)$. If G is diagonalizable, then the stability of the synchronization manifold is governed by the eigenvalues of G and the following block diagonalized variational equation for the transverse modes

$$\dot{\xi}(t) = DF\left[X_s(t)\right]\xi(t) - \varepsilon Dh\left[X_s(t-\tau)\right]\xi(t-\tau). \tag{2.2}$$

where $\xi(t)$ is a m-dimensional perturbation transverse to the synchronization manifold, which may be complex, $X_s(t)$ is the dynamics within the synchronization manifold, $DF\left[X_s(t)\right]$ is the Jacobian evaluated on the synchronization manifold and $Dh\left[X_s(t-\tau)\right]$ is an $m \times m$ matrix that determines which components of the oscillator are coupled. The normalized coupling parameter $\varepsilon = \sigma\gamma_k$, where γ_k is an eigenvalue of the coupling matrix G, $k = 0, 1, 2, \ldots, N-1$. It is to be noted that the eigenvalue γ_k is more generic because of the arbitrary G and it could be the eigenvalue corresponding to any specific topology determined by G. The synchronized state is stable only when all the $N-1$ eigenvalues, $\gamma_k, k = 1, 2, \ldots, N-1$, of the eigenmodes transverse to the synchronization manifold are negative. The eigenvalue γ_0 for $k = 0$ is associated with the perturbations within the synchronization manifold. Hence, the stability of the synchronized state of a given network topology is assured by the negative value of the largest transverse Lyapunov exponent, $\lambda_{max}(\varepsilon) < 0$, of the variational equations (2.2), which is referred to as the master stability function (MSF).

Considering the fact that G could have complex eigenvalues arising from asymmetric couplings [Fink et al., 2000], the generic variational equation, that is the MSF, can be written as

$$\dot{\xi}(t) = DF\left[X_s(t)\right]\xi(t) + (\alpha + i\beta)Dh\left[X_s(t-\tau)\right]\xi(t-\tau), \tag{2.3}$$

where, α and β are the real and imaginary parts of the eigenvalue. Separating $\xi(t)$ into

the real part $\xi_r(t)$ and the imaginary part $\xi_i(t)$, we get

$$\begin{aligned}\dot{\xi}_r(t) = &DF\left[X_s(t)\right]\xi_r(t) + \alpha Dh\left[X_s(t-\tau)\right]\xi_r(t-\tau) \\ &- \beta Dh\left[X_s(t-\tau)\right]\xi_i(t-\tau), \qquad (2.4a)\\ \dot{\xi}_i(t) = &DF\left[X_s(t)\right]\xi_i(t) + \alpha Dh\left[X_s(t-\tau)\right]\xi_i(t-\tau) \\ &+ \beta Dh\left[X_s(t-\tau)\right]\xi_r(t-\tau). \qquad (2.4b)\end{aligned}$$

The maximal transverse Lyapunov exponent (λ_{max}) estimated from Eqs. (2.4) yields a complex surface in the (α, β) plane, namely the master stability surface of the considered network of oscillators. For a given value of the coupling strength σ and the delay time τ, one can locate a point in the complex surface and the sign of λ_{max} at that point determines the stability of the synchronization manifold. When the coupling delay is zero ($\tau = 0$), then both the master stability equations (2.3) and (2.4) are identical to the generic variational equations (1.17) and (1.18) in real and imaginary space, respectively.

2.3 Delay-enhanced stable synchronization

Recently, Huang et al [Huang et al., 2009] classified the typical behaviors of MSFs into four categories by examining all possible one-component linear coupling configurations in several prototype three-dimensional systems as already pointed out in Sec. 1.3.5 of the introduction. It is to be noted that the x-component coupling in most of the dynamical systems tends the network to remain synchronized with a single crossing of the maximal transverse Lyapunov exponent with the zero-axis from positive. We recall that, according to their classification, the λ_{max} of class Γ_2 possesses two successive crossings with the zero-axis in a finite interval of the normalized coupling strength $\varepsilon \in (\varepsilon_1, \varepsilon_2)$ indicating a finite range of the stable synchronized state. Dynamical systems with different component couplings fall under different classes [Huang et al., 2009].

To demonstrate the existence of the extended regime of the stable synchronous state of a delay coupled network, i.e. delay-enhanced synchronization, it would be convenient if the original stable synchronized regime of the network without delay is limited within a finite range of the normalized coupling parameter ε. Therefore, we stick to the appropriate component couplings that are classified under the class Γ_2 for the following paradigmatic models that have been widely exploited in synchronization studies.

Now, we demonstrate our results by estimating the largest transverse Lyapunov exponent of the master stability equation (2.2) and (2.4) in both real axis and complex (α, β) planes, respectively. Numerical integrations were made by a Runge-Kutta 4th order routine with an integration step size of 0.01 and the transverse Lyapunov exponents are estimated using the algorithm of J. D. Farmer [Farmer, 1982] for time-delay systems after leaving 10^6 steps as transient, throughout this thesis.

2.3.1 Delay-enhanced Synchronization in a network of Rössler system

First, we consider the paradigmatic Rössler system governed by the equation of motions [Pecora and Carroll, 1998, Rössler, 1976, Huang et al., 2009]

$$\begin{aligned}\dot{x} &= -y - z,\\ \dot{y} &= x + 0.2y,\\ \dot{z} &= 0.2 + z(x - 9.0),\end{aligned}$$

with $x \to x$ component coupling in the network (2.1), which has a finite range of stable synchronization as a function of the normalized coupling strength as we will discuss below.

The largest transverse Lyapunov exponent λ_{max} corresponding to the master stability equation (2.2) of the delay coupled network with the Rössler system as nodes is depicted in Fig. 2.1(a) for three different values of the coupling delay τ. In the absence of the coupling delay, $\tau = 0$, the stable synchronous state exists only in the range of $\varepsilon \in (0.18, 4.61)$ as indicated by the sign of the λ_{max} (see Fig. 2.1(a)). As the coupling delay is increased, the stable synchronous regime is gradually extended in the ε parameter space up to a certain threshold. Further increase in it leads to decrease in the regime of a stable synchronous oscillations of the delay coupled network (see Figs. 2.2). In particular, for $\tau = 0.24$ in the coupling, λ_{max} has a second stable regime for $\varepsilon > 7.38$ and for $\tau = 0.4$ there exists only one single stable synchronous regime but extended in the range of $\varepsilon \in (0.18, 7.38)$, which is almost twice compared to that without delay [Shrii et al., 2012a].

In order to understand the effect of delay coupling in the network of Rössler systems more clearly, we have shown λ_{max} as a function of $\varepsilon \in (0, 6)$ and the coupling delay $\tau \in (0, 1)$ in Fig. 2.2(a). Contours in this figure correspond to different values of λ_{max}. It is evident from this figure that as the coupling delay is increased from zero, the stable synchronous regime increases slowly towards the larger coupling strength up to a certain threshold as indicated by the contour corresponding to $\lambda_{max} = 0$. This confirms the extension of the interval of the stable synchronous state induced by the coupling delay. Further increase in the delay leads to decrease in the regime of a stable synchronous state as indicated by the contour of $\lambda_{max} = 0$. Closer examination of the contour corresponding to $\lambda_{max} = 0$ in the range of coupling delay $\tau \in (0.1, 0.2)$ clearly indicates that the stable synchronous state occurs even for smaller values of ε in a narrow range in the presence of coupling delay. Nevertheless, the networks of Lorenz systems, HR neurons and Chua's circuit systems display more pronounced extended regime of stable synchronous state towards smaller coupling strengths (see Figs. 2.1), which is indeed attained for larger ε without delay in the network.

The stability issue of the synchronized state of the arbitrary network (2.1) is reduced to that of the block diagonalized variational equation, (2.2), for the transverse modes such that the sign of the largest Lyapunov exponent determines the stability. As the form of each block is the same with only the scalar multiplier $\varepsilon = \sigma\gamma_k$ differing for each [Pecora and Carroll, 1998] and hence it is straightforward to obtain a scaling rela-

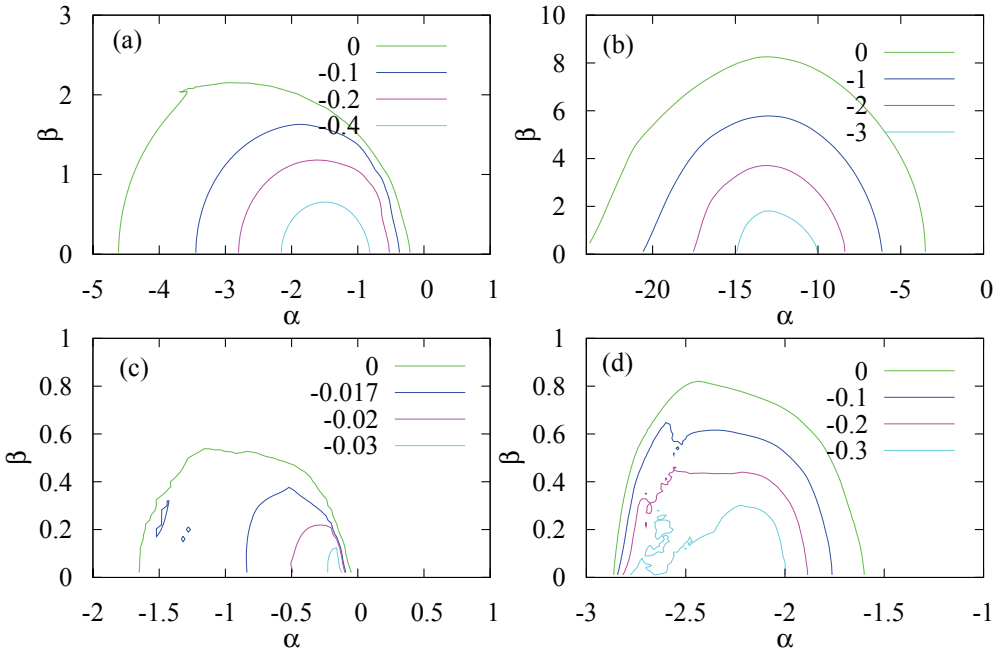

Figure 2.3: Contours of the largest transverse Lyapunov exponent λ_{max} in the complex plane of the master stability equation (2.4). (a) $x \to x$ coupled Rössler systems with $\tau = 0.24$, (b) $y \to x$ coupled Lorenz systems with $\tau = 0.05$, (c) $y \to x$ coupled Hindmarsh-Rose neurons systems with $\tau = 4.0$ and (d) $z \to x$ coupled Chua's circuit systems with $\tau = 0.3$. Contours encompasses the stable synchronous states.

tion between the eigenmodes of the connectivity matrix G. Further, one can estimate the maximal number of synchronized oscillators, N_{max}, of the network from the scaling relation in analogy with the one derived for a lattice [Heagy et al., 1995]. However, it is to be noted that the scaling relation facilitates the estimation of N_{max} only from the explicit knowledge of the eigenvalues γ_k in terms of trigonometric functions and hence the estimation of N_{max} is restricted rather to regular networks, whereas for more complex networks it remains an open problem. As N_{max} in the regular networks depends solely on ε at the two successive zero crossings of λ_{max}, namely ε_1 and ε_2. Increase in the interval between ε_1 and ε_2 reflects in increase in the N_{max} [Pecora and Carroll, 1998, Heagy et al., 1995]. As a consequence, the extended regime of a stable synchronized state as a function of ε in the delay coupled network of Rössler systems facilitates an increase in the N_{max} when compared to the same network without delay [Shrii et al., 2012a].

The largest transverse Lyapunov exponent of the MSF (2.4) for $x \to x$ coupled Rössler

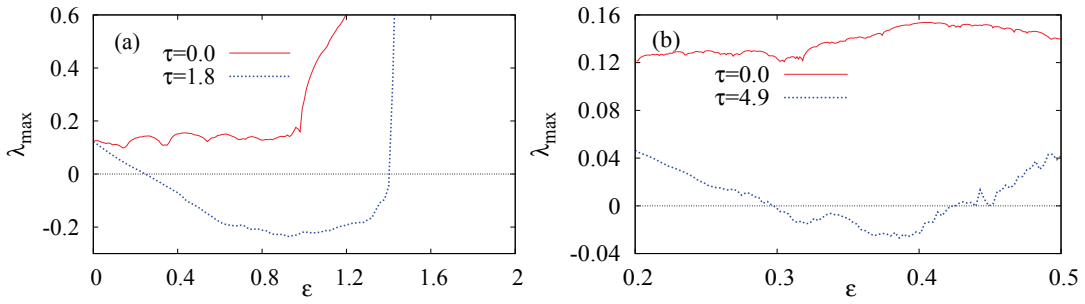

Figure 2.4: The largest transverse Lyapunov exponents λ_{max} of the MSF (2.2) of the delay-coupled network as a function of the normalized coupling parameter ε for different values of the delay τ in the coupling. (a) $x \to y$ coupled Rössler system for $\tau = 0.0$ and 1.8, and (b) $y \to x$ coupled Rössler system for $\tau = 0.0$ and 4.9.

systems is illustrated in the complex (α, β) plane in Fig. 2.3(a) for the value of the coupling delay $\tau = 0.24$. The contours encompasses the stable synchronous regimes corresponding to the negative values of λ_{max}. To the best of our knowledge, this is the first result showing stable synchronous states using the MSF of a delay coupled network of time continuous chaotic units. For $(\alpha, \beta) = (0, 0)$ in Eq. (2.4), then $\lambda_{max} > 0$ as the nodes evolve independently. Equations (2.4a) and (2.4b) become exactly the same as Eq. (2.2) for $\alpha < 0$ when $\beta = 0$ and the effect of coupling delay for this case is clearly illustrated in Figs. 2.1 and 2.2, and explained in appropriate places. The network does not synchronize at all for $\alpha > 0$. Increasing β in Eq. (2.4) for fixed α rotates the transverse modes as can be seen in Figs. 2.3 and hence the complex surface defining stability is symmetric along the real axis. Further, λ_{max} becomes positive for larger (or smaller) values of β beyond a certain threshold even if $\alpha < 0$ as depicted in Figs. 2.3 attributing to the fact that a large imaginary coupling can destabilize the system. In short, varying the real term in $\alpha + i\beta$ has the effect of damping the transverse perturbations to the synchronization manifold, whereas changes in the imaginary terms have a rotational effect between different transverse modes [Fink et al., 2000].

2.3.2 Delay-enhanced Synchronization in a network of Lorenz system

Now, we consider the network of $y \to x$ coupled Lorenz systems, whose node dynamics is represented by the equation of motions [Lorenz, 1963, Huang et al., 2009]

$$\begin{aligned} \dot{x} &= 10.0(x - y), \\ \dot{y} &= x(28.0 - z) - y, \\ \dot{z} &= xy - 2.0z \end{aligned}$$

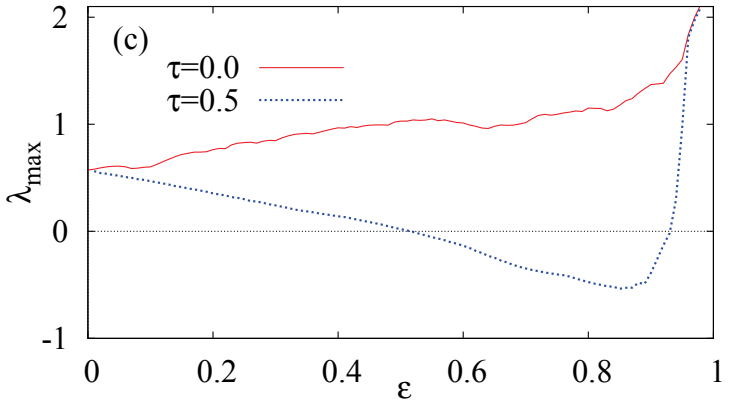

Figure 2.5: The largest transverse Lyapunov exponents λ_{max} of the MSF (2.2) of the delay-coupled network of $z \to y$ coupled Chua's circuit systems for $\tau = 0.0$ and 0.5 as a function of the normalized coupling parameter ε for different values of the delay τ in the coupling.

Figure 2.1(b) illustrates λ_{max} of the master stability equation (2.2) of a delay coupled network with the Lorenz systems as its nodes. λ_{max} depicts a finite regime of a stable synchronous chaos for the $y \to x$ coupled Lorenz systems in the range of $\varepsilon \in (4.17, 22.53)$ in the absence of delay coupling. On the other hand, the regime of a stable synchronized state is extended in both directions of the coupling strength in the range of $\varepsilon \in (3.51, 24.14)$ for $\tau = 0.05$ corroborating the extended regime of a stable synchronous states induced by the delay in the coupling. As a consequence, the number of synchronized oscillators in the delay coupled network is increased beyond that of the same network without delay. To elucidate this phenomenon of delay enhanced synchrony more clearly, λ_{max} is illustrated as contours in Fig. 2.2(b) as a function of $\varepsilon \in (0, 25)$ and $\tau \in (0, 0.3)$. The contour for $\lambda_{max} = 0$ confirms the above phenomenon up to a certain threshold value of τ and then the stable regime decreases with further increase in τ. The master stability surface of $y \to x$ coupled Lorenz systems is depicted in Fig. 2.3(b) for the coupling delay $\tau = 0.05$. Isocline lines of λ_{max} attributes to the stable synchronous state.

2.3.3 Delay-enhanced Synchronization in a network of Hindmarsh-Rose neurons

We consider HR neurons described by the equation of motions [Dhamala et al., 2004, Hindmarsh and Rose, 1984]

$$\dot{x} = y - x^3 + 3.0x^2 - z + 3.2, \tag{2.5a}$$
$$\dot{y} = 1.0 - 5.0x^2 - y, \tag{2.5b}$$
$$\dot{z} = 0.06(4.0(x + 1.6) - z). \tag{2.5c}$$

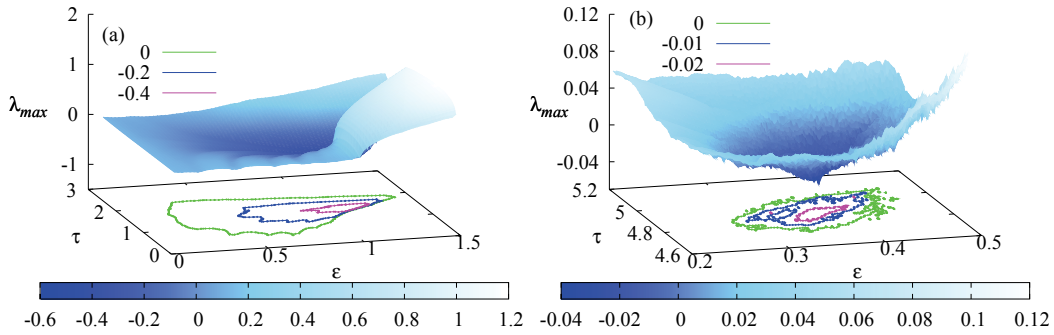

Figure 2.6: Surface of the largest transverse Lyapunov exponents λ_{max} as a function of the coupling delay τ and the normalized coupling parameter ε. An increase in the color density corresponds to a decrease in the value of λ_{max} and the contours encompasses the stable synchronized regime corresponding to $\lambda_{max} < 0$. (a) $x \to y$ coupled Rössler system, and (b) $y \to x$ coupled Rössler system.

with $y \to x$ coupling in the network (2.1) to investigate the effect of delay on its synchronization properties.

The master stability function of network of HR neurons, λ_{max} is depicted in Fig. 2.1(c). There exists a stable synchronized regime in the interval $\varepsilon \in (0.28, 1.23)$ for $\tau = 0.0$, whereas for $\tau = 0.8$ λ_{max} indeed shows a large regime of a stable synchronized state in the range $\varepsilon \in (0.036, 2.31)$ extended for both smaller and larger values of ε. It is a strong evidence that stable synchronization can occur even for smaller values of the coupling strength in the presence of the coupling delay, which is obtained only for sufficiently larger values of ε without delay in the same network. N_{max} can also be increased proportionally as discussed above. Further, the isocline line corresponding to $\lambda_{max} = 0$ as a function of $\varepsilon \in (0, 3)$ and $\tau \in (0, 6)$ in Fig. 2.2(c) also confirms the extended regime of a stable synchronized state, compared to that for $\tau = 0$, almost in the entire range of the coupling delay we have considered. Contours of λ_{max} estimated from (2.4) for $y \to x$ coupled HR neurons depicted in Fig. 2.3(c) clearly delineate the stable synchronous regimes in the complex plane of the MSF for the coupling delay $\tau = 4.0$.

2.3.4 Delay-enhanced Synchronization in a network of Chua's circuit systems

As a final example of delay-enhances synchronization, we consider a network of $z \to x$ coupled Chua's circuit systems, with the node dynamics given by the equation of

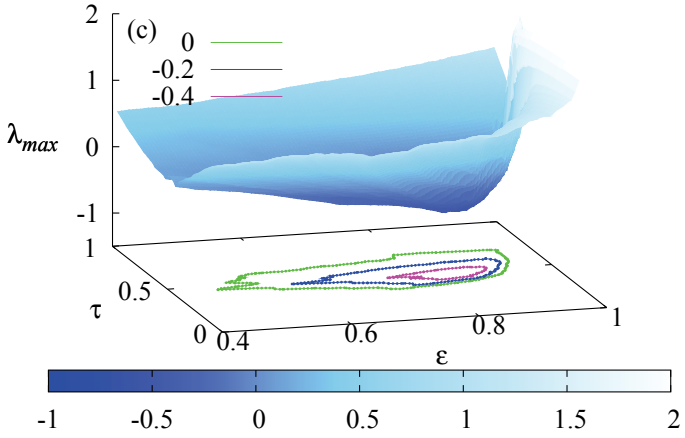

Figure 2.7: Surface of the largest transverse Lyapunov exponents λ_{max} as a function of the coupling delay τ and the normalized coupling parameter ε for $z \to y$ coupled Chua's circuit systems. An increase in the color density corresponds to a decrease in the value of λ_{max} and the contours encompasses the stable synchronized regime corresponding to $\lambda_{max} < 0$.

motions [Matsumoto et al., 1985, Chua et al., 1987, Madan, 1996]

$$\begin{aligned}\dot{x} &= 10.0(y - x + f(x)),\\ \dot{y} &= x - y + z,\\ \dot{z} &= -14.87y.\end{aligned}$$

Here, the piecewise linear function $f(x)$ is given by

$$f(x) = \begin{cases} -bx - a + b & x > 1,\\ -ax & |x| < 1,\\ -bx + a - b & x < -1,\end{cases} \tag{2.6}$$

where $a = -1.27$ and $b = -0.68$.

Figure 2.1(d) depicts λ_{max} of $z \to x$ coupled network of Chua's circuit systems illustrating stable synchronization in the interval $\varepsilon \in (1.84, 2.85)$ in the absence of delay in the coupling. On the other hand for appropriate delay in the coupling, that is for $\tau = 0.3$, λ_{max} in Fig. 2.1(d) confirms the phenomenon of delay enhanced synchrony by extending the stable synchronization to the interval $\varepsilon \in (1.52, 2.88)$. The contour for $\lambda_{max} = 0$ in Fig. 2.2(d) confirms the above phenomenon. Further, the isocline line of λ_{max} (see Fig. 2.3(d)) estimated from (2.4) for $z \to x$ coupled network of Chua's circuit systems in the complex plane also corroborates the existence of stable synchronization.

Thus, we have demonstrated the existence of an extended regime of stable synchronized states at both smaller and larger values of the coupling strength in an arbitrary network induced by the coupling delay using the framework of the master stability formalism. The generic nature of our results is also exhibited using four paradigmatic models that have been widely exploited in the literature for synchronization studies.

2.4 Delay-induced synchronization

In this section, we demonstrate the phenomenon of delay-induced synchronization, that is inducing synchronization where there is no synchronization at all without time-delay, in an arbitrary network again using the master stability formalism. In order to demonstrate the phenomenon of delay-induced synchronization, we consider the different component coupling that comes under the class Γ_0, according to the classification by Huang *etal.* [Huang et al., 2009], which does not exhibit any synchronization at all. In the following we demonstrate delay-induced synchronization in an arbitrary network of $x \to y$ and $y \to x$ coupled Rössler systems and $z \to y$ coupled Chua's circuit systems [Shrii et al., 2012b].

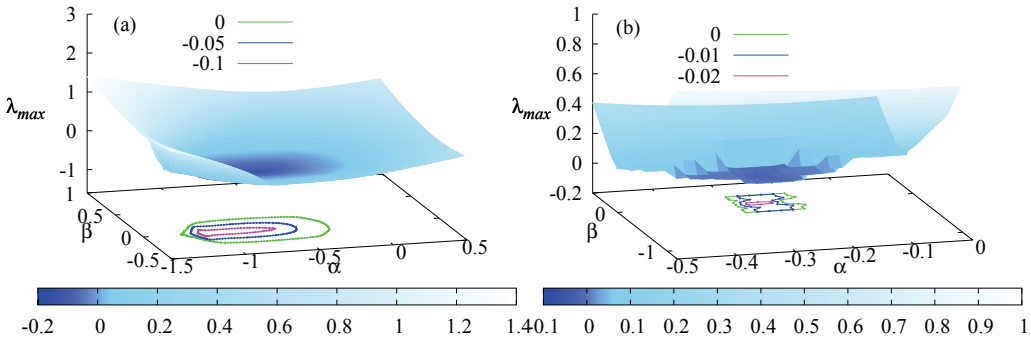

Figure 2.8: Master stability surface of the delay-coupled network. An increase in the color density corresponds to a decrease in the value of λ_{max} and the contours encompasses the stable synchronized regime corresponding to $\lambda_{max} < 0$. (a) $x \to y$ coupled Rössler system for $\tau = 1.8$, and (b) $y \to x$ coupled Rössler system for $\tau = 4.9$.

2.4.1 Delay-induced Synchronization in a network of Rössler systems

Now, we consider the network of $x \to y$ coupled Rössler systems and the largest transverse Lyapunov exponent, estimated from Eq. (2.2), depicted in Fig. 2.4(a) for $\tau = 0$ indicates that the network is in an asynchronous state as $\lambda_{max} > 0$ in the entire range of ε. In contrast, in the presence of a delay under the same coupling, the network of

Rössler systems is entrained to synchronous oscillations as confirmed by the sign of λ_{max} in Fig. 2.4(a) for $\tau = 1.8$ attributing to the phenomenon of delay-induced synchronization in the network. The effect of delay coupling can be better understood from Fig. 2.6(a), where λ_{max} is shown as a surface in the (τ, ε) plane. An increase in the color intensity corresponds to a decrease in λ_{max} and the isoclinic lines encompasses the stable synchronous regime corresponding to $\lambda_{max} < 0$. It is evident from Fig. 2.6(a) that without delay in the coupling the network of Rössler systems does not exhibit any synchronous oscillation. On the other hand, as τ is increased the network attains synchronization after an appreciable delay and the range of stable synchronization increases with it up to a certain threshold. Further increase in the delay results in a decrease in the spread of stable synchronization and finally reaches asynchronization for further larger delays. The corresponding master stability surface, i.e. the surface of λ_{max} in the complex (α, β) plane, estimated from the MSF (2.4) is illustrated in Fig. 2.8(a) for the coupling delay $\tau = 1.8$, in which the stable regimes are displayed by the contours of $\lambda_{max} < 0$.

A similar result is also observed for another choice of the delayed coupling, namely $y \to x$. The sign of λ_{max} (see Fig. 2.4(b)) as a function of ε for both with and without delay in the coupling asserts the phenomenon of delay-induced synchronization in the network of Rössler systems. The surface of λ_{max} in Fig. 2.6(b) and its contours for $\lambda_{max} < 0$ clearly illustrate the above phenomenon. Further, the complex (α, β) plane of the MSF in Fig. 2.8(b) for $\tau = 4.9$ with $\lambda_{max} < 0$ confirms the same.

2.4.2 Delay-induced Synchronization in a network of Chua's circuit systems

Next, we consider the network of $z \to y$ coupled Chua's circuit systems. Without any delay in the coupling λ_{max} remains positive in Fig. 2.5 attributing to asynchronization, whereas for the value of delay $\tau = 0.5$, $\lambda_{max} < 0$ in the range $\varepsilon \in (0.5, 0.93)$ corroborating the phenomenon of delay-induced synchronization. Further, this phenomenon is also confirmed from the contours of $\lambda_{max} < 0$ in the surface plot of λ_{max} depicted in Fig. 2.7 as a function of τ and ε. The corresponding master stability surface, estimated from the MSF (2.4) is illustrated in Fig. 2.9 for the coupling delay $\tau = 0.5$, in which the stable regimes are displayed by the contours of $\lambda_{max} < 0$.

By exploiting the framework of the master stability formalism in investigating stable synchronization in an arbitrary delay-coupled network, we have demonstrated the phenonemon of delay-induced synchronization in paradigmatic models of Rössler and Chua's circuit systems.

2.5 Conclusion

We have investigated the phenomena of delay-enhanced and delay-induced stable synchronization in an arbitrary delay coupled network using the framework of the master stability formalism. We have demonstrated that there always exist an extended regime of stable synchronous state as a function of coupling strength for appropriate coupling delays, which cannot be observed without any delay in the coupling. In addition, we have also shown that the delayed coupling can induce stable synchronization to a large

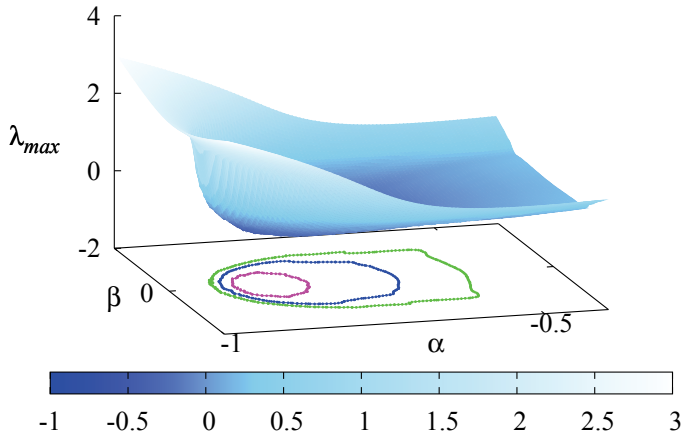

Figure 2.9: Master stability surface of the $z \to y$ delay-coupled network of Chua's circuit systems for $\tau = 0.5$. An increase in the color density corresponds to a decrease in the value of λ_{max} and the contours encompasses the stable synchronized regime corresponding to $\lambda_{max} < 0$.

parameter range in certain coupling configurations, where there is no synchronization at all. Further, the stable synchronous state is achieved even at smaller values of coupling strength with delay, which is actually attained at larger coupling strength without delay. Furthermore, the contours of the largest transverse Lyapunov exponent in the complex plane corresponding to the MSF of the delay coupled network clearly demarcates the stable synchronous state from the unstable ones. The generic nature of our results is also corroborated using four paradigmatic models, namely, Rössler, Lorenz systems, Hindmarsh-Rose neurons and Chua's circuit systems as nodes of the network, that have been widely exploited in the literature for synchronization studies.

3 Effect of partial delay on synchronization of neuronal networks

3.1 Introduction

In continuation of our work on the influence of connection delay in coupled networks of nonlinear dynamical systems, we propose a partial delay coupling in this chapter and investigate its effect on the synchronizability of a network of chaotic dynamical systems. In this, chapter we focus mainly on Hindmarsh-Rose (HR) neurons [Hindmarsh and Rose, 1984] as nodes of the network to illustrate our results. Earlier works on synchronization has considered only instantaneous coupling for the ease of analytical treatment and experimental realizations [Pikovsky et al., 2001, Boccaletti et al., 2002, Arenas et al., 2008]. Later, realizing the importance of delay arising from the finite time required by the propagation of signals among interacting dynamical units in many natural systems [Dhamala et al., 2004, Atay et al., 2004, Masoller and Marti, 2005] and the constructive role of connection delays in facilitating synchronization, despite our prior understanding that delayed flow of information does not favour synchronization, a flurry of research activities has been provoked in unveiling several fascinating features of the connection delay including delay-induced and delay-enhanced synchronization in networks of coupled dynamical systems [Soriano et al., 2013, Dhamala et al., 2004, Atay et al., 2004, Masoller and Marti, 2005, Fischer et al., 2006, Kozyreff et al., 2000, Flunkert et al., 2010, Kinzel et al., 2009, Shrii et al., 2012b,a, Lu et al., 2009, Stepan, 2009, Tang J. et al., 2011, Wang et al., 2008, 2011, Perez et al., 2011, Liang et al., 2009]. Furthermore, the trade-offs between several forms of delay coupling, for instance, discrete and distributed delays, and network architectures has also been largely investigated [Soriano et al., 2013, Dhamala et al., 2004, Atay et al., 2004, Masoller and Marti, 2005, Fischer et al., 2006, Kozyreff et al., 2000, Flunkert et al., 2010, Kinzel et al., 2009, Shrii et al., 2012b,a, Lu et al., 2009, Stepan, 2009, Tang J. et al., 2011, Wang et al., 2008, 2011, Perez et al., 2011, Liang et al., 2009].

Recent investigations in this line have been centered at understanding the role of connection delays and emergence of synchronization in coupled neuronal networks with difference architectures [Dhamala et al., 2004, Tang J. et al., 2011, Wang et al., 2008, 2011, Perez et al., 2011, Liang et al., 2009]. This is because of the natural coexistence of heterogeneous connection delays due to axons of different lengths and synchronous neural activity in the central nervous system. It is now known that axons can generate delays from a few millisecond to $300ms$ and the neuronal synchronization facilitates the information processing from different parts of the brain to induce coordination among different sensory organs [Shadlow, 1985]. In this connection, enhancement of neuronal

synchrony by delay coupling was shown in Ref. [Dhamala et al., 2004], the role of delay and diversity [Tang J. et al., 2011], effects of finite information transmission delay and rewiring probability [Wang et al., 2008] on synchronization transition in small-world neuronal network were investigated, delay effects on synchronization transitions in scale-free neuronal networks was reported in Ref. [Wang et al., 2011], effects of distributed time-delay on phase synchronization of inhibitory coupled neurons was considered in Ref. [Liang et al., 2009], effects of topology and delay interactions on synchronization of neuronal networks was examined in Ref. [Perez et al., 2011].

With one's common wisdom, it is easy to realize that either completely instantaneous or completely delay coupling are two limiting cases of a more realistic scenario: the presence of both instantaneous and delay couplings to execute a desirable task. In particular, memory effects of the medial temporal lobe, especially perirhinal cortex, is an essential feature to facilitate neural communication and to perform various cognitive process including, learning, reasoning, visual discrimination, etc [Fell and Axmacher, 2011, Shrager et al., 2008, Knuston A. R. et al., 2012]. Specifically, it is clearly understood that when the working memory capacity is exceeded then a successful implementation of cognitive processes depends at least in part on long-term memory [Knuston A. R. et al., 2012].

From a dynamical systems point of view, the working memory refers to instantaneous coupling and long-term memory naturally to the delay coupling. Recently, efforts have also been made in reducing the connection delays in networks by a selective time shift transformation that render the network dynamically equivalent to the actual network with completely delay connection [Luecken et al., 2012]. Hence, it is quite reasonable and important to understand the dynamics of neuronal networks with a combination of instantaneous coupling (working memory) and delay coupling (long-term memory) with certain weights to each, as the weights determine the proportion of both memories required for a specific task to be carried out by neuronal networks [Fell and Axmacher, 2011, Shrager et al., 2008, Knuston A. R. et al., 2012]. Such memory effects play a vital role in their evolutionary mechanisms and also quite common in nature, e. g., in physiology [Peng et al., 1993, Bunde et al., 2000], ecology [Izquierdo et al., 1998, Mery and Kawecki, 2005], epidemics [Ndungu et al., 2012] financial markets [Chow et al., 1995, Masih R. and Masih A. M. M., 2001] and climate dynamics [KoscielnyBunde et al., 1998, Kantelhardt et al., 2006, Lennartz et al., 2008].

In this chapter, we propose a partial delay coupling of the form $wx(t-\tau)+(1-w)x(t)$, where the weight w determines the proportion of instantaneous and delay couplings, and investigate effects of the partial delay on the synchronizability of networks of Hindmarsh-Rose (HR) neurons [Hindmarsh and Rose, 1984]. It is now known that completely delay coupled networks exhibit much richer synchronization properties in certain parameter space than the completely instantaneous coupled counterparts. In connection with this, one may intuitively think that partial delay coupling may result only in a weak effect of completely delay coupled networks. In contrast, we find that there exists stable synchronization in an enlarged range of parameter space for appropriate weights compared to either completely instantaneous or completely delay coupled neuronal networks. Further, we have also found that stable synchronization is achieved even for lower values

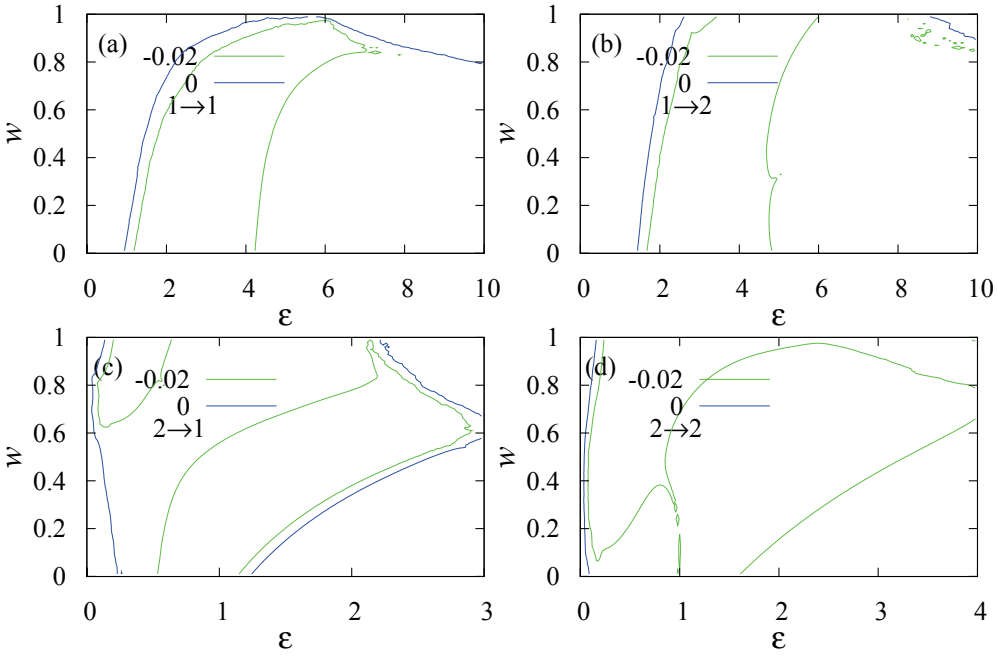

Figure 3.1: Contours of the largest transverse Lyapunov exponent λ_{max} of network of HR neurons as a function of the weight w in the partial delay coupling and the normalized coupling strength ε for the coupling delay $\tau = 1$. The notation $i \to j$ indicates the coupling as being from ith component of one oscillator to the jth component of another one.

of coupling strength for appropriate weights than in both limiting cases. Indeed, the proposed partial delay can induce synchronization, where there is no synchronization in either cases of completely instantaneous and completely delay coupling. Using the master stability formalism, we will estimate the largest transverse Lyapunov exponent of the variational equation corresponding to the largest transverse mode of an arbitrary neuronal network to determine the stable synchronized regime as a function of the weight w and the coupling strength ε to corroborate the above findings.

3.2 Stability of synchronization with partial delay coupling

We consider the following undirected, partially delay coupled network composed of N identical chaotic units with an arbitrary topology

$$\dot{X}_i(t) = F\left(X_i(t)\right) - \sigma \sum_{j=1}^{N} g_{ij} h\left(X_j(t), X_j(t-\tau)\right), \tag{3.1}$$

where $X_i \in \mathbb{R}^m, i = 1, \ldots, N$, F corresponds to the nonlinear vector function of the individual dynamical units, σ is the overall coupling strength, τ is the coupling delay, $G = g_{ij}$ is a $N \times N$ symmetric matrix determining the topology of an arbitrary network, that is, $g_{ij} = 1$ when i and j are connected otherwise $g_{ij} = 0$, while self connections are forbidden, $g_{ii} = 0$ and $h\left(X(t), X(t-\tau)\right)$ is a linear coupling function determining the nature of the coupling and the components in the coupling. It is to be noted that the dynamical equation of the network (3.1) is similar to the network equation (2.1) except for the nature of the coupling. For the proposed partial delay coupling, the coupling function h takes the form $h = wX(t-\tau)+(1-w)X(t)$ with the weight w determining the proportion of instantaneous and delay couplings. The limiting cases $w = 0$ corresponds to completely instantaneous coupling and $w = 1$ to completely delay coupling. For the intermediate values of w less than unity the coupling has linear combination of both instantaneous and delay components as its constituents. The invariant synchronization manifold is ensured by $\sum_{j=1}^{N} g_{ij} = 0 \; \forall \; i$. If the coupling matrix G is diagonalizable, then the master stability equation is deduced as [Pecora and Carroll, 1998]

$$\begin{aligned}\dot{\xi}(t) = &\left[DF\left(X_s(t)\right) - \varepsilon(1-w)Dh(X_s(t))\right]\xi(t) \\ &- \varepsilon\left[wDh(X_s(t-\tau))\right]\xi(t-\tau).\end{aligned} \tag{3.2}$$

Here, the description for all the notations remain the same as discussed in Sec. 2.2 on the master stability formalism for delay coupled network in Chapter 2.

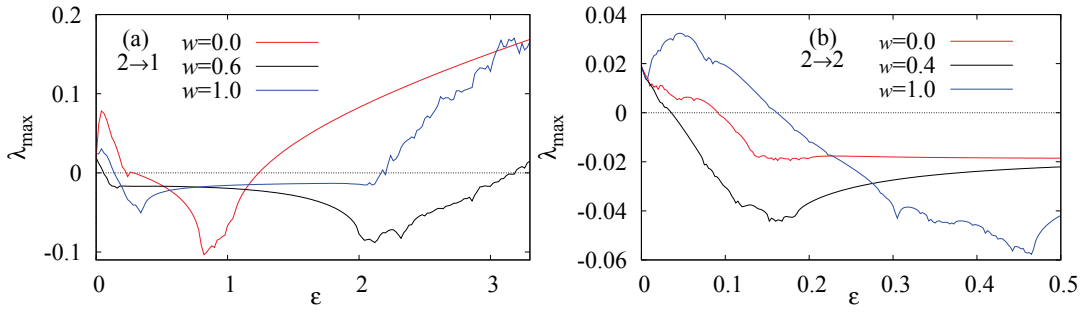

Figure 3.2: The largest transverse Lyapunov exponent λ_{max} of the network of HR neurons as a function of the normalized coupling strength ε for different values of the weight w, determining the nature of the coupling. (a) $y \to x$ coupling, and (b) $y \to y$ coupling.

Again, considering that G could have complex eigenvalues $\varepsilon = \sigma\gamma_k = -(\alpha + i\beta)$, if G is asymmetric, the master stability equation (3.2) for a network with the proposed partial delay coupling can be written as

$$\begin{aligned}\dot{\xi}(t) = &\left[DF + (\alpha + i\beta)(1-w)Dh\right]\xi(t) \\ &+ (\alpha + i\beta)\left[wDh\right]\xi(t-\tau),\end{aligned} \tag{3.3}$$

where, α and β are the real and imaginary parts of the eigenvalue. Separating $\xi(t)$ into the real part $\xi_r(t)$ and the imaginary part $\xi_i(t)$, we get

$$\dot{\xi_r}(t)\ [DF + \alpha(1-w)dh]\,\xi_r(t) - \beta(1-w)dh\xi_i(t) + \alpha w Dh\xi_r(t-\tau) - \beta w Dh\xi_i(t-\tau), \tag{3.4a}$$

$$\dot{\xi_i}(t)\ [DF + \alpha(1-w)dh]\,\xi_i(t) + \beta(1-w)dh\xi_r(t) + \alpha w Dh\xi_i(t-\tau) + \beta w Dh\xi_r(t-\tau). \tag{3.4b}$$

As we have discussed in the previous chapter, the largest transverse Lyapunov exponent, $\lambda_{max}(\alpha, \beta)$ of the above equations results in a surface in the complex (α, β) plane, the MSF of a given network of oscillators. For a specific value of the weight w, and the delay time τ, the value of the $\lambda_{max}(\alpha, \beta)$ in the complex surface determines the stability of the synchronized state.

3.3 Effect of partial delay in an arbitrary network of HR neurons

We consider the Hindmarsh-Rose neurons [Dhamala et al., 2004, Hindmarsh and Rose, 1984], designed to study the spiking-bursting behavior of the membrane potential observed in experiments made with a single neuron, in the network (3.1) with arbitrary topology. The equation of motions corresponding to the individual nodes dynamics are the same as in Eq. (2.5) of Sec. 2.3.3. We couple all the four possible combinations of the x and y-component coupling to unravel the effect of partial delay on the synchronizability of networks of HR neurons. Most of the earlier investigations on delay effects on completely delay coupled neuronal networks considered only $x \to x$ couplings [Dhamala et al., 2004, Stepan, 2009, Tang J. et al., 2011, Wang et al., 2008, 2011, Perez et al., 2011, Liang et al., 2009] and illustrated that connection delays enrich the synchronization properties of the networks for appropriate values of the delay. In our investigation, we have chosen the connection delays such that the delay in the $x \to x$ coupling does not show any enriched synchronizability for any combinations of weights including $w = 1$, where the network is completely delay coupled, and show that the other $(x \to y, y \to x, y \to y)$ coupling configurations induce enhanced regimes of stable synchronization in the network for a certain range of weight w as a function of the coupling strength ε. Further, the network is synchronized even for very low values of coupling strength for certain w when compared to completely instantaneous coupling for $w = 0$ and completely delay coupling for $w = 1$.

The largest transverse Lyapunov exponent λ_{max} corresponding to the largest transverse mode (3.2) for all the four possible combinations of x and y-component couplings is shown in Fig. 3.1 as a function of $w \in (0, 1)$ and ε. The value of the delay in the coupling is chosen as $\tau = 1$. The contours in the figure encloses the stable synchronization regime, where $\lambda_{max} < 0$. $x \to x$ coupled network of HR neurons is depicted in Fig. 3.1(a), where the completely delay coupling for $w = 1$ does not show any stable synchronization. The partial delay coupling for intermediate values of w less than unity but

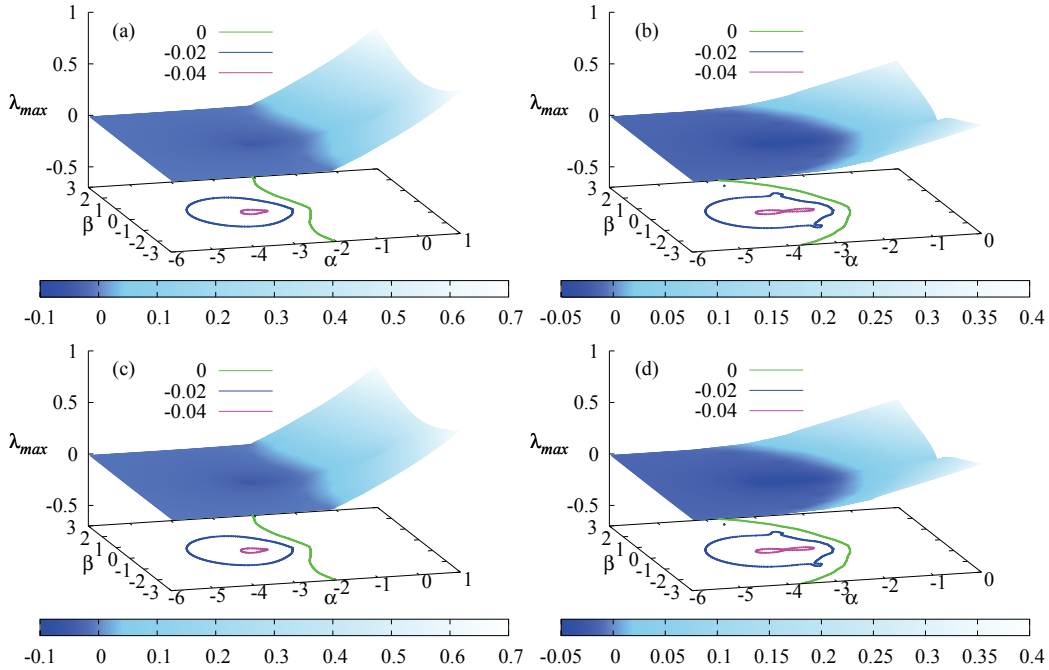

Figure 3.3: Master stability function, the surface of λ_{max} of a network of HR neurons with the partial delay coupling in the complex (α, β) plane corresponding to Fig. 3.1 for $w = 0.6$. The contours encloses the stable synchronization regimes for $\lambda_{max} < 0$.

greater than zero has stable synchronization but does not show any enhanced regime of stable synchronization compared to completely instantaneous coupling for $w = 0$. Similar results are observed for $x \to y$ coupled HR neurons for $\tau = 1$ (see Fig. 3.1(b)) even though it displays stable synchronization of $w = 1$. We will later show that for higher values of delay τ, $x \to y$ coupled HR neurons show better synchronizability for suitable values of w. The effect of partial delay is clearly seen in Fig. 3.1(c) for $y \to x$ coupled HR neurons. It is evident that upon increasing w from zero, the stable synchronization increases gradually and attains an extended range of stable synchronization for both lower and higher values of coupling strength for a certain range of w, illustrating the ability of partial delay coupling in enriching stable synchronization compared to that of the completely delay coupling.

To visualize the effect of partial delay more clearly, we have shown the largest transverse Lyapunov exponent for specific values of w in Fig. 3.2(a) as a function of ε. For $w = 0$, the completely instantaneous coupling exhibits stable synchronization only in a rather narrow range of coupling strength $\varepsilon \in (0.26, 1.24)$. For $w = 1$, the completely delay coupling shows an enlarged regime of stable synchronization in the range

$\varepsilon \in (0.14, 2.18)$ than that of $w = 0$. The effect of completely delay coupling in enhancing the stable synchronization for both lower and higher values of ε is also clearly evident. But the presence of partial delay outperforms the completely delay coupling for certain weights as illustrated for $w = 0.6$ in Fig. 3.2(a), depicting stable synchronization in a very broad range of $\varepsilon \in (0.06, 3.18)$. It is to be noted that synchronization is achieved even for very low values of the coupling strength when compared to either of the limiting cases.

The contours in the Fig. 3.1(d) depicts the stable synchronization regime for a $y \to y$ coupled network of HR neurons. Here, the contour indicates that synchronization is achieved almost in the entire range of w and ε. Nevertheless, synchronization is attained for lower values of coupling strength for appropriate weights w of the partial delay coupling compared to that of completely instantaneous or completely delay coupling. This is clearly shown in Fig. 3.2(b) as a function of ε for different values of w. For $w = 1$, the completely delay coupling induce synchronization only for $\varepsilon > 0.16$, where as for $w = 0$, the instantaneous coupling synchronizes the network for a lower coupling strength $\varepsilon = 0.091$. On the other hand, in the presence of partial delay coupling, the $y \to y$ coupled network of HR neurons synchronizes even for a very lower value of coupling strength $\varepsilon = 0.034$ compared to either cases. Thus, the partial delay facilitates synchronization even at very low coupling strengths than that of completely delay coupling, which may have relevance in the synchronization process among the neuronal network of cerebral cortex even for smaller electrical activity of neurons.

The master stability function, namely, the surface of λ_{max} characterizing the stable synchronization regime of $x \to x$, $x \to y$, $y \to x$, and $y \to y$ coupled network of HR neurons in the complex (α, β) plane is illustrated in Fig. 3.3(a-d), respectively, for the weight $w = 0.6$. The contours in the figures corresponding to $\lambda_{max} < 0$ encloses stable synchronization as a function of α and β.

Now, we increase the value of the delay in the coupling to $\tau = 5.0$ and illustrate the effect of partial delay coupling for higher values of delay in the coupling. The largest transverse Lyapunov exponent for the four possible combinations of x and y-component couplings is depicted in Fig. 3.4. For a higher value of τ, the $x \to x$ coupled HR neurons show stable synchronization in a narrow range of ε for completely delay coupling and less than that of instantaneous coupling (see Fig. 3.4(a)), while the partial delay does not have any effect as we have considered for $\tau = 1$. For $x \to y$ coupling, increasing w in the partial delay coupling from zero, the minimum value of ε necessary for stable synchronization is decreasing gradually until it reaches the value of unity as seen in Fig. 3.4(b). This again ascertains that the partial delay induces synchronization even for lower values of the coupling strength and at the same time it has an extended regime of stable synchronization compared to completely delay coupling. The effect of partial delay discussed above for $\tau = 1$ is preserved even for higher values of delay in the coupling for $y \to x$ and $y \to y$ coupled network of HR neurons as depicted in Figs. 3.4(c) and 3.4(d), respectively. The master stability function, the surface of λ_{max} in the complex (α, β) plane is shown in Fig. 3.5. For $x \to x$ and $x \to y$ coupling the surface of λ_{max} is shown in Figs. 3.5(a) and 3.5(b), respectively, for $w = 0.6$. For $y \to x$, MSF is depicted in Fig. 3.5(c) for $w = 0.4$ and for $y \to y$, MSF is illustrated in Fig. 3.5(d) for $w = 0.6$. The

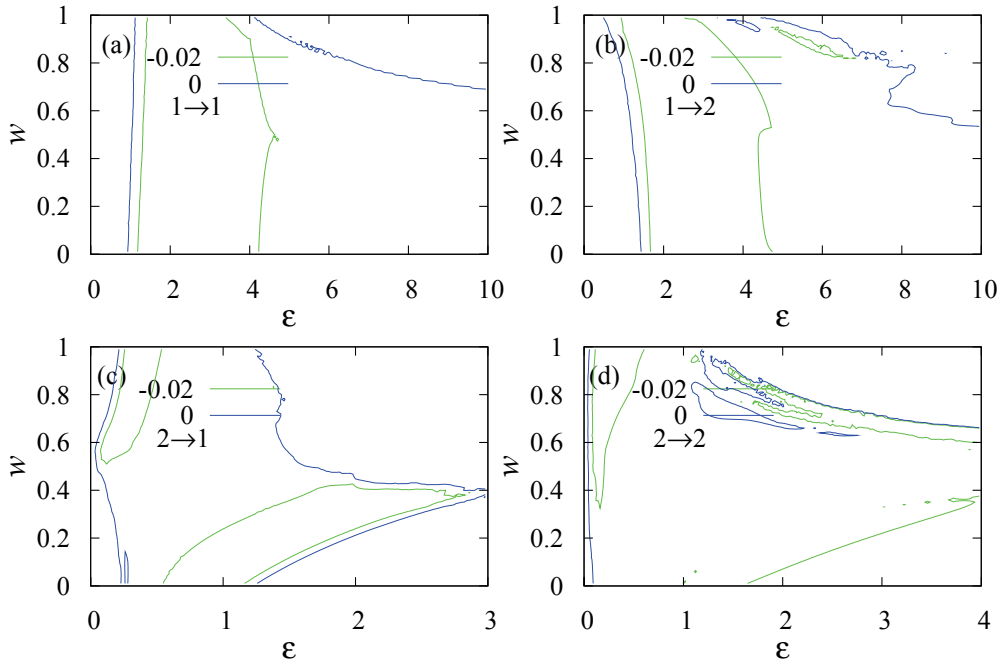

Figure 3.4: Contours of the largest transverse Lyapunov exponent λ_{max} of network of HR neurons as a function of the weight w in the partial delay coupling and the normalized coupling strength ε for the coupling delay $\tau = 5$.

contours in these figures indicate the regime of stable synchronization in the complex (α, β) plane.

3.4 Effect of partial delay in an arbitrary network of Rössler systems

We have also investigated the effect of partial delay coupling on the synchronizability of other chaotic dynamical systems and observed similar effects for appropriate weights determining the proportion of delay and instantaneous coupling. Further, the partial delay coupling induces synchronization for appropriate weights where there is no synchronization for either completely delay coupling or completely instantaneous coupling. For example, we consider the following chaotic Rössler systems [Rössler, 1976, Huang et al.,

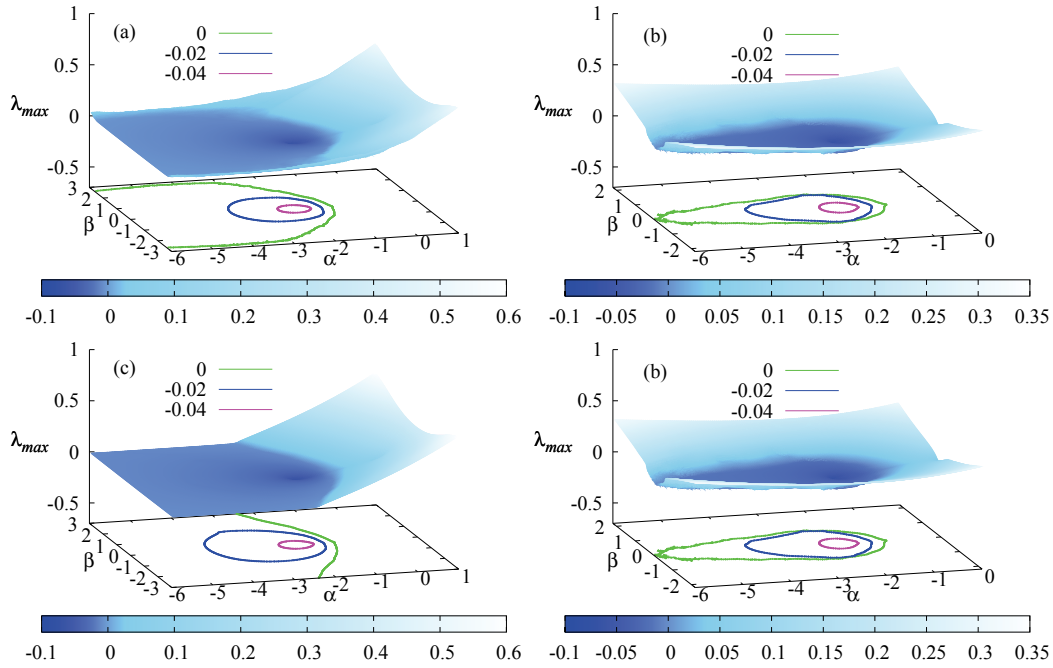

Figure 3.5: Master stability function, the surface of λ_{max} of network of HR neurons in the complex (α, β) plane corresponding to Fig. 3.4. The contours encloses the stable synchronization regimes for $\lambda_{max} < 0$. (a) $w = 0.6$, (b) $w = 0.6$, (c) $w = 0.4$ and (d) $= w = 0.6$.

2009]

$$\begin{aligned}\dot{x} &= -y - z,\\ \dot{y} &= x + 0.2y,\\ \dot{z} &= 0.2 + z(x - 9.0),\end{aligned}$$

in the arbitrary network (3.1) with $x \to x$ and $x \to y$ coupling alone for $\tau = 1$. The largest transverse Lyapunov exponent λ_{max} along with the contours enclosing the stable synchronization regimes is shown in Fig. 3.6. For $x \to x$ networks of Rössler systems, the completely delay coupling for $w = 1$ does not induce any synchronization at all (see Fig. 3.6(a)), whereas the partial delay coupling induces an extended regime of stable synchronization for appropriate weight w than the completely instantaneous coupling for $w = 0$. For $x \to y$ coupling, the network of Rössler systems is not synchronized for both completely delay and completely instantaneous coupling. On the other hand, the partial delay induces synchronization for appropriate w and ε as seen in Fig. 3.6(b).

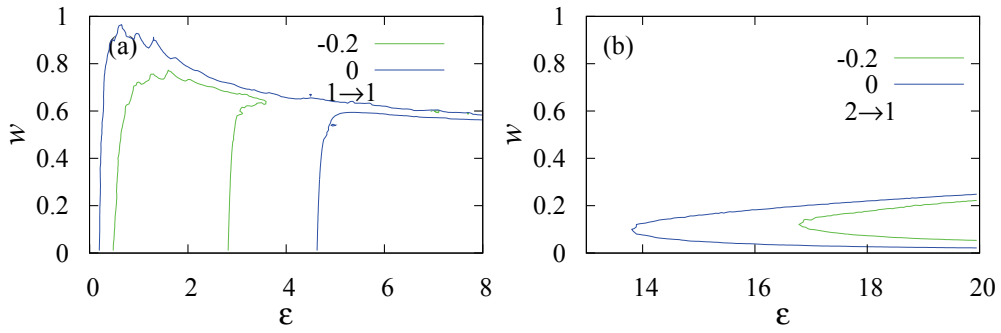

Figure 3.6: Contours of the largest transverse Lyapunov exponent λ_{max} of network of Rössler systems as a function of the weight w in the partial delay coupling and the normalized coupling strength ε for the coupling delay $\tau = 1$. (a) $x \to x$ coupling, and (b) $x \to y$ coupling.

3.5 Summary and conclusion

We have considered a partial delay coupling as a combination of both instantaneous coupling and delay coupling with a certain weight on each and investigated its effects on the synchronization properties of an arbitrary network of Hindmarsh-Rose (HR) neurons. In reality, either completely instantaneous coupling or completely delay coupling are the two limiting case that may occur rarely. In particular, the combined instantaneous and delay information transfer, referred to as working memory and long-term memory in cognitive science, is often emphasized as necessary for achieving several cognitive processes including, learning, reasoning, visual discrimination, etc [Fell and Axmacher, 2011, Shrager et al., 2008, Knuston A. R. et al., 2012]. We have shown that the partial delay coupling outperforms the completely delay coupling in inducing an extended regime of stable synchronization both at lower and higher values of coupling strength. We have also shown that the partial delay is capable of inducing synchronization where there is no synchronization in both the limiting cases. It is now understood that connection delays in networks tend to reduce local coordination of nodes to improve the global coordination [Wang et al., 2008, Hunt et al., 2010, Hod, 2010]. The presence of both the instantaneous and delay coupling with appropriate weights in the partial delay coupling may improve both the local and global coordination in achieving global synchronization for very low values of coupling strength. This effect of partial delay and the responsible mechanism needs much in-depth investigation as this will shed more light on our understanding of synchronization processes at various levels in cerebral cortex, pathological synchronization activity of neuronal network and their control mechanisms. We are also investigating the effect of partial delay coupling on various specific network topologies.

4 Stable synchronization in networks of intrinsic time-delay systems

4.1 Introduction

Investigations on synchronizing intrinsic time-delay systems have been an active area of research for more than a decade in view of its potential applications. Intrinsic time-delay systems described by delay differential equations [Senthilkumar and Lakshmanan, 2011, Erneux, 2009, Gopalsamy, 1992] are essentially infinite-dimensional in nature and exhibit high-dimensional hyperchaotic oscillations with very high frequency broadband spectrum, thereby rendering time-delay systems for several practical applications including digital information transformation at gigabyte rates [Argyris et al., 2005], high speed communication with chaotic lasers [Vanwiggeren and Roy, 1998], generating high precision random numbers [Williams et al., 2010, Li et al., 2011], cryptography [Alsing et al., 1997, Kye et al., 2005], controlling [Hövel, 2010, Schöll and Schuster, 2007], etc. An immense amount of investigations have been carried out in identifying different kinds of synchronizations and their transitions in coupled intrinsic time-delay systems [Namajunas et al., 1995, Burner and Just, 1998, Boccaletti et al., 2000, Shahverdiev et al., 2002a, Sano et al., 2007, Hramov and Koronovskii, 2004, Zhan et al., 2003, Senthilkumar et al., 2006, 2010, Soriano et al., 2013, Pyragas, 1998, Zhou et al., 2007, Chen and Kurths, 2007, Ghosh et al., 2007, Senthilkumar et al., 2009, Voss, 2000, Shahverdiev and Shore, 2005]. Further, the stability of synchronization in time-delay systems has also largely been addressed [Pyragas, 1998, Voss, 2000, Zhou et al., 2007, Senthilkumar and Lakshmanan, 2005, Shahverdiev and Shore, 2005, Chen and Kurths, 2007, Ghosh et al., 2007, Senthilkumar et al., 2009] to establish conditions for stable synchronized states.

Stability of synchronization in coupled time-delay systems has been widely investigated using the Lyapunov functional approach [Shahverdiev and Shore, 2005, Pyragas, 1998, Voss, 2000, Senthilkumar and Lakshmanan, 2005, Zhou et al., 2007, Chen and Kurths, 2007, Ghosh et al., 2007, Senthilkumar et al., 2009], which is most often restricted to just two-coupled time-delay systems. The Lyapunov functional approach results in sufficiency condition for asymptotic stable synchronization. Recently, exact synchronization bound for coupled time-delay system using the generalized Halanay inequality has been deduced, which assures an exponential stabilization of the synchronization manifold [Senthilkumar et al., 2013a]. But this approach is also restricted to two coupled time-delay systems and it lacks a general approach to determine stable synchronized states in networks of time-delay systems.

As, we have discussed in the previous chapters, the framework of the master stabil-

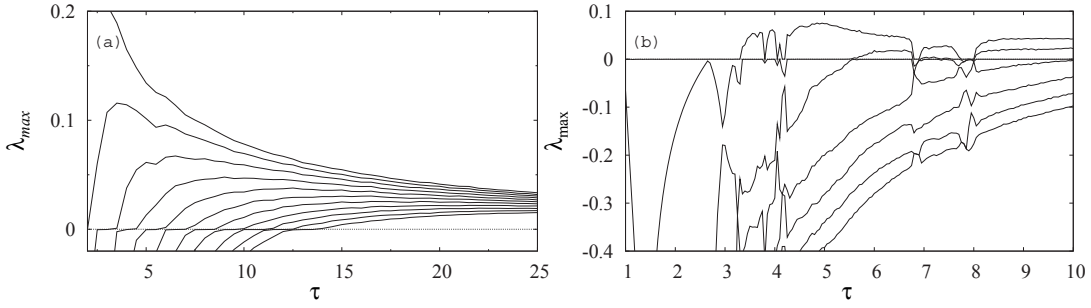

Figure 4.1: (a) First eleven largest Lyapunov exponent λ_{max} of the Ikeda time-delay system, and (b) First six largest Lyapunov exponent λ_{max} of the Mackey-Glass time-delay system with the threshold nonlinearity.

ity formalism has been largely exploited in analysing the stability of networks, in general, which separates the local dynamics from the network topology [Pecora and Carroll, 1998, Fink et al., 2000]. The master stability function (MSF) attributes to a necessary condition for stable synchronization by requiring that the largest transverse Lyapunov exponent corresponding to the largest transverse mode to be negative. This framework has even been extended to deal with network topologies with asymmetric connectivity matrix [Nishikawa and Motter, 2006a]. Only recent investigations on synchronization of networks, whose constituents are composed of low-dimensional dynamical systems described by ordinary differential equations and discrete dynamical systems [Dhamala et al., 2004, Kinzel et al., 2009, Flunkert et al., 2010, Choe et al., 2010, Englert et al., 2011] with delay coupling have been using the MSF in probing stable synchronized states.

On the one hand, the master stability formalism has not yet been extended to intrinsic time-delay systems represented by delay differential equations. On the other hand, there does not exists a general approach to determine the stability of synchronization in networks of intrinsic time-delay systems. Further the behavior of the MSF in typical low-dimensional nonlinear dynamical systems are distinguished into three major classes [Boccaletti et al., 2006, Arenas et al., 2008, Huang et al., 2009]. Delay differential equations being an important class of dynamical systems and synchronization in such systems are being widely investigated. However, the behavior of the MSF with intrinsic time-delay systems as individual units of the network is not yet known. It is worth to emphasize that this may be due to difficulty in estimation of transverse Lyapunov exponents of intrinsic time-delay systems, which are characterized by an infintedimensional phase-space and correspondingly by a large number of variables depending on the value of the delay time and the integration step. In particular, it is computationally changelling and very expensive.

This chapter aims at filling this gap by employing the master stability formalism to an arbitrary network of time-delay systems in determining its stable synchronized states. We have considered undirected networks and estimated the largest Lyapunov exponent

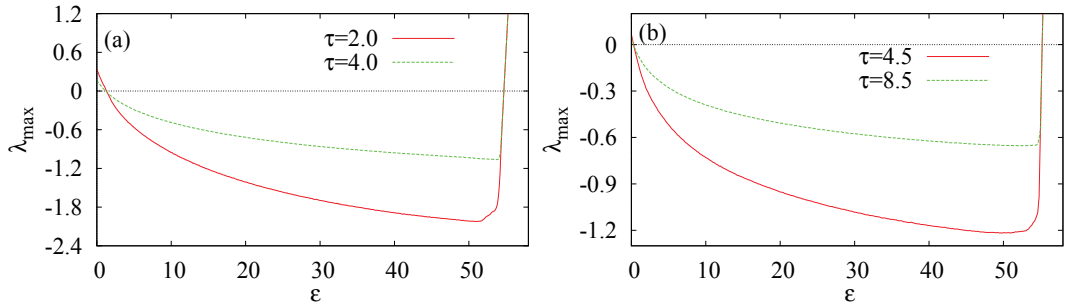

Figure 4.2: The largest transverse Lyapunov exponent λ_{max} of (4.2) as a function of ε in chaotic regimes for lower value of delay τ and hyperchaotic regimes for higher value of delay τ. (a) For the network of Ikeda time-delay system, and (b) For the network of Mackey-Glass time-delay system.

corresponding to the largest transverse mode resulting from the master stability formalism to determine the stability of the synchronized network of time-delay systems. We have examined the nature of the MSF for four paradgamatic scalar time-delay systems, that have been widely used in the synchronization studies, as individual constituents of the arbitrary network. We have found that the MSF exhibits a similar behavior with all the four different scalar time-delay systems we have considered. The MSF is characterized by a finite range of stable synchronization with two zero crossings of the largest Lyapunov exponent as a function of the normalized coupling parameter, thereby falling under the class Γ_2 according to the classification scheme in Ref. [Huang et al., 2009]. This enables us to analyse specific network topologies unambiguously using the eigen-ratio R, to characterize the synchronizability of a given network of scalar time-delay systems.

4.2 Master stability formalism for a network of time-delay systems

We analyse the following undirected network of N identical time-delay systems with an arbitrary topology

$$\dot{X}_i(t) = F\left(X_i(t), X_i(t-\tau)\right) - \sigma \sum_{j=1}^{N} g_{ij} h\left(X_j(t)\right), \tag{4.1}$$

where $X_i, i = 1, \ldots, N$, in general. $F(X_i(t), X(t-\tau))$ is the nonlinear vector function of the individual time-delay systems units, τ is the delay time. The other details are the same as discussed in the previous chapters while discussing the stability of the delay coupled networks. If the coupling matrix G is diagonalizable, then the following block

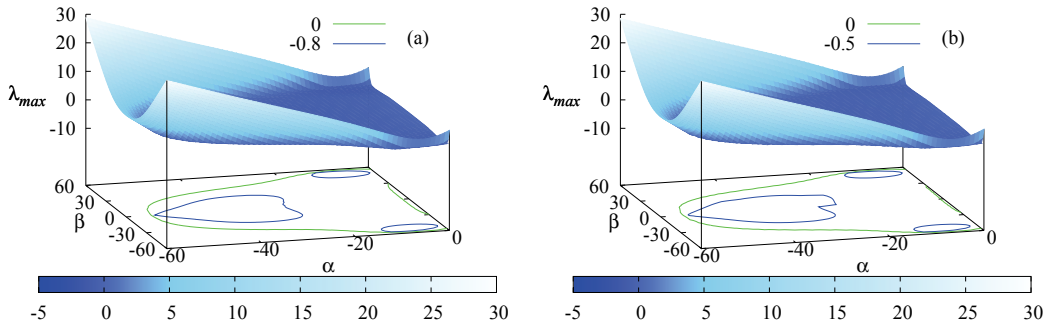

Figure 4.3: The master stability function, the surface of λ_{max} of the network of (a) Ikeda, and (b) Mackey-Glass time-delay systems, in the complex (α, β) plane for $\tau = 2.0$ and 4.5, respectively. The contours encloses the stable synchronization regimes for $\lambda_{max} < 0$.

diagonalized variational equation for the transverse modes can be obtained as

$$\dot{\xi}(t) = DF\left(X_s(t-\tau)\right)\xi(t-\tau) + \left[DF\left(X_s(t)\right) - \varepsilon Dh(X_s(t))\right]\xi(t), \tag{4.2}$$

The definitions on the notations are the same as in the previous chapters. It is to be noted that for the sake of generality, our discussions on the stability aspects are for nodes with m-th order delay differential equations.

As discussed earlier, the negative value of the largest transverse Lyapunov exponent, $\lambda_{max}(\varepsilon) < 0$, of the variational equations (4.2) assures the stable synchronization of the arbitrary network of intrinsic time-delay systems.

Considering the fact that G could be asymmetric and may have complex eigenvalues $\varepsilon = \sigma\gamma_k = -(\alpha + i\beta)$, the master stability equation (4.2) can be written as

$$\begin{aligned}\dot{\xi}(t) = &DF\left(X_s(t-\tau)\right)\xi(t-\tau) + \left[DF\left(X_s(t)\right)\right.\\ &\left. + (\alpha + i\beta)Dh\right]\xi(t),\end{aligned} \tag{4.3}$$

where, α and β are the real and imaginary parts of the eigenvalue. Separating $\xi(t)$ into the real part $\xi_r(t)$ and the imaginary part $\xi_i(t)$, we get

$$\begin{aligned}\dot{\xi}_r(t) = &DF(X_s(t-\tau))\xi_r(t-\tau) + [DF(X_s(t))\\ &+ \alpha Dh(X_s(t))]\xi_r(t) - \beta Dh(X_s(t))\xi_i(t),\end{aligned} \tag{4.4a}$$

$$\begin{aligned}\dot{\xi}_i(t) = &DF(X_s(t-\tau))\xi_i(t-\tau) + \alpha Dh(X_s(t))\xi_i(t)\\ &+ \left[DF(X_s(t)) + \beta Dh(X_s(t))\right]\xi_r(t).\end{aligned} \tag{4.4b}$$

Now, the largest transverse Lyapunov exponent, $\lambda_{max}(\alpha, \beta)$ determines the stability of the synchronization of the network of time-delay systems.

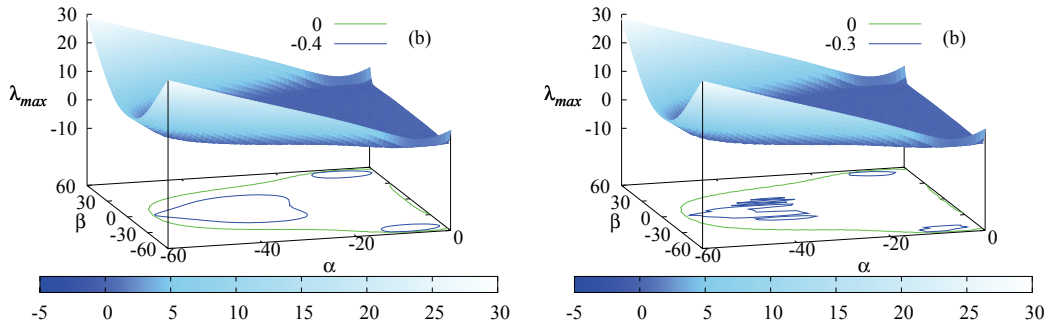

Figure 4.4: The master stability function, the surface of λ_{max} of the network of (a) Ikeda, and (b) Mackey-Glass time-delay systems, in the complex (α, β) plane for $\tau = 4.0$ and 8.5, respectively, exhibiting hyperchaotic attractors. The contours encloses the stable synchronization regimes for $\lambda_{max} < 0$.

4.3 Synchronization in network of scalar time-delay systems

We consider the scalar delay differential equation of the form

$$\dot{x}(t) = -ax(t) + bf\left(x(t-\tau)\right), \tag{4.5}$$

as individual units of the network. Here, a and b are parameters, τ is the delay time and $f(x(t-\tau))$, the nonlinear function, is different for different time-delay systems we have employed. First, we consider the widely studied Ikeda [Ikeda et al., 1980] and Mackey-Glass [Mackey and Glass, 1977] time-delay systems as nodes of the network in both chaotic and hyperchaotic regimes.

4.3.1 Synchronization in network of the Ikeda time-delay systems

The nonlinear function for the Ikeda system [Ikeda et al., 1980] is of the form

$$f(x(t-\tau)) = \sin(x(t-\tau)). \tag{4.6}$$

The parameter for the Ikeda system are chosen as $a = 1.0, b = 5.0$, $\tau = 2.0$ for chaotic oscillations and $\tau = 4.0$ for hyperchaotic oscillations. First eleven largest Lyapunov exponents of the Ikeda time-delay system are depicted in Figs. 4.1(a) and for the above parameter values. It is evident from Fig. 4.1(a) that the Ikeda system exhibits chaotic oscillations for $\tau = 2.0$ with only one positive Lyapunov exponent and hyperchaotic oscillations with three positive Lyapunov exponents for $\tau = 4.0$.

The behavior of the largest transverse Lyapunov exponent, λ_{max}, corresponding to the master stability equation of the network of Ikeda time-delay system is depicted in Fig. 4.2(a) as a function of the normalized coupling strength in both chaotic and hyper-

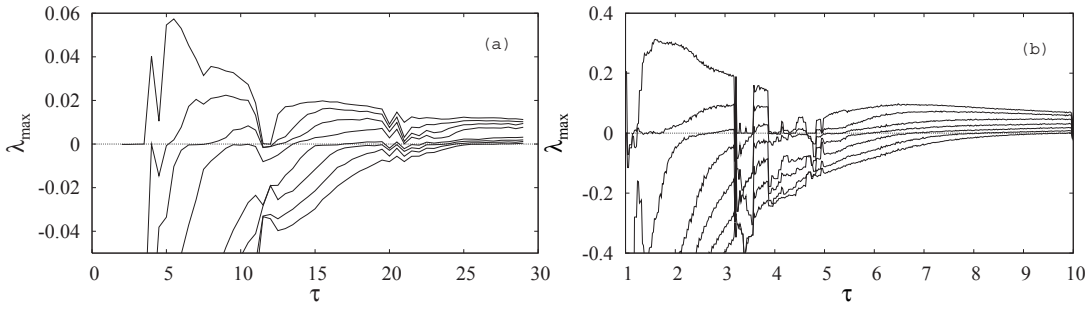

Figure 4.5: (a) First eight largest Lyapunov exponent λ_{max} of the piecewise linear time-delay system, and (b) First seven largest Lyapunov exponent λ_{max} of the piecewise linear time-delay system with the threshold nonlinearity.

chaotic regimes. It is to be noted that as the network is synchronized in a broad range of the coupling strength ε, where $\lambda_{max} < 0$, the first transition point of λ_{max}, that is the first crossing of the zero-axis by λ_{max}, looks identical for both chaotic and hyperchaotic attractors but they transit the zero-axis at different values of ε. Nevertheless, the second crossing of λ_{max} from negative to positive values takes place almost at the same value of the coupling strength. This nature of transition is found to be common for all the four scalar time-delay systems we have considered. Intuitively, one may expect network of chaotic attractors may synchronized first for smaller value of ε than that of the network with hyperchaotic attractors. But, except for a single case, the network of hyperchaotic attractors synchronize first at a lower value of ε and then the network of chaotic attractors synchronize for a slightly higher value of ε with all the other three time-delay systems as we will demonstrate in the remaining part of this chapter.

The largest transverse Lyapunov exponent, λ_{max}, of the network of the Ikeda system with hyperchaotic attractors transits the zero-axis first at $\varepsilon \approx 1.19$ (see Fig. 4.2(a)) and then the network with chaotic attractors at $\varepsilon \approx 1.29$ confirming the existence of synchronization in the networks with chaotic and hyperchaotic attractors. The network remains synchronized for a large range of the coupling strength and becomes desynchronized at a higher value of coupling strength. The network with both chaotic and hyperchaotic attractors of Ikeda time-delay system desynchronized at $\varepsilon \approx 54.7$ as indicated by the second crossing of the zero-axis by the λ_{max}. The master stability function, namely, the surface of λ_{max} in the complex (α, β) plane is illustrated in Fig. 4.3(a) for $\tau = 2.0$. The surface with $\lambda_{max} < 0$ corroborates the stable synchronization regime of network of Ikeda system with chaotic attractors. This is clearly visualized using the contours with different values of $\lambda_{max} \leq 0$ enclosing the stable synchronization as a function of α and β. The contour with $\lambda_{max} = 0$ is the critical stability curve demarcating the stable synchronized and desynchronized regimes in the complex plane. Similar surface of λ_{max} for the network of Ikeda time-delay systems with hyperchaotic attractor is shown in Fig. 4.4(a).

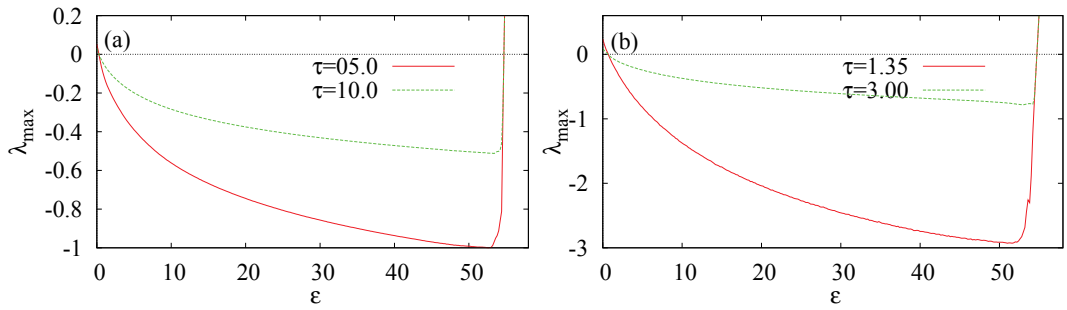

Figure 4.6: The largest transverse Lyapunov exponent λ_{max} of (4.2) as a function of ε in chaotic regimes for lower value of delay τ and hyperchaotic regimes for higher value of delay τ. (a) For the network of piecewise linear time-delay system, and (b) For the network of piece-wise linear time-delay system with threshold nonlinearity.

4.3.2 Synchronization in network of the Mackey-Glass time-delay systems

The nonlinear function $f(x(t-\tau))$ in Eq. (4.5) corresponding to the Mackey-Glass time-delay [Mackey and Glass, 1977] is of the form

$$f(x(t-\tau)) = \frac{x(t-\tau)}{(1+(x(t-\tau)^{10}))}. \tag{4.7}$$

We have fixed $a = 0.5, b = 1.0$, $\tau = 4.5$ and $\tau = 8.5$ for chaotic and hyperchaotic regimes, respectively, of the Mackey-Glass time-delay system. First six largest Lyapunov exponents of the Mackey-Glass time-delay system are depicted in Fig. 4.1(b) for the above parameter values. It is evident from Fig. 4.1(b) that the Mackey-Glass system is characterized by chaotic attractor with one positive Lyapunov exponents for $\tau = 4.5$ and by hyperchaotic attractor with two positive Lyapunov exponents for $\tau = 8.5$.

The network of the Mackey-Glass time-delay systems with hyperchaotic attractors is also synchronized first at $\varepsilon = 0.27$ and then the network with chaotic attractors is synchronized at $\varepsilon = 0.29$ as confirmed by the transition of λ_{max} from positive to negative values below the zero-axis as illustrated in Fig. 4.2(b). The networks with both chaotic and hyperchaotic attractors remain synchronized in a broad range and desynchronized simultaneously at $\varepsilon \approx 55.2$ as indicated by the value of λ_{max}. The corresponding MSF in the complex (α, β) plane is shown in Fig. 4.3(b) for $\tau = 4.5$. We have also obtained similar MSF for $\tau = 8.5$. The contours correspond to different values of λ_{max} encompassing the stable synchronous states. The MSF of the network of the Mackey-Glass time-delay systems with hyperchaotic attractors is illustrated in Fig. 4.4(b) for $\tau = 8.5$.

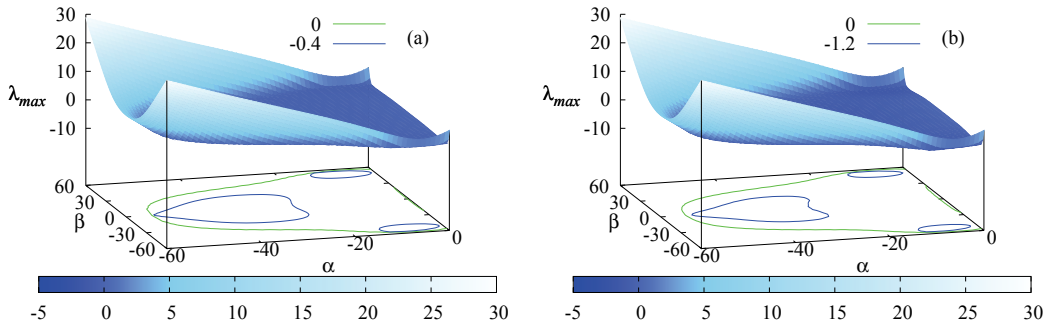

Figure 4.7: The master stability function, the surface of λ_{max} in the complex (α, β) plane, of the network of (a) Piecewise linear time-delay system for $\tau = 5.0$, and(b) Piecewise linear time-delay system with threshold nonlinearity for $\tau = 1.35$. Contours correspond to different values of λ_{max} encompassing the stable synchronous states.

4.3.3 Synchronization in network of a piecewise linear time-delay systems

Now, we consider two other time-delay systems, whose nonlinearity is of the piecewise linear form, to demonstrate the generic behaviour of the MSF in network of scalar delay differential equation. Now, we consider the nonlinearity of a piecewise linear time-delay system, represented by [Senthilkumar and Lakshmanan, 2005]

$$f(x) = \begin{cases} 0, & x \leq -4/3 \\ -1.5x - 2, & -4/3 < x \leq -0.8 \\ x, & -0.8 < x \leq 0.8 \\ -1.5x + 2, & -0.8 < x \leq 4/3 \\ 0, & x > 4/3. \end{cases} \tag{4.8}$$

The first eight largest Lyapunov exponents of the piecewise linear time-delay system are depicted in Fig. 4.5(a) for the parameter values $a = 1, b = 1.2$. We fix $\tau = 5$ and $\tau = 10$ for chaotic with one positive Lyapunov exponent and hyperchaotic attractors with three positive Lyapunov exponents, respectively.

The largest transverse Lyapunov exponent, λ_{max}, of the network of PWL with chaotic attractor becomes negative first at $\varepsilon = 0.28$ and then that with hyperchaotic attractor at $\varepsilon = 0.3$ as illustrated in Fig. 4.6(a), indicating the emergence of synchronization in the network. Similar to the network with Ikeda and MG systems, the network of PWL time-delay system with both chaotic and hyperchaotic attractors remains synchronized in a large range of ε and desynchronized at a larger value of $\varepsilon = 54.8$ as seen in Fig. 4.6(a). The surface of λ_{max} in the complex (α, β) plane is shown in Fig. 4.7(a) for $\tau = 5.0$. The contour corresponding to $\lambda_{max} < 0$ exhibits the stable synchronized regime of the network of PWL time-delay systems. The MSF of the network with hyperchaotic

attractors is illustrated in Fig. 4.8(a) for $\tau = 10.0$.

4.3.4 Synchronization in network of a piecewise linear time-delay systems with threshold nonlinearity

The nonlinear function $f(x)$ for the piecewise linear time-delay system with threshold nonlinearity is of the form [Senthilkumar et al., 2010]

$$f_3(x) = AF^* - Bx. \tag{4.9}$$

Here

$$F^* = \begin{cases} -x^*, & x < -x^* \\ x, & -x^* \leq x \leq x^* \\ x^*, & x > x^*. \end{cases} \tag{4.10}$$

We have chosen the parameters for the piecewise linear time-delay system with threshold nonlinearity system as $a = 1.0, b = 1.2$, $\tau = 1.35$ for chaotic and $\tau = 3.0$ hyperchaotic regimes with three positive Lyapunov exponents. The number of positive Lyapunov exponents are confirmed from the first seven largest Lyapunov exponents depicted in Fig. 4.5(b).

The network of piecewise linear time-delay system with threshold nonlinearity becomes synchronized first for its hyperchaotic behavior at $\varepsilon = 0.66$ and then the network with chaotic attractor is synchronized at $\varepsilon = 0.69$ as shown by λ_{max} in Fig. 4.6(b). The network is desynchronized at $\varepsilon = 54.8$ as the λ_{max} transits the zero-axis from negative to positive values. The corresponding MSF is depicted in Fig. 4.7(b) for the network with chaotic attractor. The contour in the figure encloses the stable synchronization regimes for $\lambda_{max} < 0$. The surface of λ_{max} in the complex (α, β) plane for hyperchaotic attractors of the piecewise linear time-delay systems with threshold nonlinearity is shown in Fig. 4.8(b).

It is to be noted that even though the structure of the contours in the MSFs of all the scalar time-delay systems are almost identical, the value of λ_{max}, quantifying the degree of convergence, corresponding to the contours are clearly distinct for different systems.

4.4 Summary and conclusion

We have investigated the stability of synchronization in an arbitrary network of scalar time-delay systems using the master stability formalism. Using four different scalar time-delay systems that have been widely used from synchronization studies in the literature, we have examined the behavior of the MSF, that is λ_{max} of the largest transverse mode of the variational equations. We have found that a network of scalar time-delay systems are characterized by finite range of stable synchronized states as corroborated by two crossing of the zero-axis by the λ_{max} in the finite range of the coupling strength ε with $\lambda_{max} < 0$. Thus, the MSF with the network of scalar time-delay systems exhibits a generic behavior by falling under the class Γ_2 according to the classification of the MSF

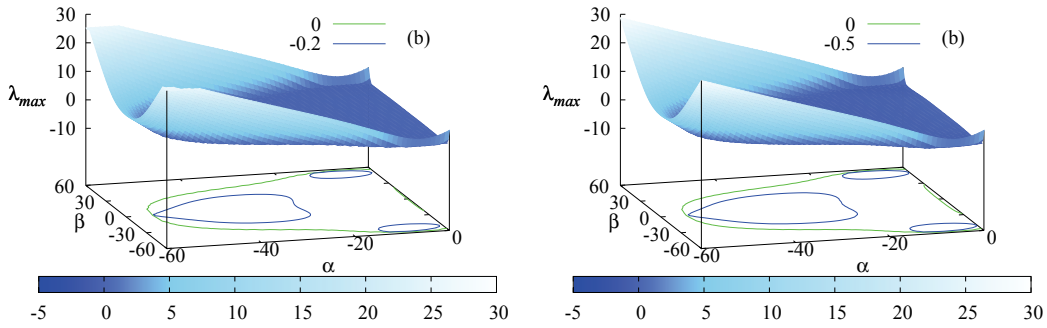

Figure 4.8: The master stability function, the surface of λ_{max} in the complex (α, β) plane, of the network with hyperchaotic attractors of (a) Piecewise linear time-delay system for $\tau = 10.0$, and(b) Piecewise linear time-delay system with threshold nonlinearity for $\tau = 3.0$. Contours correspond to different values of λ_{max} encompassing the stable synchronous states.

in Ref. [Huang et al., 2009]. Our study bridges the gap in the literature by applying the framework of master stability formalism to the network of intrinsic time-delay systems. Furthermore, our results allows unambiguously to analyse networks of scalar time-delay systems with specific topologies using the eigenratio R.

5 Noise-enhanced phase synchronization in time-delayed systems

5.1 Introduction

Synchronization of interacting dynamical systems is an evergreen research topic receiving flurry of attention because of its fundamental importance in understanding numerous natural phenomena [Pikovsky et al., 2001, Boccaletti et al., 2002, Arenas et al., 2008]. Recent investigations in this line of research are focusing on dynamical systems with intrinsic delay and delay couplings [Senthilkumar and Lakshmanan, 2011, Flunkert et al., 2010, Dhamala et al., 2004, Masoller and Marti, 2005, Atay et al., 2004, Englert et al., 2011, Senthilkumar et al., 2006, Suresh et al., 2010, Senthilkumar et al., 2010] due to a rich variety of dynamical behaviors induced by delay [Sethia et al., 2008, Prasad et al., 2006]. Among different kinds of synchronization, phase synchronization (PS) plays a crucial role in understanding large class of weekly interacting dynamical systems [Pikovsky et al., 2001, Boccaletti et al., 2002, Arenas et al., 2008]. For instance, PS forms the basic mechanism of large-scale integration of neural process in neural assemblies of the brain [Varela et al., 2001]. Recently, it has also been shown that PS links the working memory and long-term memory by facilitating neural communication and by promoting neural plasticity [Fell and Axmacher, 2011]. Further, the key role of coupling, delay and noise in understanding the "resting state" of human brain associated with day-dreaming, inner rehearsal, etc., have been reported [Deco et al., 2009].

Effects of noise on synchronization have also been studied extensively [Pikovsky et al., 2001, Boccaletti et al., 2002, Arenas et al., 2008]. The phenomenon of "bubbling", i.e., noise-induced desynchronization due to local instability of the synchronization manifold [Ashwin et al., 1994] is an example of a non-constructive effect of noise. Nevertheless, noise can also induce and enhance synchronization in coupled/uncoupled oscillators [Zhou et al., 2002, Zhou and Kurths, 2002]. The influence of stochastic forces on dynamical systems are also of great importance in various applications [Anishchenko et al., 2002, Horsthemke and Lefever, 1984]. For instance, stochastic process in the central nervous system is essential for the expression of spatiotemporal patterns [Deco et al., 2009]. It has been shown that the neural connections are of variable loops such that the propagation of a signal through the loops can result in a large time-delay (synaptic delay), and it is also reported that the axons can generate a time-delay up to 300 ms [Shadlow, 1985, Aboitiz et al., 1992]. As a consequence, the neural networks have intrinsic delay in their dynamics. Hence investigating noise effects on PS of delay dynamical systems will provide a better understanding on the stochastic process mediating the information processing in neurons.

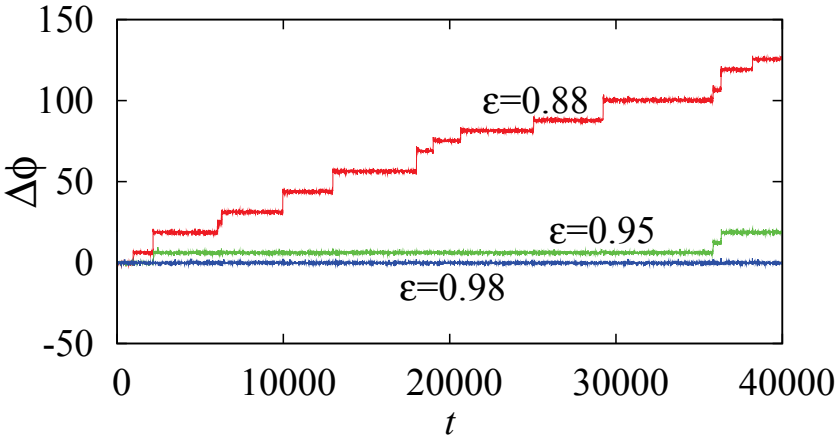

Figure 5.1: Phase difference for different values of the coupling strength ε, while the noise intensity $\sigma = 0.0$.

In this chapter, we will investigate the phenomenon of noise-enhanced PS in coupled time-delay systems along with its mechanism. Delay dynamical systems are essentially an infinite-dimensional in nature exhibiting highly non-phase-coherent chaotic/hyperchaotic attractors. In contrast to low-dimensional dynamical systems described by ordinary differential equations as studied in [Zhou et al., 2002, Zhou and Kurths, 2002], time-delayed systems described by delay differential exhibit strongly pronounced multiple characteristic time scales [Senthilkumar and Lakshmanan, 2011]. As PS is the coincidence of characteristic time scales of interacting dynamical systems, it is cruical and interesting to understand the interplay of noise and the multiple time scales in achieving PS in such systems for various applications. Indeed, only a very few studies have been reported on PS in coupled time-delay systems [Senthilkumar et al., 2006, Suresh et al., 2010, Senthilkumar et al., 2010], despite the difficulty in estimation of the phase explicitly in such systems. Recently, we have demonstrated PS experimentally using electronic circuits in a piecewise linear time-delay system with a threshold nonlinearity [Senthilkumar et al., 2010]. In particular, we will consider the same system with parameter mismatches and demonstrate that both an independent and a common additive noise can enhance PS. Interestingly, multiple time scales of a time-delay system are clearly identified from the return times of the flow to a Poincaré section. We find noise-enhanced PS in both basic coupling configurations: unidirectional and bidirectional. On the one hand the response system adjust its time scales to that of the drive in achieving PS in an unidirectional coupling configuration. On the other hand, both subsystems adjust their rhythms to the main time scale of the uncoupled system to achieve PS in bidirectionally coupled systems. Further, we will show that phase slips are accompanied by small and large return times, which are not present in the noise-free system, due to the unlocked unstable periodic orbits present in the coupled system.

5.2 Coupled time-delay system

We consider the following coupled scalar piecewise linear time-delay system

$$\begin{aligned}\dot{x} &= \omega_x \left(-x(t) + bf\left[x(t-\tau)\right]\right) + \varepsilon_x(y(t) - x(t)) + \sigma\xi_x(t),\\ \dot{y} &= \omega_y \left(-y(t) + bf\left[y(t-\tau)\right]\right) + \varepsilon_y(x(t) - y(t)) + \sigma\xi_y(t),\end{aligned} \tag{5.1}$$

where $\omega_x = 1.0$ and $\omega_y = 1.1$ contributes to the frequency mismatch, $b = 1.2$ is the nonlinear parameter, $\tau = 1.33$ the delay, $\varepsilon_{x,y}$ the coupling strength, $\xi_{x,y}(t)$ an added Gaussian noise with zero mean and unit variance, and σ the noise intensity. When $\varepsilon = \varepsilon_x = \varepsilon_y$, then the systems are bidirectionally coupled, whereas $\varepsilon_x = 0$ corresponds to a unidirectional coupling configuration. When $\xi_x = \xi_y$, the Gaussian noise is common otherwise it is independent. The function $f(x(t-\tau))$ is taken to be a piecewise linear function with threshold nonlinearity defined by Eq. (4.9) of Chapter 4. The parameter values are fixed in accordance with the values of the circuit elements [Senthilkumar et al., 2010].

5.3 Noise-enhanced PS in unidirectionally coupled time-delay systems

Now, we will demonstrate the results for unidirectional coupling. For the drive system $A_x = 5.2$ and for the response system $A_y = 5.0$, while B is fixed as $B = 3.5$. The first seven largest Lyapunov exponents of the drive system is shown in Fig. 4.5(b). It is to be noted that the results presented in the entire chapter remain valid irrespective of the values of the parameters $A_{x,y}$, B and b, which are chosen such that the individual systems exhibit chaotic behavior. The coupled system (5.1) is integrated using the Runge-Kutta fourth order integration scheme with step size 0.01 and the additive Gaussian noise is added at every integration step. Interacting chaotic dynamical systems are said to be in phase synchronized state when there exists an entrainment between phases of the systems, while their amplitudes may remain chaotic and uncorrelated. In other words, PS exists when their respective frequencies and phases are locked [Pikovsky et al., 2001, Boccaletti et al., 2002]. The phase of a chaotic attractor can also be defined based on an appropriate Poincaré section which the chaotic trajectory crosses once for each rotation, please refer to [Pikovsky et al., 2001, Boccaletti et al., 2002] for various other possible estimators (definition) of the phase. Each crossing of the orbit with the Poincaré section corresponds to an increment of 2π of the phase, and the phase in between two crosses is linearly interpolated as [Pikovsky et al., 2001, Boccaletti et al., 2002],

$$\Phi(t) = 2\pi k + 2\pi \frac{t - t_k}{t_{k+1} - t_k}, \qquad (t_k < t < t_{k+1}) \tag{5.2}$$

where t_k is the time of kth crossing of the flow with the Poincaré section.

The Poincaré section is chosen at $x(t-\tau) = 0.8$ and $x(t) < 0.8$ on the attractor throughout this chapter. The unidirectionally coupled, for $\varepsilon_x = 0$ and $\varepsilon = \varepsilon_y$, piece-

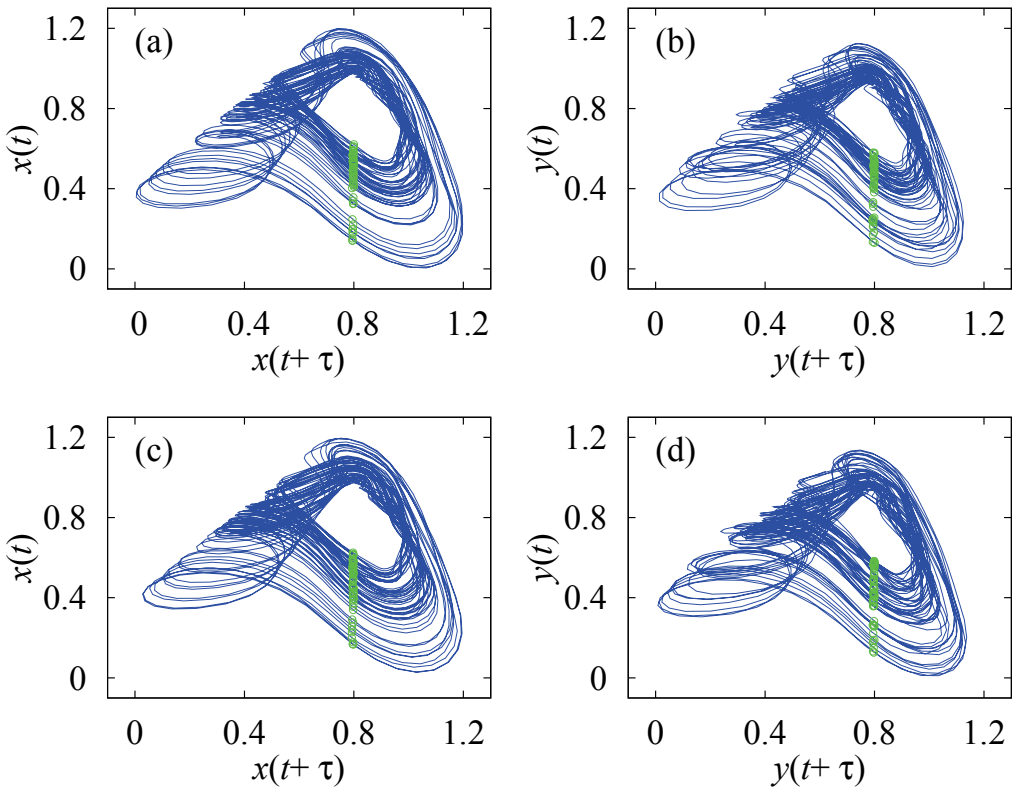

Figure 5.2: Attractors of the coupled piecewise linear time-delay systems (5.1) along with the Poincaré section, represented as filled squares, both with and without the additive noise. (a) Attractor of the drive system for $\varepsilon = 0.98$ and $\sigma = 0$, (b) Attractor of the response system for $\varepsilon = 0.98$ and $\sigma = 0$, (c) Attractor of the drive system for $\varepsilon = 0.88$ and $\sigma = 0.006$ and (d) Attractor of the response system for $\varepsilon = 0.88$ and $\sigma = 0.006$.

wise linear time-delay system exhibit PS for appropriate values of the coupling strength without noise $\sigma = 0$, which is indeed demonstrated in Fig. 5.1. In the absence of the coupling, both systems evolve independently with different frequencies due to the frequency mismatch $\omega_x \neq \omega_y$. For $\varepsilon = \varepsilon_y = 0.88$, the coupled systems are in their transition to PS regime. Further increase in the coupling strength leads to increase in the duration of the phase synchronized epochs, finally resulting in the perfect PS. In particular, the coupled systems are at the onset of PS at $\varepsilon = 0.95$ and in perfect phase synchrony for $\varepsilon = 0.98$. The attractors of the drive and the response systems along with their Poincaré section, represented as filled squares, for the above parameter values are shown in Figs. 5.2(a) and 5.2(b), respectively.

The mean frequency of the chaotic oscillations is defined as [Pikovsky et al., 2001,

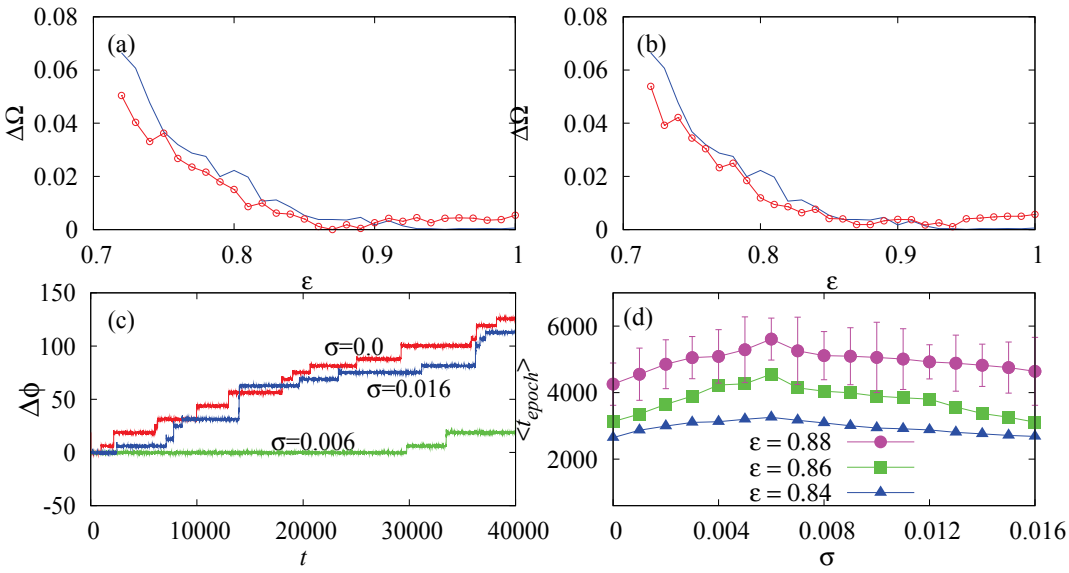

Figure 5.3: Frequency difference $\Delta\Omega$ vs coupling strength ε with a common noise (a) and with an independent noise (b) for unidirectional coupling. Solid line correspond to $\sigma = 0$ and open circles to $\sigma = 0.006$. (c) Phase difference for different noise intensity σ and (d) Average duration of PS epochs vs σ for different ε. The standard deviation is shown with error bars for $\varepsilon = 0.88$.

Boccaletti et al., 2002],

$$\Omega_{x,y} = \langle d\phi_{x,y}(t)/dt \rangle = \lim_{T\to\infty} \frac{1}{T} \int_0^T \dot{\phi}_{x,y}(t)dt \tag{5.3}$$

and the $1:1$ PS between the coupled systems can also be characterized by the equality of their mean frequencies $\Omega_x = \Omega_y$. The mean frequency difference $\Delta\Omega = \Omega_y - \Omega_x$ as a function of $\varepsilon \in (0, 1)$ for both a common and an independent noise with $\sigma = 0.006$, represented as connected open circles, are shown in Figs. 5.3(a) and 5.3(b), respectively. The solid line corresponds to the mean frequency difference in the absence of noise, $\sigma = 0$. Smaller values of the mean frequency difference $\Delta\Omega$, below the onset of exact PS at $\varepsilon_{PS} = 0.95$, for the connected circles compared to that of the solid line clearly illustrate the phenomenon of noise-enhanced PS for both a common and an independent noise.

To demonstrate this phenomenon more clearly, we analyse the duration of PS epochs t_{epoch} as σ is increased. We choose $\varepsilon = 0.88$ well below ε_{PS} and $\xi_x = \xi_y$, that is, a common noise. The instantaneous phase difference $\Delta\phi$ for different σ is depicted in Fig. 5.3(c). In the absence of noise, $\sigma = 0$, the average phase difference displays several PS epochs, whereas longest possible PS epochs are observed for $\sigma = 0.006$, which is indeed confirmed by the maximal value of the average duration of PS epochs $\langle t_{epoch} \rangle$

shown in Fig. 5.3(d) ($\langle t_{epoch} \rangle$ is estimated by averaging over 10 different realization, each of duration $t = 2,000,000$). Note that, as we have fixed the coupling strength well below the onset of perfect PS, we did not achieve perfect PS with noise. However, we have confirmed that if the coupling strength is chosen very close to the onset of perfect PS, noise can induce perfect PS in the coupled time-delay systems. Further increase in the noise intensity results in shortening of the duration of PS epochs as depicted for $\sigma = 0.016$ in Fig. 5.3(c) and lower values of the average duration of PS epochs $\langle t_{epoch} \rangle$ (see Fig. 5.3(d)). Hence, increasing σ from zero increases the average duration of PS epochs attaining a maximum for appropriate σ, attributing to noise-enhanced PS, and then $\langle t_{epoch} \rangle$ decreases for larger σ, like the resonance phenomenon due to the competing effects of the noise and the mutual locking of time scales of the coupled system as we will discuss below. This behavior is also observed for the other values of the coupling strength as illustrated in Fig. 5.3(d). We have also obtained qualitatively similar results for $\xi_x \neq \xi_y$, an independent noise.

Now, we investigate the return times T_k to a Poincaŕe section to understand the constructive role of noise in increasing the duration of PS epochs t_{epoch}. Periodic orbits are manifested by almost vanishing $\Delta X_k = |x_{t+k} - x_t|$ at the Poincaŕe section for every k returns with the corresponding return times T_k. PS is characterized by mutual phase locking of unstable periodic orbits (UPOs) of the coupled chaotic systems and the phase slips are manifested by a few pairs of unlocked UPOs of the coupled system similar to periodically driven chaotic oscillators [Pikovsky et al., 2001, Boccaletti et al., 2002, Zhou et al., 2002, Zhou and Kurths, 2002, Pikovsky et al., 1997, Zaks et al., 1999]. Noise is capable of preventing the systems from following unlocked UPOs for a long time and also forcing the systems to follow them for a long time resulting in both short and long return times, which do not happen in noise-free systems [Zhou et al., 2002, Zhou and Kurths, 2002]. This is illustrated in Fig. 5.4 for $\varepsilon = 0.88$ and for the small noise intensity $\sigma = 0.002$. A phase synchronized epoch along with the accompanying phase slips at its both end is depicted in Figs. 5.4(a) and 5.4(d). Note that both these figures are the same and shown here to compare the region of phase slips with the other figures. The difference between the same variables ΔX_2 and ΔY_1 for every second and first returns, with return times T_2 and T_1, to the Poincaŕe section is shown in Figs. 5.4(b) and 5.4(c), respectively, along with their corresponding period-2 and period-1 UPOs in the insets. It is to be noted that the large fluctuation in the difference ΔX_2 and ΔY_1 is due to the oscillations with different (multiple) time scale return to the Poincaŕe section at different instant in contrast to the mutually coupled systems (see below). phase slip at $t \approx 9950$ is indeed caused by these pairs of unlocked UPOs, which is followed by the system for sufficiently long time to a phase slip to occur. Nevertheless, one can also find other pairs of unlocked UPOs at the phase slip while the majority of the UPOs of the coupled systems are mutually locked. Those pairs with small and large return times (see Fig. 5.4(f)), corresponding to a large mismatch in their time scales, require a large value of coupling strength for a fixed noise intensity to become locked. On contrary, a large value of the noise intensity, less than a certain threshold for a fixed coupling strength, can also change their time scales to become locked and consequently increasing the duration of PS epochs t_{epoch} resulting in noise-enhanced PS as shown in Figs. 5.3.

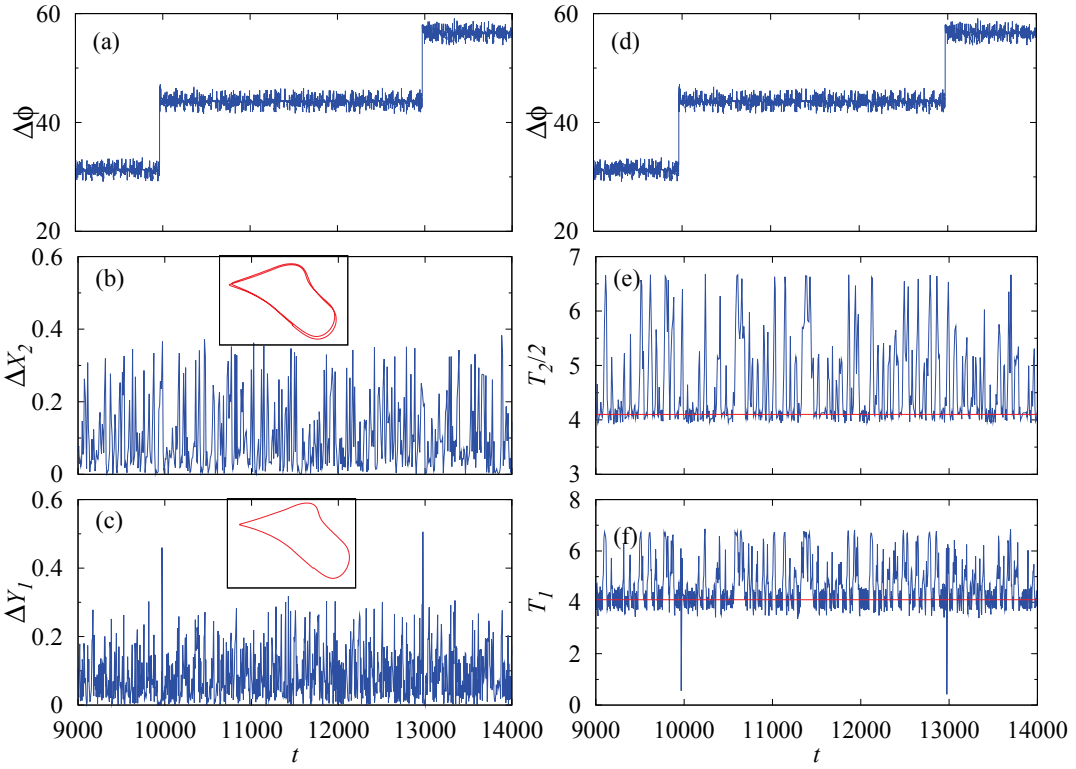

Figure 5.4: (a) Phase slips induced by unlocked UPOs are illustrated in (a) and (d). Difference between x and y variables, ΔX_2 and ΔY_1, to the Poincarè section is shown in (b) and (c), respectively, with the insets illustrating period-2 and period-1 unlocked UPOs around $t \approx 9950$ and their corresponding return times T_2 and T_1 in (e) and (f), respectively.

Multiple time scales of the individual system are clearly identified from their return times (Figs. 5.4(e) and 5.4(f)). The principle time scale, around which majority of the return times are fluctuating, is indicated by a horizontal line at 4.3, while the other two pronounced time scales are seen at 5.3 and 6.6. It is to be noted that the time scales of the drive system remain unaffected (see Fig. 5.4(e)), while most of the time scales of the response system become entrained to that of the drive system except those return times with a large difference in the time scales of unlocked UPOs manifesting phase slips (compare Figs. 5.4(d) and 5.4(f)).

5.4 Noise-enhanced PS in bidirectionally coupled time-delay systems

In the following, we will demonstrate the phenomenon of noise-enhanced PS in bidirectionally coupled time-delay systems where both subsystems adjust their time scales of

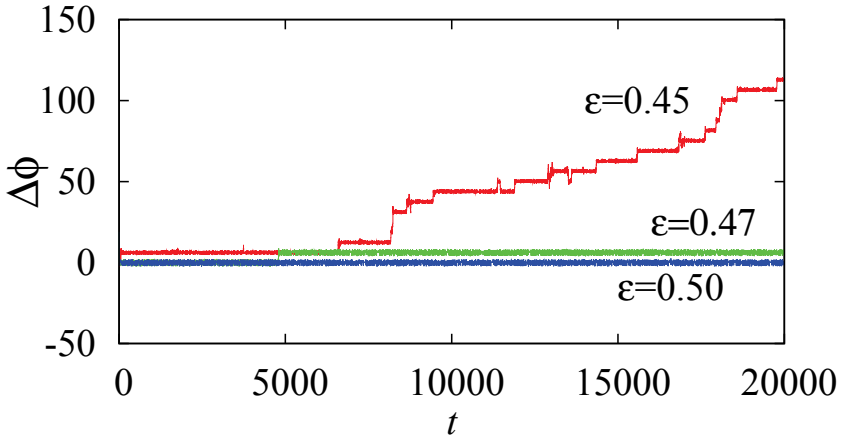

Figure 5.5: Phase difference for different values of the coupling strength ε, while the noise intensity $\sigma = 0.0$, for the bidirectionally coupled piecewise linear time-delay systems.

oscillation to their principle time scale in achieving PS. Now, we fix the same parameters as above except for $A_x = A_y = 5.2$, that is, parameter mismatch only in the frequencies. The instantaneous phase difference of the bidirectionally coupled piecewise linear time-delay system is shown in Fig. 5.5 for different ε but without noise $\sigma = 0.0$. Because of the frequency mismatch, both systems evolve independently for $\varepsilon = 0.0$. The coupled systems are in their transition to PS for both $\varepsilon = 0.45$ and 0.47, while they are in perfect PS for $\varepsilon = 0.5$. The average frequency difference $\Delta\Omega$ is depicted in Figs. 5.6(a) and 5.6(b) in the presence of a common and an independent noise with $\sigma = 0.04$, indicated by connected open circles, respectively. The solid line corresponds to $\Delta\Omega$ without any noise. $\Delta\Omega$ acquire small values in the presence of noise rather than without noise in almost the entire range of the coupling strength below $\varepsilon_{PS} = 0.5$, which clearly indicates the phenomenon of noise-enhanced PS in bidirectionally coupled systems. The phase difference $\Delta\phi$ for different values of the noise intensity σ with a common Gaussian noise and $\varepsilon = 0.45$ are shown in Fig. 5.6(c). The average duration of PS epochs $\langle t_{epoch} \rangle$ for three different values of the coupling strength ε is illustrated in Fig. 5.6(d). From these figures, it is observed that the duration of PS epochs increases with noise intensity and reaches a maximum for an optimal value of the noise intensity with further increase in it resulting in decreasing in the value of $\langle t_{epoch} \rangle$, similar to the phenomenon of resonance due to the competition between the noise and the mutual locking of UPOs. Similar results are obtained for other analyzed values of the coupling strength and for an independent noise.

A phase synchronized epoch with its accompanying phase slips is shown in Figs. 5.7(a) and 5.7(d) for $\varepsilon = 0.45$ and $\sigma = 0.01$. Difference between the same variables, ΔX_1 and ΔY_2, at every first and second returns to the Poincarè section are shown in Figs. 5.7(b) and 5.7(c), respectively. The phase slip around $t \approx 6600$ is occurred between the un-

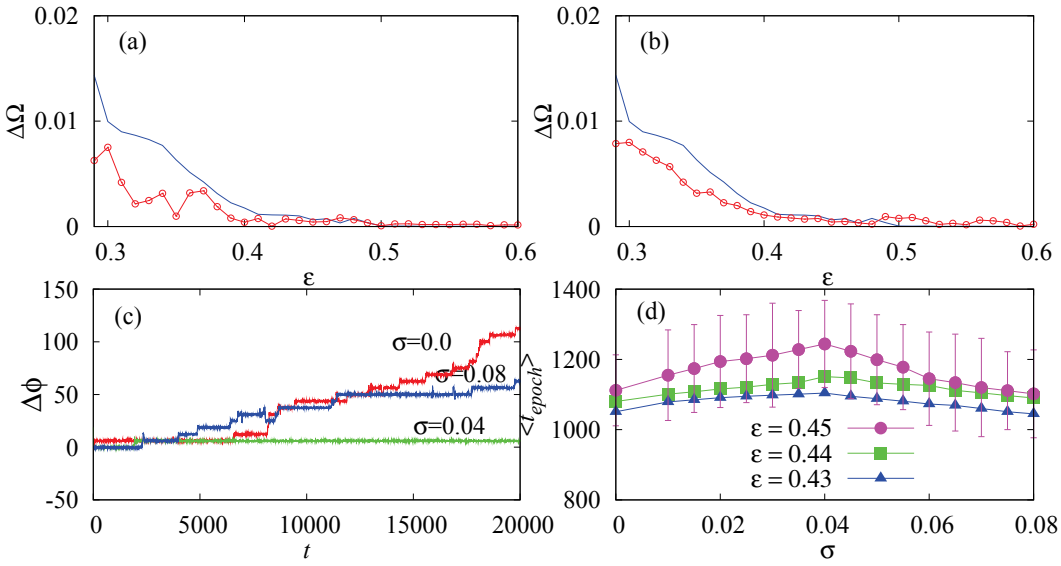

Figure 5.6: Bidirectional coupling: Frequency difference $\Delta\Omega$ vs coupling strength ε with a common noise (a) and with an independent noise (b). Solid line correspond to $\sigma = 0$ and open circles to $\sigma = 0.04$. (c) Phase difference for different noise intensity σ and (d) Average duration of PS epochs vs σ for different ε. The standard deviation is shown with error bars for $\varepsilon = 0.45$.

locked period-2 and period-1 UPOs depicted in the insets. One can also find other pairs of unlocked UPOs at this phase slip. Being bidirectionally coupled system, the subsystems adjust their time scales to their principle time scale, indicated by the horizontal line at 4.05, around which the majority of the return times fluctuate attributing to the majority of locked UPOs. The small and large return times in both subsystems at $t \approx 6600$ and $t \approx 8250$ in Figs. 5.7(e) and 5.7(f) is due to the large difference in the time scales of the pair of unlocked UPOs. As discussed for the unidirectional coupling, it requires a large coupling strength or a large noise less than a threshold value to induce changes in their time scales such that the UPOs now become locked. The latter is indeed demonstrated in Fig. 5.6(c), for the noise intensity $\sigma = 0.04$, and in Fig. 5.6(d) illustrating the increase in the duration of PS epochs resulting in noise-enhanced PS for fixed values of the coupling strength.

5.5 Summary and Conclusion

In summary, we have demonstrated the phenomenon of noise-enhanced PS in both unidirectionally and bidirectionally coupled time-delay systems. It is to be noted that the time scales of the drive system remain unaffected, while most of the time scales of the response system are entrained to that of the drive system in unidirectionally coupled time-delay systems, whereas both systems adjust their rhythms to their principle time

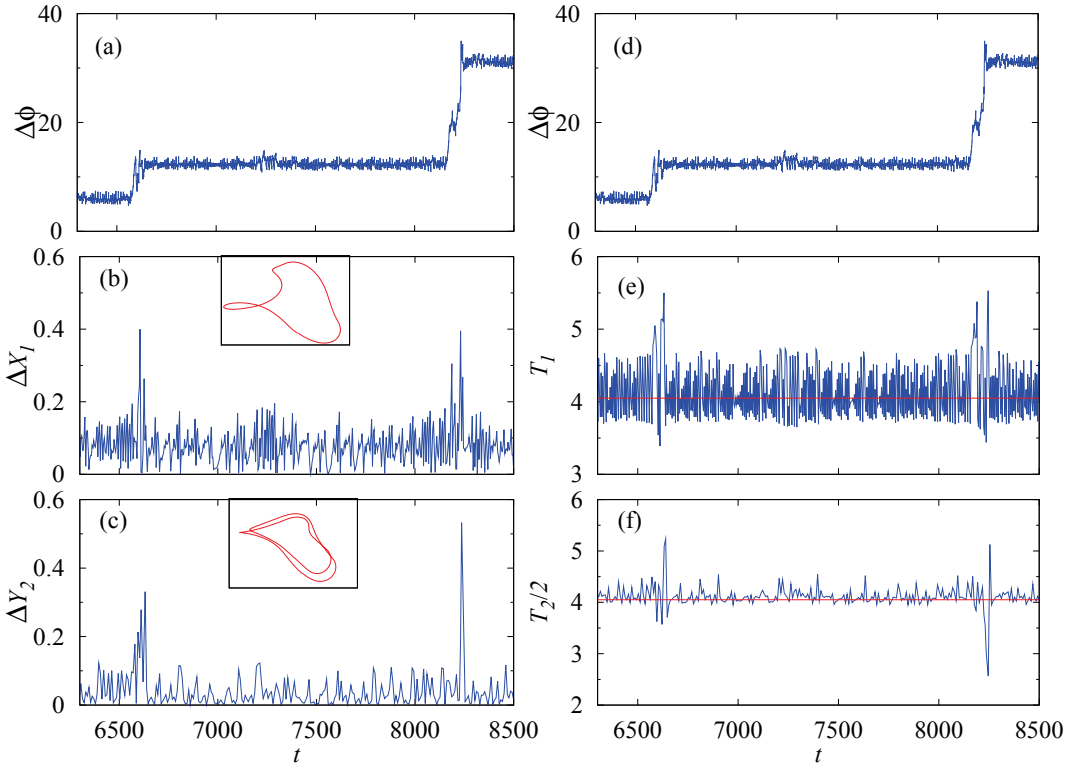

Figure 5.7: (a) Phase slips induced by unlocked UPOs are illustrated in (a) and (d). Difference between x and y variables, ΔX_1 and ΔY_2, on the Poincarè section is shown in (b) and (c), respectively, with the insets illustrating period-2 and period-1 unlocked UPOs around $t \approx 6600$ and their corresponding return times T_1 and T_2 in (e) and (f), respectively.

scale for mutual coupling. In particular, the return time clearly indicates the multiple time scales of the delay system. Several rather complicated techniques, such as permutation information theory [Soriano et al., 2011], principle component analysis [Jolliffe, 2002], etc., have been developed to identify the time scales, whereas our result shows that this could be clearly seen from the return times. Entrainment of the oscillations to the principle time scale in mutually coupled systems despite of the presence of intrinsic multiple time scales could shed more light on our understanding of information processing in neural networks where the connections naturally involves delay and exhibit multiple time scale. Further, synchronizing to a particular time scale, correspondingly to a specific frequency, for instance alpha and beta waves in the brain [Llinas and Yarom, 1991], could enrich our knowledge on synchronization and its control of several pathological disorders, in chaotic semiconductor lasers [Soriano et al., 2011], etc. Experimental confirmation of the above results are in progress using electronic circuits [Senthilkumar et al., 2010]. We have confirmed that the reported phenomenon does change for a range of values of

the parameters in the chaotic regime and hence our results remain robust against the changes in the parameters.

6 Summary, conclusions and future outlook

6.1 Summary and Conclusions

Stability of synchronization is one of the most prominent issue in the synchronization studies. Several analytical approaches such as mean field theory, generalized mean-field approach and their variants, Lyapunov stability, the master stability formalism, etc., has been proposed to deal with the stability aspects. Among these approaches, the framework of master stability formalism is widely employed in probing the stability of networks from regular to complex topological structure. Effects of delay coupling on the phenomenon of synchronization in networks of dynamical systems have been intensively investigated in recent times. This is because of finite time required by the signals to propagate from one node to the other in real world networks that are spatially separated and/or due to nature of the communication channel. Only a few recent investigations has employed the framework of master stability formalism in investigating the stability of synchronization in delay coupled networks and that too widely in networks, whose node dynamics are described by discrete dynamical systems. In this thesis, we have employed the master stability formalism to investigate stable synchronization in delay coupled networks of time-continuous nonlinear dynamical systems and the important results are listed below.

1. We have investigated the phenomena of delay-enhanced and delay-induced stable synchronization in an arbitrary delay coupled network using the framework of the master stability formalism. We have demonstrated that there always exist an extended regime of stable synchronous state as a function of coupling strength for appropriate coupling delays, which cannot be observed without any delay in the coupling. Further, we have elucidated that the stable synchronization in the delay coupled networks are achieved even at smaller values of coupling strength with delay, which is actually attained at larger coupling strength without delay. The generic nature of our results is also corroborated using four paradigmatic models, namely, Rössler, Lorenz systems, Hindmarsh-Rose neurons and Chua's circuit systems as nodes of the network, that have been widely exploited in the literature for synchronization studies.

2. We have proposed a partial delay coupling as a combination of both instantaneous coupling and delay coupling with a certain weight on each and investigated its effects on the synchronization properties of an arbitrary network. The combined instantaneous and delay information transfer, referred to as working memory and long-term memory in cognitive science, is often emphasized as necessary for achieving several cognitive processes including, learning, reasoning, visual discrimination,

etc Fell and Axmacher [2011], Shrager et al. [2008], Knuston A. R. et al. [2012]. We have shown that the partial delay coupling outperforms the completely delay coupling in inducing an extended regime of stable synchronization both at lower and higher values of coupling strength. We have also shown that the partial delay is capable of inducing synchronization where there is no synchronization in both the limiting cases.

3. We have investigated the stability of synchronization in an arbitrary network of scalar time-delay systems using the master stability formalism. Using four different scalar time-delay systems that have been widely used from synchronization studies in the literature, we have examined the behavior of the MSF, that is λ_{max} of the largest transverse mode of the variational equations. We have found the network of scalar time-delay systems are characterized by finite range of stable synchronized states as corroborated by two crossing of the zero-axis by the λ_{max} in a finite range of the coupling strength ε with $\lambda_{max} < 0$. Thus, the MSF with the network of scalar time-delay systems exhibits a generic behavior by falling under the class Γ_2 according to the classification of the MSF in Ref. [Huang et al., 2009]. Our study bridges the gap in the literature by applying the framework of the master stability formalism to the network of intrinsic time-delay systems. Furthermore, our results allows unambiguously to analyze networks of scalar time-delay systems with specific topologies using the eigenratio R.

4. We have also demonstrated the phenomenon of noise-enhanced PS in both unidirectionally and bidirectionally coupled time-delay systems. It is to be noted that the time scales of the drive system remain unaffected, while most of the time scales of the response system are entrained to that of the drive system in unidirectionally coupled time-delay systems, whereas both systems adjust their rhythms to their principle time scale for mutual coupling. In particular, the return time clearly indicates the multiple time scales of the delay system. Several rather complicated techniques, such as permutation information theory [Soriano et al., 2011], principle component analysis [Jolliffe, 2002], etc., have been developed to identify the time scales, whereas our result shows that this could be clearly seen from the return times. Entrainment of the oscillations to the principle time scale in mutually coupled systems despite of the presence of intrinsic multiple time scales could shed more light on our understanding of information processing in neural networks where the connections naturally involves delay and exhibit multiple time scale.

6.2 Future outlook

There are several open and challenging problems which remain to be explored from different aspects of the problems and their results discussed in this thesis. We present here some of the potential problems which we hope to investigate in the near future.

1. The mechanism behind the phenomenon of delay-enhanced and delay-induced stable synchronization remains unclear and is an open problem to be explored.

2. It is now understood that connection delays in networks tend to reduce local coordination of nodes to improve the global coordination Wang et al. [2008], Hunt et al. [2010], Hod [2010]. The presence of both the instantaneous and delay coupling with appropriate weights in the partial delay coupling may improve both the local and global coordination in achieving global synchronization for very low values of coupling strength. This effect of partial delay and the responsible mechanism needs much in-depth investigation as this will shed more light on our understanding of synchronization processes at various levels in cerebral cortex, pathological synchronization activity of neuronal network and their control mechanisms. We are also investigating the effect of partial delay coupling on various specific network topologies.

3. We plan to carry out experimental confirmation of our results in possible cases. In particular, we are already working on the experimental confirmation of noise-enhanced phase synchronization in coupled time-delay systems using electronic circuits [Senthilkumar et al., 2010].

4. The interplay of connection delays and several other factors of complex networks remain largely unexplored. For example, the effect of connection delays proportional to the path length between the nodes in a complex network may be investigated.

5. As far as coupled chaotic dynamical systems are considered, there exists many different scenarios by which synchronization is lost. For example, existence of short wave length bifurcation, existence of upper limit in the number of chaotic oscillators that can be synchronized, upper limit in the value of coupling strength, etc. In connection with this, we will investigate the desynchronization dynamics along with the mechanism responsible for loss of synchronization and the influence of the delay on the desynchronization mechanism in the network of delay dynamical systems.

We hope to pursue these and other related problems in the near future.

Bibliography

Abbott L. F. and Vreeswijk C. von . Asynchronous states in networks of pulse-coupled oscillators. *Phys. Rev. E*, 48:1483, 1993.

Aboitiz F., Scheibel A. B., Fisher R. S., and Zaidel E. Fiber composition of the human corpus callosum. *Brain Res.*, 598:143–153, 1992.

Abrams D. M. and Strogatz S. H. Chimera states for coupled oscillators. *Phys. Rev. Lett.*, 93:174102, 2004.

Acebron J. A., Boneilla L. L., Perez Vincente C. J., Ritort F., and Spigler R. The kuramoto model: a simple paradigm forsynchronization phenomena. *Rev. Mod. Phys.*, 77:137–185, 2005.

Afraimovich V. S., Verichev N. N., and Rabinovich M. I. Stochastic synchronization of oscillation in dissipative systems. *Radio Phys. Quantum Electron*, 29:795–803, 1986.

Albert R. and Barbasi A. L. Statistical mechanics of complex networks. *Rev. Mod. Phys.*, 72:47, 2002.

Alsing P., Gavrielides A., Kovanis V., Roy R., and Thornburg K. S. Encoding and decoding messages with chaotic lasers. *Phys. Rev. E.*, 56:6302–6310, 1997.

Amritkar R. E. and Rangarajan G. Exploring the dynamics of conjugate coupled chua circuits: Simulations and experiments. *Phys. Rev. Lett*, 96:258102, 2006.

Anishchenko V. S., Astachov V. V., Neiman A. B., Vadivasova T. E., and Schimansky-Geier L. *Nonlinear Dynamics of Chaotic and Stochastic Systems*. Springer, Berlin, 2002.

Appleton E. V. The automatic synchronization of triode oscillator. *Proc. of the Cambridge Phil. Soc. (Math. and Phys. Sci.)*, 21:231–248, 1922.

Arenas A., Diaz-Guilera A., Moreno Y., Kurths J., and Zhou C. S. Synchronization in complex networks. *Phys. Rep.*, 469:93–153, 2008.

Argyris A., Syvridis D., Larger L., Annovazzi-lodi V., Colet P., Fischer I., Mirasso C. R., Garcia-Ojalvo J., Pesquera L., and Shore K. A. Chaos-based communications at high bit rates using commercial fibre-optic links. *Nature*, 438:343, 2005.

Ashwin P., Buescu J., and Stewart I. Bubbling of attractors and synchronisation of chaotic oscillators. *Phys. Lett. A*, 193:126–139, 1994.

Atay F. M., Jost J., and Wende A. Delays, connection topology, and synchronization of coupled chaotic maps. *Phys. Rev. Lett.*, 92:144101, 2004.

Barahona M. and Pecora L. M. Synchronization in small-world systems. *Phys. Rev. E.*, 89:054101, 2002.

Blekhman I. I. *Synchronization in Science and Technology.* ASME Press, New York, 1988.

Boccaletti S. and Valladares D. L. Characterization of intermittent lag synchronization. *Phys. Rev. E.*, 62:7497–7500, 2000.

Boccaletti S., Kurths J., Valladares D. L., Maza D., and Mancini H. Synchronization of chaotic structurally nonequivalent systems. *Phys. Rev. E.*, 61:3712–3715, 2000.

Boccaletti S., Pecora L. M., and Pelaez A. Unifying framework for synchronization of coupled dynamical systems. *Phys. Rev. E.*, 63:66219, 2001.

Boccaletti S., Kurths J., Osipov G., Valladares D. L., and Zhou C. S. The synchronization of chaotic systems. *Phys. Rep.*, 366:1–101, 2002.

Boccaletti S., Latora V., Moreno Y., Chavez M., and Hwang D. U. Complex networks: Structure and dynamics. *Phys. Rep.*, 424:175, 2006.

Braiman Y., Linder J. F., and Ditto W. L. Taming spatiotemporal chaos with disorder. *Nature*, 378:465, 1995.

Brown R. Approximating the mapping between systems exhibiting generalized synchronization. *Phys. Rev. Lett.*, 81:4835–4838, 1998.

Brown R. and Kocarev L. unifying definition of synchronization for dynamical systems. *Chaos*, 10:344–349, 2000.

Bunde A., Havlin S., Kantelhardt J. W., Penzel T., Peter J. P., and Voigt K. Correlated and uncorrelated regions in heart-rate fluctuations during sleep. *Phys. Rev. Lett.*, 85: 3736–3739, 2000.

Burner M. J. and Just W. Synchronization of time-delay systems. *Phys. Rev. E.*, 58: 4072–4075, 1998.

Buscarino A., Fortuna L., and Frasca M. Separation and synchronization of chaotic signals by optimization. *Phys. Rev. E*, 75:016215, 2007.

chaos. Focus issue: Stability and pattern formation in dynamics on networks. *Chaos*, 16, 2006.

Chen M. and Kurths J. Synchronization of time-delayed systems. *Phys. Rev. E.*, 76: 036212, 2007.

Choe C. U., Dahms T., HÃ¶vel P., and Schöll E. Controlling synchrony by delay coupling in networks :from in-phase to splay and cluster states. *Phys. Rev. E.*, 81:025205, 2010.

Chow K. V., Denning K. C., Ferris S., and Noronha G. longterm and shortterm price mermory in the share market. *Economic Lett.*, 49:287, 1995.

Chua L. O., Desoer C. A., and Kuh E. S. *Linear and Nonlinear Circuits*. Mcgraw Hill, Singapore, 1987.

CollinsJ. J., Chow C. C., and Imhoff T. T. Stochastic resonance without tuning. *Nature*, 376:236, 1995.

Deco G., Jirsa V., McIntosh A. R., Sporns O., and Kötter R. Key role of coupling, delay, and noise in resting brain fluctuations. *Proc. Natl Acad. Sci. USA*, 106:10302–10307, 2009.

Dhamala M., Jirsa V. K., and Ding M. Enhancement of neural synchrony by time-delay. *Phys. Rev. Lett.*, 92:074104, 2004.

Earl M. G. and Strogatz S. H. Synchronization in oscillator networks with delayed coupling: A stability criterion. *Phys. Rev. E.*, 67:036204, 2003.

Englert A., Heiligenthal S., Kinzel W., and Kanter I. Synchronization of chaotic networks with time−delayed couplings: An analytic study. *Phys. Rev. E.*, 83:046222, 2011.

Erneux T. *Applied Delay differential equations*. Springer, Berlin, 2009.

Farmer J. D. Chaotic attractors of an infinite dimensional dynamical system. *Physica D*, 4:366, 1982.

Fell J. and Axmacher N. The role of phase synchronization in memory processes. *Neuroscience (Nat. Rev.)*, 12:105, 2011.

Fink K. S., Johnson G. A., Carroll T. L., Mar D. J., and Pecora L. M. Three coupled oscillators as a universal probe of synchronization stability in coupled oscillator arrays. *Phys. Rev. E*, 61:5080, 2000.

Fischer I., Vicente R., Buldu J. M., Mirasso C. R., Torrent M. C., and Garcia-Ojalvo J. Zero-lag long-range synchronization via dynamical relaying. *Phys. Rev. Lett.*, 97: 123902, 2006.

Flunkert V., Yanchuk S., Dahms T., and Schöll E. Synchronizing distant nodes: A universal classification of networks. *Phys. Rev. Lett.*, 105:254101, 2010.

Fujisaka H. and Yamada T. Stability theory of synchronized motion in coupled-oscillator systems iii. *Prog. Theor. Phys.*, 72:885–894, 1984.

Fujisaka H. and Yamada T. A new intermittency in coupled dynamical systems. *Prog. Theor. Phys.*, 74:918–921, 1985.

Fujisaka H. and Yamada T. Stability theory of synchronized motion in coupled-oscillator systems. iv instability of synchronized chaos and new intermittency. *Prog. Theor. Phys.*, 75:1087–1184, 1986.

Fujisaka H. and Yamada T. Stability theory of synchronized motion in coupled-oscillator systems ii. *Prog. Theor. Phys.*, 69:32–47, 1983.

Gade P. K. and Hu C. K. Synchronous chaos in coupled map lattices with small world interactions. *Phys. Rev. E.*, 62:6409–6413, 2000.

Gerhardt M. and Schuster H. A cellular automaton of excitable media including curvature and dispersion. *Science*, 247:1563–1566, 1990.

Ghosh D., Banarjee S., and Chowdury A. R. Synchronization between variable time-delayed systems and cryptography. *Europhys. Lett.*, 80:30006, 2007.

Gonzalez C. M, Masoller C., Torrent M. C, and Garcia-Ojalvo J. Synchronization via clustering in a small delay-coupled laser network. *Europhys. Lett.*, 79:64003, 2007.

Gopalsamy K. *Stability and Oscillations in Delay Differential Equations of Population Dynamics*. Kluwer Academic Press, The Netherlands, 1992.

Heagy J. F., Pecora L. M., and Carroll T. L. Short wavelength bifurcations and size instabilities in coupled oscillator systems. *Phys. Rev. Lett.*, 74:4185, 1995.

Hindmarsh J. L. and Rose R. M. A model of neuronal bursting using three coupled first order differential equations. *Proc. R. Soc. London, Ser. B*, 221:87–102, 1984.

Hod S. Analytic treatment of the network synchronization problem with time-delays. *Phys. Rev. Lett.*, 105:208701, 2010.

Horsthemke W. and Lefever R. *Noise-Induced Transitions: Theory and Applications in Physics, Chemistry and Biology*. Springer, Berlin, 1984.

Hövel P. *Control of Complex Nonlinear Systems with Delay*. Springer, Berlin Heidelberg, 2010.

Hramov A. E. and Koronovskii A. A. An approach to chaotic synchronization. *Chaos*, 14:603(1–8), 2004.

Huang L., Chen Q., Lai Y. C., and Pecora L. M. Generic behavior of master stability functions in coupled nonlinear dynamical systems. *Phys. Rev. E*, 80:036204, 2009.

Hunt D., Korniss G., and Szymanski B. J. Network synchronization in a noisy environment with time-delays: Fundamental limits and trade-offs. *Phys. Rev. Lett.*, 105: 68701, 2010.

Huygens, Christiaan. *Horologium oscillatorium sive de motu pendularium*. (theory and design of the pendulum clock, dedicated to Louis XIV of France), France, 1673.

Huys O. D, Vincente R., Erneux T., Danckert J., and Fischer I. Synchronization properties of network motifs: Influence of coupling delay and symmetry. *Chaos*, 18:037116, 2008.

Ikeda K., Diado H., and Akimoto O. Optical turbulence: Chaotic behavior of transmitted light from a ring cavity. *Phys. Rev. Lett.*, 45:709, 1980.

Izquierdo I., Barros D. M., desouza T. M., Izquierdo L. A., and Medina J. H. Mechanisms for memory types differ. *Nature*, 393:635, 1998.

Jalan S. and Amritkar R. E. Self-organized and driven phase synchronization in coupled maps. *Phys. Rev. Lett*, 90:014101, 2003.

Jiang Y., Lozada-Cassou M., and Vinet A. Synchronization and symmetry-breaking bifurcations in constructive networks of coupled chaotic oscillators. *Phys. Rev. E*, 68: 065201, 2003.

Jirsa V. K. Dispersion and time-delay effects in synchronized spike burst networks. *Cognit. Neurodynamics*, 2:29, 2008.

Jolliffe I. T. *Principal Component Analysis*. Springer, NewYork, 2002.

Jost J. and Joy M. P. Spectral properties and synchronization in coupled map lattices. *Phys. Rev. E.*, 65(3):016201, Feb 2002.

Kantelhardt J.W., KoscielnyBunde E., Rysbki D., Braun P., Bunde A., and Havlin S. Long-term persistence and multifractality of precipitation and river runoff records. *J. Geophys. Res. Atoms.*, 111:D01106, 2006.

Karnatak R., Prasad A., Dana S. K., and Ramaswamy R. Amplitude death in the absence of time-delays in identical coupled oscillators. *Phys. Rev. E.*, 76:035201, 2007.

Kauffman S. A. Homeostasis and differentiation in random genetic control networks. *Nature*, 22:437, 1969.

Kinzel W., Englert A., Reents G., Zigzag M., and Kanter I. Synchronization of networks of chaotic units with time-delayed couplings. *Phys. Rev. E.*, 79:056207, 2009.

Knuston A. R., Hopkins R. O., and Squire L. R. Visual discrimination performance, memory, and medial temporal lobe function. *Proc. Natl. Acad. Sci. USA*, 109:13106, 2012.

Kocarev L. and Parlitz U. Generalized synchronization, predictability, and equivalence of unidirectionally coupled dynamical systems. *Phys. Rev. Lett.*, 76:1816–1819, 1996.

Kocarev L., Halle K. S., Eckert K., Chua L. O., and Parlitz U. Experimental demonstration of secure communications via chaotic synchronization. *Int. J. Bifurcation and Chaos*, 2:973, 1992.

KoscielnyBunde E., Bunde A., Havlin S., Roman H. E., Goldreich Y., and Schnellhuber H. J. Indication of a universal persistence law governing atmospheric variability. *Phys. Rev. Lett.*, 81:729, 1998.

Koseska A. , Volkov E., Zaikin A., and Kurths J. Inherent multistability in arrays of autoinducer coupled genetic oscillators. *Phys. Rev. E.*, 75:31916, 1998.

Kozyreff G., Vladimirov A. G., and Mandel P. Global coupling with time-delay in an array of semiconductor lasers. *Phys. Rev. Lett.*, 85:3809, 2000.

Krasvoskii N. N. *Stability of motion*. Stanford University Press, Stanford, 1963.

Kuramoto Y. *Chemical Oscillations, Waves, and Turbulence*. Springer, Berlin, 1984.

Kurths J. Special issue on phase synchronization. *Int. J. Bifurcation and Chaos*, 10, 2000.

Kye W. H., Choi M., Kim C. M., and Park Y. J. Encryption with synchronized time-delayed systems. *Phys. Rev. E.*, 71:045202(1–4), 2005.

Lakshmanan M. and Murali K. *Chaos in Nonlinear Oscillators: Controlling and Synchronization*. World Scientific, Singapore, 1996.

Lakshmanan M. and Rajasekar S. *Nonlinear Dynamics:Integrability, Chaos and Patterns*. Springer, Berlin, 2003.

Lee D. S. Synchronization transition in scale-free networks: Clusters of synchrony. *Phys. Rev. E*, 72:26208, 2005.

Lennartz S., Livina V. N., Bunde A., and Havlin S. Long-term memory in earthquakes and the distribution of interoccurrence times. *Europhys. Rev. Lett.*, 81:69001, 2008.

Li C., Sun W., and Kurths J. Synchronization between two coupled complex networks. *Phys. Rev. E.*, 76:046204, 2007.

Li X., Cohen A. B., Roy R., and Murphy T. E. Scalable parallel physical random number generator based on a superluminescent led. *Optics Lett.*, 36:1020–1022, 2011.

Liang X., Tang M., Dhamala M., and Liu Z. Phase synchronization of inhibitory bursting neurons induced by distributed time-delays in chemical coupling. *Phys. Rev. E.*, 80: 066202, 2009.

Llinas R. R. and Grace A. A.and Yarom Y. In vitro neurons in mammalian cortical layer 4 exhibit intrinsic oscillatory activity in the 10 to 50hz frequency range. *Proc. Natl. Acad. Sci. USA*, 88:897–901, 1991.

Locquet A., Rogister F., Sciamanna M., Megret P., and Blandel M. Two types of synchronization in unidirectionally coupled chaotic external cavity semiconductor lasers. *Phys. Rev. E.*, 64:045203, 2001.

Locquet A., Masoller C., and Mirasso C. R. Synchronization regimes of optical feedback induced chaos in unidirectionally coupled semiconductor lasers. *Phys. Rev. E.*, 65: 056205, 2002.

Lorenz E. N. . Deterministic nonperiodic flow. *J. Atmos. Sci.*, 20:130–141, 1963.

Lu J., , Ho D. W. C, and Kurths J. Consensus over directed static networks with arbitrary finite communication delays. *Phys. Rev. E*, 80:066121, 2009.

Luecken L., Pad J. P., Rysbki D., and Yanchuk S. Reduction of interaction delays in networks. *ArXiv1206170v1*, -, 2012.

Mackey M. C. and Glass L. Oscillation and chaos in physiological control systems. *Science*, 197:287–289, 1977.

Madan R. N. *A Paradigm for Chaos*. World Scientific, Singapore, 1996.

Masih R. and Masih A. M. M. Long and short-term dynamic causal transmission amongst international stock markets. *J. International Money and Finance*, 20:563, 2001.

Masoller C. Anticipation in the synchronization of chaotic semiconductor lasers with optical feedback. *Phys. Rev. Lett.*, 86:2782, 2001.

Masoller C. and Atay F. M. Complex transitions to synchronization in delay coupled networks of logistic maps. *Eur. Phys. J. D*, 62:119, 2011.

Masoller C. and Marti A. C. Random delays and the synchronization of chaotic maps. *Phys. Rev. Lett.*, 94:134102, 2005.

Matsumoto T., Chua L. O., and Komuro M. The double scroll. *IEEE Trans. Circuits Syst. CAS*, 32:797–818, 1985.

Mery F. and Kawecki T. J. A cost of long-term memory in drosophila. *Science*, 308: 1148, 2005.

Mokhov I. I., Smirnov D. A., Nakonechny P. I., Kozlenko S. S., Seleznevv E. P., and Kurths J. Exploring the dynamics of conjugate coupled chua circuits: Simulations and experiments. *Geophys. Res. Lett*, 38:L00F04, 2011.

Moreno Y. and Pacheco A. F. Synchronization of kuramoto oscillators in scale-free networks. *Europhys. Lett.*, 68:603, 2004.

Motter A. E., Zhou C., and Kurths J. Network synchronization, diffusion, and the paradox of heterogeneity. *Phys. Rev. E*, 90:016116, 2005.

Nagai K. H. and Kori H. Noise-induced synchronization of a large population of globally coupled nonidentical oscillators. *Phys. Rev. E*, 81:065202(R), 2010.

Namajunas A., Pyragas K., and Tamasevicius A. An electronic analog of the mackey-glass system. *Phys. Lett. A*, 42:201, 1995.

Ndungu F.M., Olotu A., Mwacharo J., Nyonda M., Apfeld J., Mramba L. K., Fegan G. W., Bejon P., and Marsh K. Memory b cells are a more reliable archive for historical antimalarial responses than plasma antibodies in no-longer exposed childre. *Proc. Natl. Acad. Sci. USA*, 109:8247, 2012.

Nishikawa T. and Motter A. E. Maximum performance in minimum cost in network synchronization. *Physica D*, 224:77–89, 2006a.

Nishikawa T. and Motter A. E. Network synchronization landscape reveals compensatory structures, quantisation and the positive effects of negative interactions. *Proc. Natl. Acad. Sci. USA*, 107:10343–10347, 2010.

Nishikawa T. and Motter A. E. Synchronization is optimal in nondiagonazible networks. *Phys. Rev. E.*, 73:05106, 2006b.

Nishikawa T., Motter A. E., Lia Y. C., and Hoppensteadt F. C. Heterogeneity in oscillator networks: Are smaller worlds easier to synchronize? *Phys. Rev. Lett.*, 91: 014101, 2003.

Oguchi O. D, Nijmeijer R., and Yamamoto T. Synchronization in networks of chaotic systems with time-delay coupling. *Chaos*, 18:037108, 2008.

Pecora L. Special focus issue on chaotic synchronization. *Chaos*, 7, 1997.

Pecora L. M. and Barahona M. Synchronization of oscillators in complex networks. *Chaos and Complexity Letters*, 72:61–91, 2002.

Pecora L. M. and Carroll T. L. Driving systems with chaotic signals. *Phys. Rev. A.*, 44: 2374–2383, 1991.

Pecora L. M. and Carroll T. L. Synchronization in chaotic systems. *Phys. Rev. Lett.*, 64:821–824, 1990.

Pecora L. M. and Carroll T. L. Master stability functions for synchronized coupled systems. *Phys. Rev. Lett.*, 80:2109, 1998.

Pecora L. M., Carroll T. L., Johnson G. A., Mar D. J., and Heagy J. F. Fundametals of synchronization in chaotic systems, concepts and applications. *Chaos*, 7:520–542, 1997.

Pecora L. M., Carroll T. L., Johnson G. A., Mar D. J., and Heagy J. F. Synchronization stability in coupled oscillator arrays:solution for arbitrary configuration. *International Journal of Bifurcation and chaos*, 10:273–290, 2000.

Peng C. K., Meitus J., Hausdroff J. M., Havlin S., Stanley H. E., and Goldberger A. L. Long-range anticorrelations and non-gaussian behavior of the heartbeat. *Phys. Rev. Lett.*, 70:1343–1346, 1993.

Perez T., Garcia G. C, Eguiluz V. M, Vincente R., Pipa G., and Mirasso C. R. Effect of the topology and delayed interactions in neuronal networks synchronization. *PLoS ONE*, 6:19900, 2011.

Pikovsky A. S. On the interaction of strange attractors. *Z. Phys. B*, 55:149–154, 1984.

Pikovsky A. S., Osipov G., Rosenblum M. G., Zaks M., and Kurths J. Attractor-repeller collision and eyelet intermittency at the transition to phase synchronization. *Phys. Rev. Lett.*, 79:47–50, 1997.

Pikovsky A. S., Rosenblum M. G., and Kurths J. *Synchronization - A Unified Approach to Nonlinear Science*. Cambridge University Press, Cambridge, 2001.

Pisarchik A. N., Reategui R. J., Villalobos-Salazar J. R., Garcia-Lopez J. H., and Boccaletti S. Synchronization of chaotic systems with coexisting attractors. *Phys. Rev. Lett.*, 96:244102, 2006.

Ponce M., Masoller C., and Marti A. C. Synchronizability of chaotic logistic maps in delayed complex networks. *Europhys. J. B*, 67:83, 2009.

Prasad A., Kurths J., Dana S. K., and Ramaswamy R. Phase-flip bifurcation induced by time-delay. *Phys. Rev. E.*, 74:035204, 2006.

Pyragas K. Synchronization of coupled time-delay systems: Analytical estimations. *Phys. Rev. E.*, 58:3067–3071, 1998.

Lord Rayleigh. *Theory of sound*. Macmillan and co., London, 1877.

Reddy D. V. R., Sen A., and Jhonston G. L. time-delay induced death in coupled limit cycle oscillators. *Phys. Rev. Lett.*, 80:5109–5112, 1998.

Rim S., Kim I., Kang P., Park Y. J., and Kim C. M. Routes to complete synchronization via phase synchronization in coupled nonidentical chaotic oscillators. *Phys. Rev. E.*, 66:015205, 2002.

Rosenblum M. G., Pikovsky A. S., and Kurths J. Phase synchronization of chaotic oscillators. *Phys. Rev. Lett.*, 76:1804–1807, 1996.

Rosenblum M. G., Pikovsky A. S., and Kurths J. From phase to lag synchronization in coupled chaotic oscillators. *Phys. Rev. Lett.*, 469:4193–4196, 1997.

Rössler O. E. An equation for continuous chaos. *Phys. Let. A*, 57:397–398, 1976.

Rulkov N. F., Sushchik M. M., Tsimring L. S., and AbarbanelH. D. I. Generalized synchronization of chaos in directionally coupled chaotic systems. *Phys. Rev. E.*, 51: 980–994, 1995.

Sano S., Uchida A., Yosgimori S., and Roy R. Dual synchronization of chaos in mackey-glass electronic circuits with time-delayed feedback. *Phys. Rev. E.*, 75:016207(1–6), 2007.

Scheibel A. B., Fischer R. S., and Zaidel E. Fiber composition of the human corpus callosum. *Brain. Res.*, 598:143–153, 1992.

Schöll E. and Schuster H. G. *Hand Book of Chaos Control*. Kluwer Academic Press, The Netherlands, 2007.

Schuster H. G. and Wagner P. Mutual entrainment of two limit cycle oscillators with time-delayed coupling. *Prog. Theor. Phys.*, 81:939, 1989.

Senthilkumar D. V. and Lakshmanan M. Transition from anticipatory to lag synchronization via complete synchronization in time-delay systems. *Phys. Rev. E.*, 71:016211, 2005.

Senthilkumar D. V. and Lakshmanan M. *Dynamics of Nonlinear Time-Delay Systems*. Springer, Berlin, 2011.

Senthilkumar D. V., Lakshmanan M., and Kurths J. Phase synchronization in time-delay systems. *Chaos*, 74:035205, 2006.

Senthilkumar D. V., Lakshmanan M., and Kurths J. Stability of synchronization in coupled time-delay systems using krasovskii-lyapunov theory. *Phys. Rev. E.*, 79:66208(1–4), 2009.

Senthilkumar D. V., Srinivasan K., Murali K., Lakshmanan M., and Kurths J. Experimental confirmation of chaotic phase synchronization in coupled time-delayed electronic circuits. *Phys. Rev. E.*, 82:065201(1–4), 2010.

Senthilkumar D. V., Pesquera L., Banerjee S., Ortin S., and Kurths J. Exact synchronization bound for coupled time-delay systems. *Phys. Rev. E.*, 87:44902(1–5), 2013a.

Senthilkumar D. V., Manju Shrii M., and Kurths J. *Chapter on Phase and Complete Synchronizations in Time-Delay Systems, in the book entitled CNN, Memristors and Beyond: A Festschrift for Leon Chua dedicated to Prof. Leon. O. Chua on the occasion of his 75th Birthday, Eds. A. Adamatzky and G. Chen*. World Scientific, Singapore, 2013b.

Sethia G. C., Sen A., and Atay F. M. Clustered chimera states in delay-coupled oscillator systems. *Phys. Rev. Lett.*, 100:144102, 2008.

Shadlow H. A. Physiological properties of individual cerebral axons studied in vivo for as long as one year. *Neurphysiol.*, 54:1346, 1985.

Shahverdiev E. M. and Shore K. A. Generalized synchronization in time-delayed systems. *Phys. Rev. E.*, 71:016201, 2005.

Shahverdiev E. M., Sivaprakasam S., and Shore K. A. Parameter mismatches and perfect anticipating synchronization in bidirectionally coupled external cavity laser diodes. *Phys. Rev. E.*, 66:017206, 2002a.

Shahverdiev E. M., Sivaprakasam S., and Shore K. A. Lag synchronization in time-delayed systems. *Phys. Lett. A*, 292:320, 2002b.

Sharma A., Shrimali M. D., Prasad A., Ramaswamy R., and Feudel U. Phase-flip transition in relay-coupled nonlinear oscillators. *Phys. Rev. E.*, 84:016226, 2011.

Shrager Y., Levy D. A., Hopkins R. O., and Squire L. R. Working memory and the organization of brain systems. *J. Neurosci*, 28:4818, 2008.

Manju Shrii M., Senthilkumar D. V., and Kurths J. Delay-induced synchrony in complex networks with conjugate coupling. *Phys. Rev. E*, 85:057203, 2012a.

Manju Shrii M., Senthilkumar D. V., and Kurths J. Delay coupling enhances synchronization in complex networks. *Europhys. Lett.*, 98:100003, 2012b.

Singala T., Pawar N., and Pramananda P. Exploring the dynamics of conjugate coupled chua circuits: Simulations and experiments. *Phys. Rev. E.*, 83:026210, 2011.

Soriano M. C., Zunino L., Rosso O. A., Fischer I., and Mirasso C. R. Time scales of a chaotic semiconductor laser with optical feedback under the lens of a permutation information analysis. *IEEE J. Quantum Electron.*, 47:252–261, 2011.

Soriano M. C., Garcia-Ojalvo J., Mirasso C. R., and Fischer I. Complex photonics: Dynamics and applications of delay-coupled semiconductors lasers. *Rev. Mod. Phys.*, 85:421–470, 2013.

Stepan G. Delay effects in brain dynamics. *Phil. Trans. R. Soc. A*, 367:1059, 2009.

Strogatz S. H. coupled oscillators and biological synchronization. *Sci. Am.*, 269:102, 1993.

Suresh R., Senthilkumar D. V., Lakshmanan M., and Kurths J. Global phase synchronization in an array of time-delay systems. *Phys. Rev. E*, 82:016215(1–10), 2010.

Taherion S. and Lai Y. C. Observability of lag synchronization of coupled chaotic oscillators. *Phys. Rev. E.*, 59:6247–6250, 1999.

Takens F. *Detecting Strange Attractors in Turbulence, Lecture Notes in Mathematics, edited by D. Rand and L. Young.* Springer, New York, 1981.

Tang J., Ma J., Yi H., Xia M., and Yang X. Delay and diversity-induced synchronization transitions in a small-world neuronal network. *Phys. Rev. E.*, 83:046207, 2011.

van der Pol B. and van der Mark J. Frequency demultiplication. *Nature*, 120:363–364, 1927.

Vanwiggeren G. D. and Roy R. Communication with chaotic lasers. *Science*, 279:1198, 1998.

Varela F., Lachaux J. P, Rodriguez E., and Martinerie J. The brainweb: Phase synchronization and large-scale integration. *Neuroscience (Nat. Rev.)*, 2:229, 2001.

Voss H. U. Anticipating chaotic synchronization. *Phys. Rev. E.*, 61:5115–5119, 2000.

Voss H. U. Dynamic long term anticipation of chaotic states. *Phys. Rev. Lett.*, 87: 014102, 2001.

Voss H.U. Anticipating chaotic synchronization. *Phys. Rev. E.*, 61:5115, 2000.

Wang Q., Perc M., Duan Z., and Chen G. Synchronization transitions on small-world neuronal networks: Effects of information transmission delay and rewiring probability. *Europhys. Lett.*, 83:50008, 2008.

Wang Q., Perc M., Duan Z., and Chen G. Synchronization transitions on scale-free neuronal networks due to finite information transmission delays. *Phys. Rev. E*, 80: 026206, 2009.

Wang Q., Chen G., and Perc M. Synchronous bursts on scale-free neuronal networks with attractive and repulsive coupling. *PLoS ONE*, 6:15851, 2011.

Wang Q. Y., Duan Z. S., Perc M., and Chen G. R. Synchronization transitions on small-world neuronal networks: Effects of information transmission delay and rewiring probability. *Eur. Phys. Lett.*, 83:50008, 2008.

Watts D. J. *The Dynamics of Networks between Order and Randomness*. Princeton University Press, Princeton, NJ, 1999.

Watts D. J. and Strogatz S. H. Collective dynamics of small-world networks. *Nature*, 393:440, 1998.

Wiesenfeld K. New results on frequency-locking dynamics of disordered josephson arrays. *Physica B*, 222:315, 1996.

Williams C. R. S., Salevan J. C., Li X., Roy R., and Murphy T. E. Fast physical random number generator using amplified spontaneous emission. *Optics Express*, 18:23584, 2010.

Winfree A. T. *The Geometry of Biological Time*. Springer, New York, 1980.

Wolf A., Swift J. B., Swinney H. L., and Vastano J. A. Determining lyapunov exponents from a time series. *Physica D*, 16:285–317, DOI: 1985.

Wu W. C. *Synchronization in Complex Networks of Nonlinear Dynamical Systems*. World Scientific, Singapore, 2007.

Wylie C. R. and Barrett L. C. *Advanced Engineering Mathematics*. Mcgraw Hill, New York, 1995.

Yalcinkaya T. and Lai Y. C. Phase characterization of chaos. *Phys. Rev. Lett.*, 79: 3885–3888, 1997.

Zaks M., Park E. H., Rosenblum M. G., and Kurths J. Alternating locking ratios in imperfect phase synchronization. *Phys. Rev. Lett.*, 82:4228–4232, 1999.

Zhan M., Wei G. W., and Lai C. H. Transition from intermittency to periodicity in lag synchronization in coupled roessler oscillators. *Phys. Rev. E.*, 65:036202, 2002.

Zhan M., Wang Y., Gang X., Wei G. W., and Lai C. Complete synchronization and generalized synchronization of one way coupled time-delay systems. *Phys. Rev. E.*, 68:36208(1–4), 2003.

Zhou C. and Kurths J. Dynamical weights and enhanced synchronization in adaptive complex networks. *Phys. Rev. Lett*, 96:164102, 2006.

Zhou C. and Kurths J. Noise-induced phase synchronization and synchronization transitions in chaotic oscillators. *Phys. Rev. Lett.*, 88:230602, 2002.

Zhou C., Kurths J., Kiss I. Z., and Hudson J. L. Noise-enhanced phase synchronization of chaotic oscillators. *Phys. Rev. Lett.*, 89:014101, 2002.

Zhou C., Motter A. E., and Kurths J. Universality in the synchronization of weighted random networks. *Phys. Rev. Lett*, 96:034101, 2006a.

Zhou C., ZemanovÃ¡ L., Zamora G., Hilgetag C. C., and Kurths J. Hierarchical organization unveiled by functional connectivity in complex brain networks. *Phys. Rev. Lett*, 97:238103, 2006b.

Zhou S., Li H., and Wu Z. Synchronization threshold of a coupled time-delay systems. *Phys. Rev. E.*, 75:037203(1–6), 2007.

Zhu L. and Lai Y. C. Experimental observation of generalized time-lagged chaotic synchronization. *Phys. Rev. E.*, 64:045205, 2001.

Selbständigkeitserklärung

Ich erkläre, dass ich die vorliegende Arbeit selbständig und nur unter Verwendung der angegebenen Literatur und Hilfsmittel angefertigt habe.

Berlin, den. 18.06.2013 Manju Shrii Murugesan